



# Open Science Grid

## Annual Report

June 2017

Miron Livny	University of Wisconsin	Principal Investigator
Michael Ernst	BNL	co-PI
Ruth Pordes	FNAL	co-PI
Frank Würthwein	UCSD	co-PI

Supported by the National Science Foundation and the US Department of Energy's Office of Science



## Contents

1	Executive Summary .....	4
2	Science Enabled by OSG .....	10
2.1	ATLAS .....	10
2.2	CMS .....	13
2.3	FabrIc for Frontier Experiments .....	16
2.4	Nuclear Physics.....	19
2.5	Laser Interferometer Gravitational-Wave Observatory (LIGO) .....	21
2.6	IceCube .....	23
2.7	Astronomy.....	26
2.8	Campus Researchers .....	34
3	The OSG Fabric of Services .....	45
3.1	Technology Investigations .....	45
3.2	Software .....	46
3.3	Release Management .....	48
3.4	Operations.....	49
3.5	Network Monitoring .....	52
3.6	Security .....	55
3.7	Production Support .....	57
3.8	User Support and Campus Grids.....	60
4	Project, Consortium, and Partners .....	72
4.1	Project Institutions .....	72
4.2	OSG Council and Consortium .....	72
5	Education, Communications, and Other Outreach .....	73
5.1	Education .....	73
5.2	Communications .....	74
5.3	Outreach.....	75
	Appendix: Science Publications Enabled by OSG .....	77
	ATLAS .....	77
	CTC (University of Wisconsin–Madison) .....	89
	CMS .....	91
	FIFE .....	103
	IceCube .....	104
	Other .....	106

The prior year (March 2016) OSG Annual Report is available at

<http://osg-docdb.opensciencegrid.org/cgi-bin>ShowDocument?docid=1220>

Sections of this report were provided by the scientific members of the OSG Council, OSG PIs and co-PIs, and OSG staff and partners.

Edited by:

- Miron Livny, OSG Principal Investigator
- Frank Würthwein, OSG Executive Director
- Tim Cartwright, OSG Chief of Staff

## 1 Executive Summary

The Open Science Grid (OSG) is a large-scale collaboration that is advancing scientific knowledge through distributed high-throughput computing (DHTC) by operating and evolving a cross-domain, distributed cyber-infrastructure. The OSG program consists of a consortium of contributing communities (users, resource administrators, and software providers) and a funded project; this collaborative ecosystem advances the science of DHTC for researchers. OSG provides a production-quality facility, connecting a broad variety of researchers to distributed computing centers at university campuses, national laboratories, supercomputing centers, other community resources, and commercial clouds, within the United States as well as worldwide. This facility depends on a range of common services, support activities, software, and operational principles that coordinate the production of scientific knowledge through the DHTC model. In April 2012, the OSG project was extended until 2017 as a jointly funded project by the Department of Energy and the National Science Foundation. This annual report functions as the final report for the DOE, and as Year 5 annual report for the NSF. The NSF project is presently extended at present by one more year with an estimated end date of approximately May 2018.

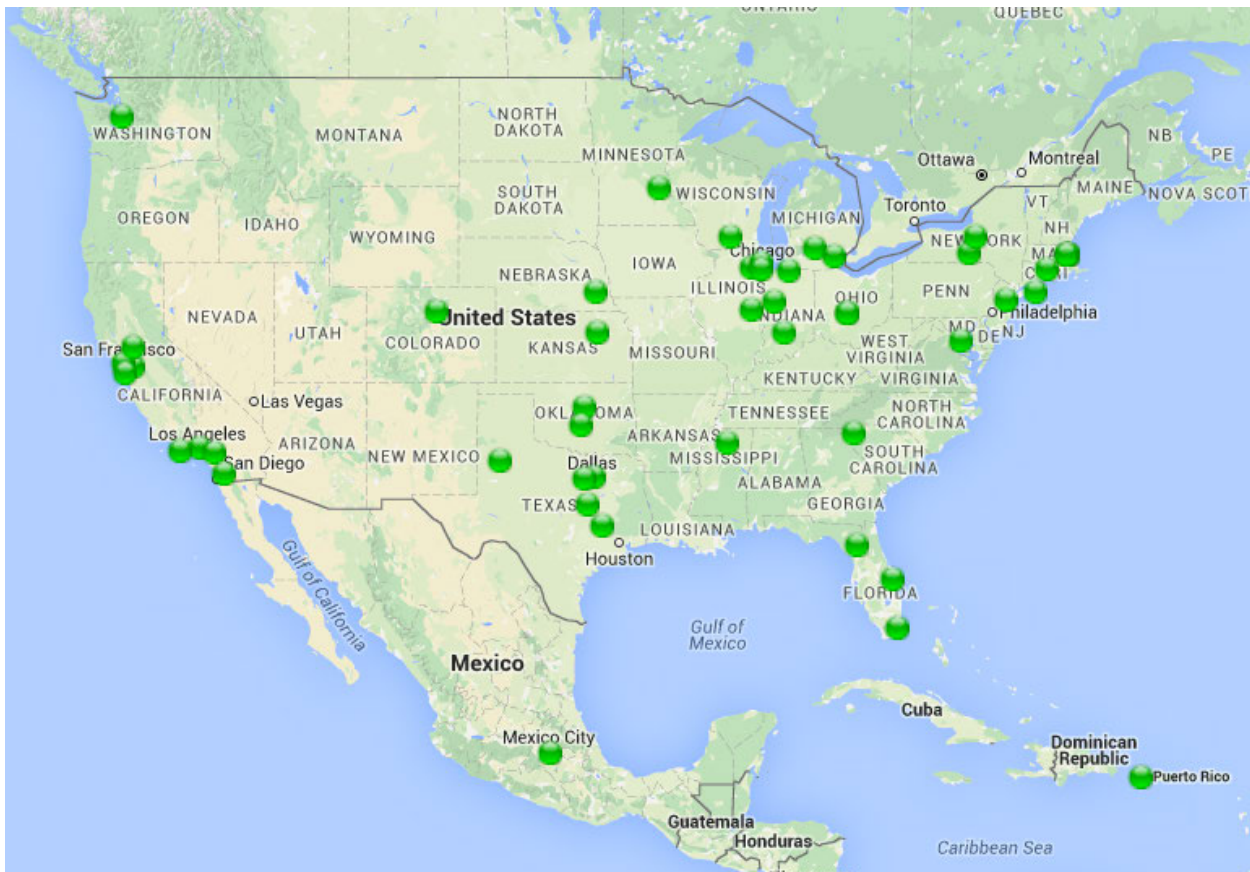


Figure 1: Open Science Grid US sites

Figure 1 shows the clusters integrated into OSG in the US alone. Figure 2 depicts the total core hours of wall time consumed via OSG interfaces across these clusters versus time since 2006. It shows clearly that the Large Hadron Collider (LHC) experiments dominated the resource consumption on OSG throughout its entire lifetime. It also shows an overall growth in resource consumption by roughly 25% within the last year, and a doubling in the last two years. The peaks seen in Figure 2 of 130 million core hours per month imply a 24 hours times 30 days non-stop operations in excess of 180,000 cores of computing. On an annual basis, this amounts to more than 1.4 billion core hours consumed by 130 million jobs, involving 2 billion data transfers that move in excess of 160,000 terabytes of data.

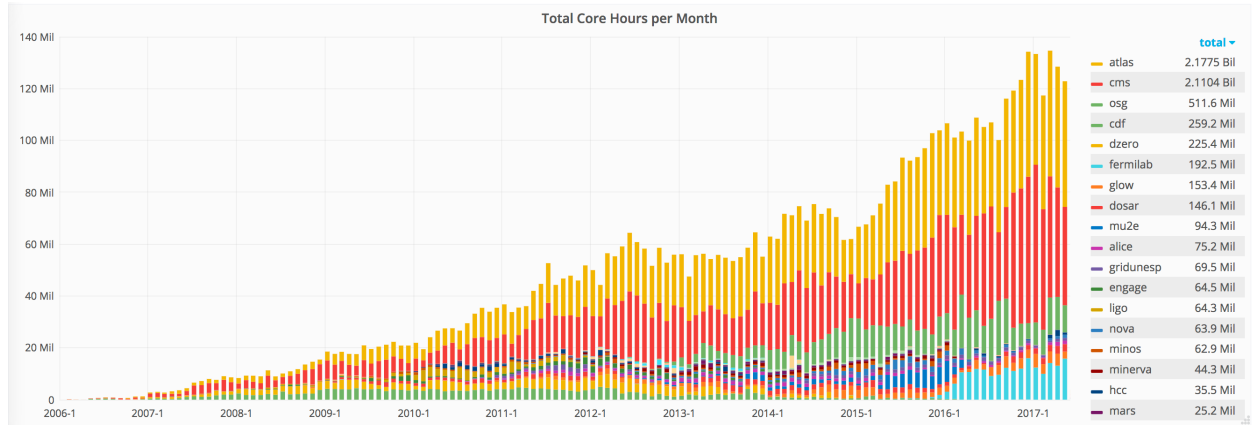


Figure 2: OSG total core hours consumed per month

OSG serves the needs of the LHC experiments by providing a platform for their contribution and consumption of distributed computing resources. The US LHC experiments continued to rely on OSG to accomplish their science; not only do they rely on OSG for computing resources, but also for operational, consulting, and software services. In addition, in the US, OSG is a natural conduit for collaboration and joint initiatives among the LHC experiments and the Worldwide LHC Computing Grid (WLCG) project.

While meeting the needs of the US LHC experiments, OSG continues to expand the access to DHTC for other sciences, nationally and especially internationally. International integration for US-based science programs including Laser Interferometer Gravitational-wave Observatory (LIGO), IceCube, NOvA, Deep Underground Neutrino Experiment (DUNE), and XENON1T has been a special focus during the last year as can be seen in Figure 3.

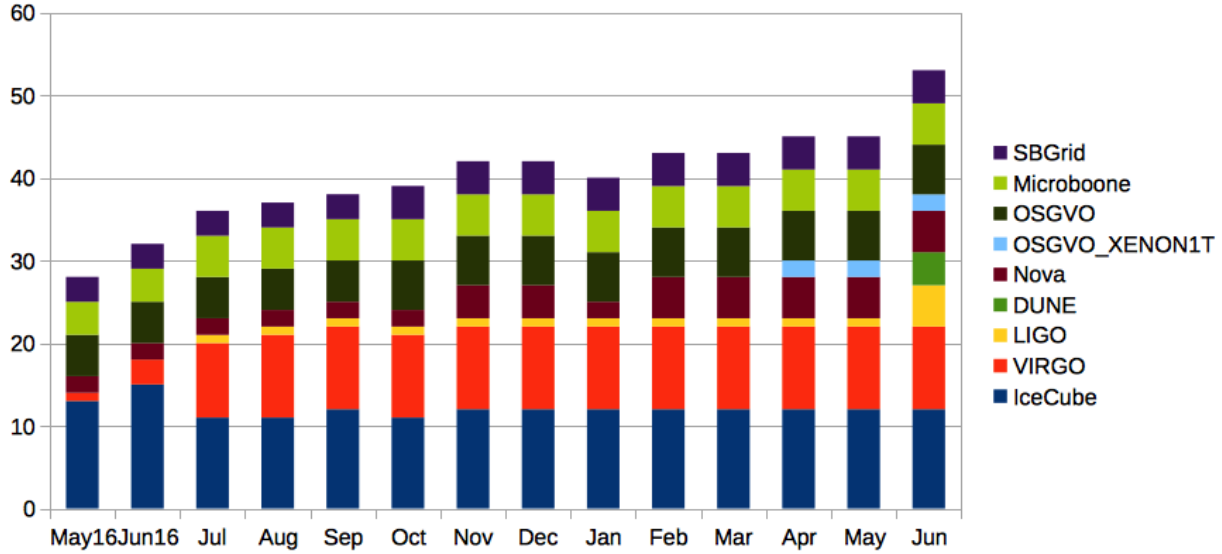


Figure 3: Number of international clusters integrated versus time by virtual organization

Figure 3 shows that we roughly doubled the number of international clusters that can be accessed by US based science communities via OSG. Figure 4 shows the weekly core hours consumed at those international clusters for the last 6 months. There is a clear increase visible within the last 6 months that is dominated by IceCube, LIGO, and NOvA. As we will discuss in the detailed sections for these three experiments below, these contributions from international collaborators comprise a significant contribution to their respective operations.

Initially, these international contributions were a direct benefit from the WLCG interoperability work OSG has been engaged in for years. Institutions that support the LHC experiments were easy to integrate into OSG also for other experiments. However, within the last couple of months, we increasingly have integrated institutions for IceCube and LIGO that are not part of WLCG.

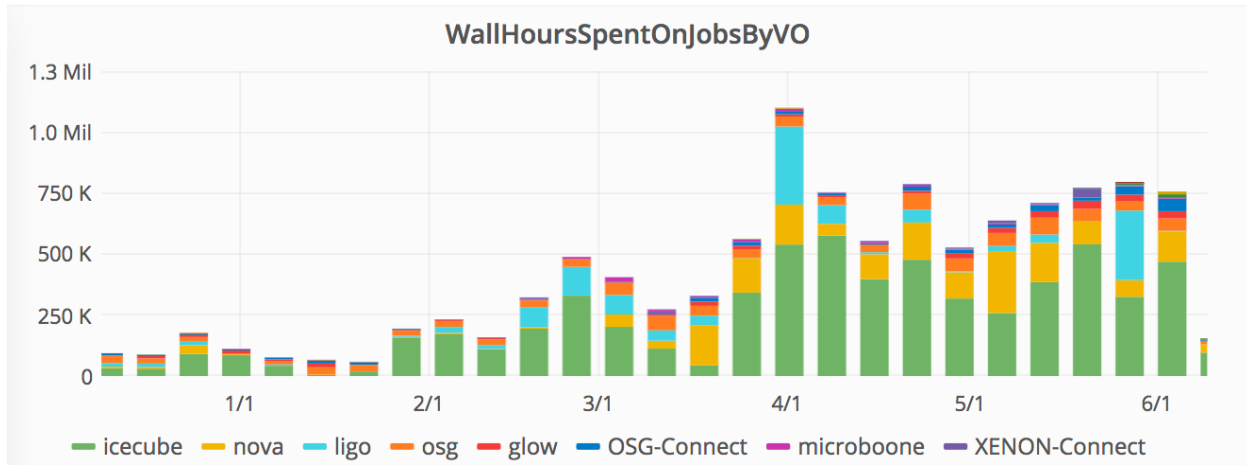


Figure 4: Core hours consumed by US-based science communities at clusters operated by their collaborating institutions outside the US

In addition to resource access, we see a strong technical cross fertilization between the US LHC community and other sciences. In years past, this was mostly a one-way street, science other than LHC benefitted from infrastructure technologies driven by LHC needs. Within the last year this has changed dramatically. Increasingly, science other than the LHC is more agile, and more adventurous, and thus drives technology adoption that the US LHC experiments will ultimately benefit from. Examples of this are:

- The Singularity container technology was introduced first for the OSG virtual organization (VO), with the OSG user group, and thus the general open science community being the stakeholder to drive technology integration and ultimately adoption. Both ATLAS and CMS have expressed interest in use of Singularity on OSG. For CMS, this is an essential part of the strategy for managing the upcoming OS transition from RHEL 6 to 7.
- Machine learning on GPUs is being driven on OSG by biomedical informatics. This is an interesting case of technology convergence. The GPU integration was driven in previous years by IceCube and SBGrid. Singularity containers are driven this year by the OSG user group. Machine learning depends on both of these, and is driven by biomedical informatics. We expect this capability to become increasingly of interest to the US LHC community in the future.
- XRootD caching was developed for the LHC but first adopted at anything resembling scale by a few genomics users on OSG. Figure 5 shows the volume of data read from StashCache, the OSG deployment of XRootD caches, for the last 60 days. Peaks of close to 15 TB per hour are clearly visible. This use is dominated by two meta- or exo-genomics projects, one from the University of Nebraska–Lincoln, and a second one from Clemson University. This capability is expected to be deployed more and more also by US ATLAS and US CMS in the future.

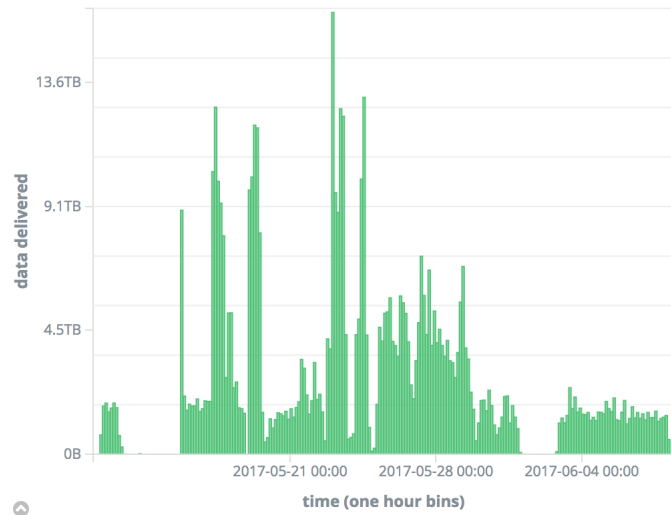


Figure 5: OSG StashCache data reads for 60 days

- The use of NSF eXtreme Digital (XD) resources in OSG is driven by LIGO, XENON1T, IceCube, and others. The LHC experiments are lagging far behind in sophistication of NSF supercomputing use.
- The “hosted CE” technology was driven by the desire to integrate non-LHC clusters into OSG at minimal effort cost to the cluster owner. All the initial deployments are integrating clusters with no LHC affiliation. Recently, the CMS experiment has taken notice, and is expressing an interest in using this technology to integrate institutional clusters at CMS institutions. An initial presentation by the University of Chicago members of the OSG User Support team at the CMS Tier-3 meeting was organized in May, 2017, and the University of Colorado Boulder was identified as potential institution interested in integrating their institutional cluster into OSG in this way.
- Rucio as a data management infrastructure was developed by ATLAS, and has been talked about but not acted upon as potential replacement of the aging PhEDEx infrastructure in CMS for a couple of years. In contrast, the OSG User Support group helped the XENON1T collaboration to adopt this software for their production use. OSG thus showed a proof of principle that Rucio can be successfully run outside the ATLAS context with very modest human effort. It is expected that the OSG experience will influence the CMS evaluation of Rucio.
- Finally, the Connect platform is primarily driven by the general open science community as it is the backbone of OSG-Connect. Both US ATLAS and US CMS have adopted this technology at some level. However, its continued evolution is clearly driven by the OSG User Support group and OSG-Connect.

Finally, OSG once again enabled a wide range of exciting science. Highlights include:

- LIGO detected their second and third gravitational waves. The first two were detected during their first science run with Advanced LIGO. The third and most recent detection was done in their second science run. All three are identified as black hole mergers.
- XENON1T produced their first science result, exceeding the world’s best sensitivity for dark matter direct detection across a wide mass range within their first 30 days of science quality data taking.
- The Alpha Magnetic Spectrometer (AMS) project presented an updated analysis of their positron energy spectrum. They have now enough statistics at high energies to see a clear indication of the kind of positron energy shape that one might expect from dark matter annihilation for a dark matter weakly interacting massive particle (WIMP) of around 1 TeV. Whether or not this is indeed due to dark matter annihilation remains to be seen.
- Last year, the Dark Energy Survey (DES) project published a discovery of a dwarf planet that is currently the second-most distant object known in our solar system. These techniques, along with opportunistic OSG resources, are also being used in the ongoing DES search for the hypothetical Planet Nine, and for its search for an optical counterpart to the three LIGO gravitational wave detections.
- Steffen Bass’s group presented a new way of analyzing heavy ion collision data from the Relativistic Heavy Ion Collider (RHIC) and the LHC at last year’s Quark Matter conference, the most important annual event for heavy ion physics. This new paradigm setting phenomenology depended crucially on processing on OSG.

- In addition, there are hundreds of results from ATLAS and CMS from Run 1 at 8 TeV, and Run 2 at 13 TeV.

We are, of course, very excited to see not just these seminal physics results but also a wide range of results from virtually all scientific domains enabled by DHTC on OSG. The next section is thus dedicated to discussion of some of the details across our major science stakeholders.

## 2 Science Enabled by OSG

### 2.1 ATLAS

The ATLAS collaboration, consisting of 189 institutes from 38 countries, completed construction of the ATLAS detector at the LHC, and began first colliding-beam data taking in late 2009. The 45 institutions of US ATLAS made major and unique contributions to the construction of the ATLAS detector, provided critical support for the ATLAS computing and software program and detector operations, and contributed significantly to physics analysis, results, and papers published.

Experience gained during the first several years of ATLAS data taking has given us confidence that the grid-based computing model provides sufficient flexibility to process, reprocess, distill, disseminate, and analyze ATLAS data in a way that utilizes both computing and manpower resources efficiently. In an era where budgets for maintaining dedicated data centers are flat or falling, substantial use of resources outside of the traditional grid infrastructure such as commercial clouds, campus clusters, and supercomputers is becoming routine.

The computing facilities in the US are based on the OSG middleware fabric of services. The Tier-1 center at Brookhaven National Laboratory (BNL) and the five Tier-2 centers located at nine universities (Boston University, Harvard University, Indiana University, Michigan State University, University of Chicago, University of Illinois in Urbana Champaign, University of Michigan, University of Oklahoma, and University of Texas at Arlington) and at SLAC have contributed to the worldwide computing effort at the 28% level (near the level expected by sharing agreements). Time-critical reprocessing tasks were completed at the Tier-1 center within the foreseen time limits, while the Tier-2 centers were widely used for centrally managed production and user analysis.

A large fraction (~60%) of the available CPU resources available to the ATLAS collaboration at the Tier-1 and the Tier-2 centers is used for simulated event production, although the fraction of analysis jobs on the facilities has been increasing. The ATLAS simulation requirements are completely driven by the physics community in terms of analysis needs and corresponding physics goals.

The primary focus for ATLAS in 2016 has been on the analysis of the 13 TeV collision data collected during Run 2. In 2016, The LHC delivered  $\sim 40 \text{ fb}^{-1}$  of integrated luminosity, of which  $36 \text{ fb}^{-1}$  was collected by the ATLAS experiment and used for analysis. In 2016, there were 151 papers published in peer-reviewed journals with a large number of Run 2 analyses in the final stage of formal collaboration review.

The OSG has enabled timely dissemination of the vast body of physics results from ATLAS, including discovery of a Higgs boson, searches for new phenomena, and precision measurement of Standard Model processes. The ATLAS collaboration presented many 13 TeV results at number international and regional conferences. The most exciting were searches for new phenomena which matched or exceeded the Run-1 sensitivity, including searches for strongly produced supersymmetry (SUSY) and new resonances in dileptons, dijets, and dibosons (including those involving the Higgs boson).

Many of the published analyses involve measurements, most of which were not evaluated in detail prior to the arrival of data. These analyses are critical to our understanding of the Standard Model at 7, 8, and 13 TeV center-of-mass energies, and are also key ingredients to tuning and validating the existing Monte Carlo (MC) generators so that they can reliably be used for background estimates in search analyses. The search analyses rely heavily on very large background samples, with higher equivalent luminosity than the data samples and very precise modeling. Although data-driven techniques are used wherever possible, in the end, these techniques are most often used to normalize the MC background samples, but the shape

determinations in multi-dimensional spaces require pure signal samples that do not exist in the data. The statistical precision of the background estimates needs to be significantly better than that of the data samples themselves, in order to take maximum advantage of the data. All of this adds up to a large need for high quality MC samples. There would have been a significant impact to physics if ATLAS would not have been able to take advantage of services and the amount of resources as they are provided through OSG in the US and sites in other regions contributing to ATLAS computing.

ATLAS decided to dedicate significant effort to using their best understanding of how Higgs, SUSY, and Exotics analyses are being done today in order to predict how well ATLAS could do with  $300 \text{ fb}^{-1}$  of 14 TeV data, as well as  $3000 \text{ fb}^{-1}$  of data. These studies were a critical input to the European Strategy and US Snowmass processes, so ATLAS could provide a forecast of their physics reach for the High Luminosity Large Hadron Collider (HL-LHC) based on their best knowledge today. This work was done with very simple parameterized simulations of the detector response, tuned against the full simulation results. However, they required generating hundreds of millions of events at the generator level in order to properly estimate background levels in these searches in a new energy regime. This is important work that needs to continue in view of the design optimization of a HL-LHC detector upgrade.

To further improve efficient usage of resources, ATLAS has invested significant effort in innovative approaches to simulation, which is also a current area of active development. One relies on large samples of “zero bias” data acquired during data taking in 2012, which can then be merged with precise simulations of high-pT physics signal events, to provide a very accurate and efficient simulation of the ATLAS performance at high levels of pileup. The other relies on an advanced framework (the Integrated Simulation Framework) that provides the ability to use different levels of accuracy in simulating different particles in a single event. For example, full GEANT simulation can be used for the critical simulation of the leptons in an event, while simpler models of the calorimeter response can be used to simulate the impact of pileup events. Both of these approaches require considerable validation against the current 13 TeV and data samples, effectively generating large parallel samples of MC events using these new tools. Again, without the OSG fabric of services and resources at least at the present level, this key validation work would have had to be reduced in priority compared to the more urgent analysis of the 13 TeV data for publications.

Figure 6 shows the breakdown of the CPU consumption by site for US ATLAS Tier-1 and Tier-2 centers. Three of the US ATLAS centers were in the top ten ATLAS federations and all US centers were in the top 16 ATLAS-wide. Figure 7 shows the CPU consumption in the US cloud as compared with the rest of ATLAS which shows that 28% of the ATLAS processing in 2016 was performed by US ATLAS centers.

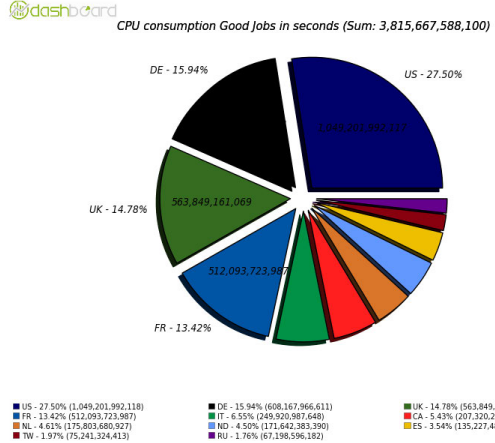


Figure 6: CPU contribution of US ATLAS sites for 2016

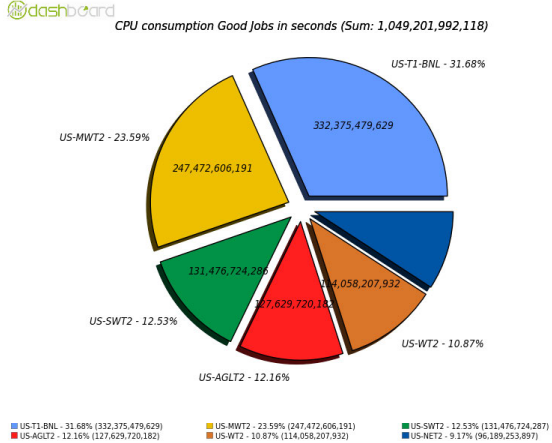


Figure 7: US ATLAS CPU contribution vs. others for 2016

Moving from the computational side to data storage and data access, US ATLAS has added the capability of direct access to data that is not available locally, meaning rather than requiring a process to wait until a programmatic replication of a dataset is completed the process is using a mechanism that allows to transparently discover the location of the needed data and access it over the Wide Area Network (WAN). US ATLAS is currently using XRootD at both the individual site level and the US ATLAS computing facility level and is working with OSG on a strategy for distributed XRootD caches. Tier-2 sites at SLAC and University of Texas at Arlington use XRootD as their baseline storage system, while the Tier-1 at BNL, University of Chicago, and University of Michigan are using XRootD as an interface system on top of their dCache-managed storage to serve user analysis activities. The sites each have between 3 PB and 12 PB of usable disk storage installed and serve heavy user analysis activities.

US ATLAS has deployed a Federated ATLAS XRootD system (FAX) aimed at providing direct data access over the WAN. The system allows users to access any data file in the federation via its global unique file name using the XRoot protocol. FAX is implemented via a global XRootD redirector at BNL and some regional redirectors deployed at Tier-2 sites. In addition to Tier-1 and Tier-2 sites, Tier 3 sites are important members of this federation because quite often, “hot” user analysis data are initially produced at Tier-3 institutions.

US ATLAS (contributing to ATLAS as a whole) relies extensively on services and software provided by OSG, as well as on processes and support systems that have been developed and implemented by OSG. OSG is essential for the operation of the worldwide-distributed ATLAS computing facility and the OSG efforts have aided the integration with WLCG partners in Europe and Asia. The derived components and procedures are the basis for support and operation covering the interoperation between OSG, EGI, and other grid sites relevant to ATLAS data analysis. OSG provides software components that are interoperable with European ATLAS grid sites, including selected components from the gLite middleware stack such as client utilities.

In addition to the services and operations mentioned above, US ATLAS has also benefited from activities with OSG in the areas of network monitoring, development of the next generation Computing Element, Grid User Mapping Service (GUMS), OSG architecture, native packaging, and configuration

management. US ATLAS is also participating in the OSG campus grids and inter-campus bridging efforts through the OSG Campus Infrastructures Community, and contributes to the pool of opportunistic resources in OSG in support of the GLOW, HCC, Engage, UCSD, UC3, and OSG virtual organizations, as well the larger community of users which access US ATLAS resources via the OSG-XSEDE Glide-in service.

Substantial effort in US ATLAS computing during 2016 has been put into developing ways to best provide access to resources beyond the boundaries of the Tier-1 and Tier-2 facilities, including US Tier-3 (institutional) computing, campus clusters, commercial clouds, and leadership-class facilities (supercomputers) in preparation for the LHC Run 2. A key part of this thrust is ATLAS Connect service. ATLAS Connect is a set of computing services designed to augment existing tools and resources used by the US ATLAS physics community, focusing on batch-like analysis processing familiar to Tier-3 users. It draws the majority of its functionality from the OSG Connect environment, which is already quite mature as a means of connecting data and CPU cycles to scientific applications. A single sign-on service provides direct institutional and working group access to the US ATLAS Computing Facility, potentially using your campus network identity if your institution participates in the InCommon identity federation. A login host allows HTCondor job submission to the Midwest Tier-2 Center, the Tier-3 center at Fresno State University, the University of Chicago Computing Cooperative campus grid, and others. The Remote Cluster Connect Factory (RCCF) allows a local cluster, such as a Tier-3 cluster managed by HTCondor, to be logically extended to use Tier-1, Tier-2, campus grids, or Amazon cloud resources using HTCondor flocking mechanisms. As an example, ATLAS Connect is currently being used as a vector for PanDA jobs in the Stampede supercomputer at Texas Advanced Computing Center (TACC). Additionally, ATLAS Connect has a storage service called FAXBox for staging user job input and output datasets.

Over the last year, the RHIC and ATLAS Computing Facility (RACF) at Brookhaven National Laboratory has been collaborating with Amazon on a pilot project to overcome challenges in utilizing Amazon's Elastic Compute Cloud (EC2) service, and move the usage of the Amazon Web Services (AWS) and the EC2 Spot market from theoretical possibility to a practical, production-grade, 100,000-core platform for doing science.

## 2.2 CMS

The scientific research performed by collaborators in the Compact Muon Solenoid (CMS) experiment at CERN's Large Hadron Collider (LHC) has captivated the interest of the general public around the world, and many of the results have been powered by the OSG. CMS is a world-wide collaboration of nearly 3,000 physicists working in 198 institutes in 45 countries. The approximately 700 signing authors from the United States make up about 30% of the collaboration, coming from 51 universities and federal labs.

Run 2 of the LHC started in 2015, with a beam energy of 6.5 TeV. The resulting proton collisions, with a center-of-mass energy of 13 TeV, have the highest energy ever achieved in the laboratory. This gives the experiment the ability to discover new massive particles that were not accessible during previous collider runs. Theoretical physics gives very strong motivations for the existence of such particles that should be observed with the new data. Indeed, should they not be observed, the paradigms that have successfully described particle physics for decades will face significant challenges.

After a disappointing 2015, in which the LHC collision rate was smaller than hoped for and the CMS detector had a number of operational problems, 2016 turned out to be a banner year for both the accelerator and detector. The LHC delivered  $41.1 \text{ fb}^{-1}$  of proton collision data. This was a factor of ten more than was delivered in 2015, and in fact more data than delivered in all previous LHC runs combined. It was also 60% more data than was originally anticipated, which led to high demand for computing resources. CMS was able to use  $36.1 \text{ fb}^{-1}$  for physics measurements. The experiment expects

to receive similar amounts of data in both 2017 and 2018, which will provide many opportunities for discovery, but will also require steadily increasing amount of computing power to store and analyze the data.

The physics output of the experiment continues to be quite strong. The CMS Collaboration submitted 107 papers for publication in calendar year 2016. 36 of these papers are based on the Run 2 dataset, while the others are based on the earlier Run 1 in 2010–2012, when the collision energy was 8 TeV. The physics papers cover a wide range of topics. These included searches for supersymmetry in a wide range of experimental signatures, for new resonances decaying to pairs of different species of particles, and for more exotic phenomena such as heavy stable charged particles, leptoquarks, dark matter, and quantum black holes. No new physics was observed, but significant limits were set on many models. In addition, there have been many studies of known particles, in particular the Higgs boson, first observed in 2012. All measurements so far of the Higgs indicate that it is the particle that is expected in the standard model. The doubling of the 13 TeV dataset expected in 2017 gives great hope for new knowledge and discoveries soon.

The development of these physics results relies on tremendous computing resources that are used to process and store recorded data, and to run the simulations of physics processes and detector response that are needed to understand the recorded data. When the experiment is operating, it produces 1–2 PB of data per month. The LHC experiments have deployed a world-wide infrastructure of computing sites to perform all of the computing tasks. The infrastructure is tiered, with sites at each tier having specific computing responsibilities, and a configuration that is matched to those responsibilities. In the US, the DOE and NSF support the operation of the Tier-1 and Tier-2 centers. All of those US centers are members of the OSG, which provides the middleware that allows CMS to use the distributed centers as an integrated high-throughput infrastructure for data processing and storage.

The US CMS facilities include the Tier-1 center at Fermi National Accelerator Laboratory (Fermilab) and the seven Tier-2 centers at seven universities (California Institute of Technology, University of Florida, Massachusetts Institute of Technology, University of Nebraska–Lincoln, Purdue University, University of California San Diego, and University of Wisconsin–Madison). In total, these centers provide about 79,000 batch slots, 44 PB of disk space and 40 PB of tape library space. (This does not include the site at Vanderbilt University, which is funded separately by the DOE Nuclear Physics program.) This is about 40% of the total computing resources for the CMS experiment. At such a large fraction, it is safe to say that the experiment’s scientific productivity depends strongly on these computing sites. Because all the sites are part of the OSG, these resources are also available for opportunistic use by other OSG virtual organizations. About 16% of the processing time was used by other VOs, with the OSG VO for new OSG users using the largest amount of that resource (11% of the 16%).

The US sites have been excellent performers. Figure 8 shows the fractional contribution of CPU hours used in successful jobs at all Tier-2 centers throughout CMS during 2016. As can be seen, the US sites provided about 45% of these processing resources, with each site among the top performers. This demonstrates the impressive impact that the OSG has had on the productivity of the CMS experiment.

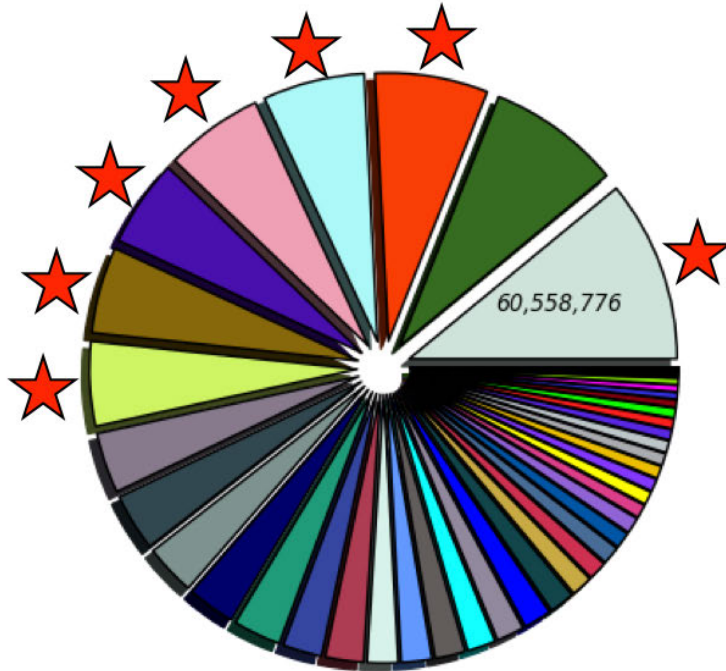


Figure 8: Fractional contributions of processing time in successful jobs by all CMS Tier-2 facilities; the seven US CMS sites are indicated with red stars

The CMS computing infrastructure also includes Tier-3 facilities that are owned and operated by collaborating institutions. Many university groups rely on these computing clusters to carry out their local data analysis projects. About fifteen Tier-3 sites have joined the OSG. In doing so, CMS as a whole, beyond the local groups, can make opportunistic use of these facilities, as can other OSG VOs at lower priority. These sites can also be considered “beachheads” for the OSG as it works with university campuses around the country to broaden participation in high-throughput computing.

The OSG provides tremendous value to US CMS through the critical services it provides to the experiment. OSG provides infrastructure software maintenance and integration, through its packaging of all of the components that make up the OSG software releases. This software forms the backbone of the US CMS distributed high-throughput computing efforts. OSG distributes the CMS software to US CMS sites through its CernVM File System (CVMFS) service. It handles registration, monitoring and accounting activities for sites, allowing CMS to track usage of OSG resources and then report it to the Worldwide LHC Computing Grid (WLCG). CMS has taken great advantage of the job submission infrastructure operated by OSG; CMS has chosen GlideinWMS as its workflow management system for all of its workflows, and OSG operates the pilot factories that facilitate job submission to CMS sites. The CMS Connect login hosts for some Tier-3 users are operated by OSG. OSG operates the cybersecurity infrastructure necessary for authorization on the grid. The OSG Grid Operations Center (GOC) provides support for individual sites, operates a ticketing system to facilitate that, and handles security advisories and wide-area networking issues for sites. Finally, OSG provides representation to the WLCG, cybersecurity communities and national and international scientific network partners on behalf of US CMS. A recent study of the value provided by OSG to US CMS has estimated that approximately 9.4 FTE are required to provide all of these critical services.

OSG has partnered with US CMS and international CMS as a whole in a number of development efforts that have benefitted the experiment. For instance, OSG has worked with CMS and the HTCondor project to improve the scalability and robustness of the HTCondor batch scheduling system, which has demonstrated the operation of over 240,000 CPU cores in a single pool. All US CMS sites have adopted the HTCondor-CE, developed in part by OSG, as the job submission interface for sites. OSG has also been working actively with US CMS on a drastic simplification of the infrastructure software. Many elements of the OSG software stack have now been retired and replaced (such as BDII, BeStMan, SRM, GRAM, and Gratia), while others have these transitions planned for the future (gLExec, VOMS Admin, GUMS, RSV). Over time, these efforts have allowed us to reduce the needed staffing levels at the US CMS Tier-2 sites to run OSG services, freeing up effort for other operations and development projects within CMS. OSG has been a long-time partner in the development of XRootD-based data federations. The CMS data federation, known as “Any Data, Anytime, Anywhere”, has provided significant new flexibility to CMS operations, as it allows for easier distribution of workflows across many sites, and also greatly simplifies data discovery and access issues for users who are performing the physics measurements. This technology is now becoming a core service of OSG for data storage and access, thanks to the deployment of StashCache at larger OSG sites which gives access to data caches serving many VOs through XRootD interfaces. In this way, CMS has seeded support for the work of a broader set of scientific communities.

All of these efforts have enabled the recent scientific success of the CMS experiment. Looking ahead, the entire particle physics community remains excited about the prospects for discovery. The LHC has a 20-year program of physics ahead, and only 2% of the total expected integrated luminosity has been collected so far. CERN and CMS are now planning for the HL-LHC, which will begin operation in 2026 with beam intensities that will be more than double what they are now. There are still significant uncertainties in the estimates of computing resources needed for HL-LHC data processing, storage and analysis, but the demands could easily be a factor of ten to one hundred from where we are now, with approximately flat budgets anticipated. New technologies and new computing models will have to be brought to bear on the problem. US CMS looks forward to partnering with OSG to meet these future challenges in our exploration of the highest energy scales ever realized in the laboratory.

### 2.3 FabrIc for Frontier Experiments

The FabrIc for Frontier Experiments (FIFE) is an initiative at Fermilab to create and maintain a modular, robust set of common software tools for non-LHC experiments, as well as to bring experiments and computing professionals together to develop a computing model for these experiments. Generally speaking, the FIFE experiments are either probing neutrino physics or precision muon physics, although some experiments in dark matter detection and astrophysics do use some of the FIFE toolset. There are FIFE experiments spanning the entire range of experiment lifecycle, from the recently-completed MINOS+ to the still under-construction muon g-2 and Mu2e experiments.

Most of the FIFE experiments are at least an order of magnitude smaller than LHC collaborations, and the Fermilab General Purpose Grid cluster (GPGGrid) can satisfy most of their computational needs. Opportunistic OSG resources are however a critical part of the FIFE strategy to satisfy demand during peak periods, and to meet the project long-term growth in demand as experiments like g-2 transition from construction to operations. OSG resources were indispensable in providing enough resources for all FIFE experiments to meet their conference result and publication targets in 2016. Taken together the FIFE experiments ran on 27 different sites in five different countries during 2016. They consumed over 26 million wall hours outside of the GPGGrid cluster and commercial clouds, as shown in Figure 9. Below we discuss some recent progress from a selection of the FIFE experiments.

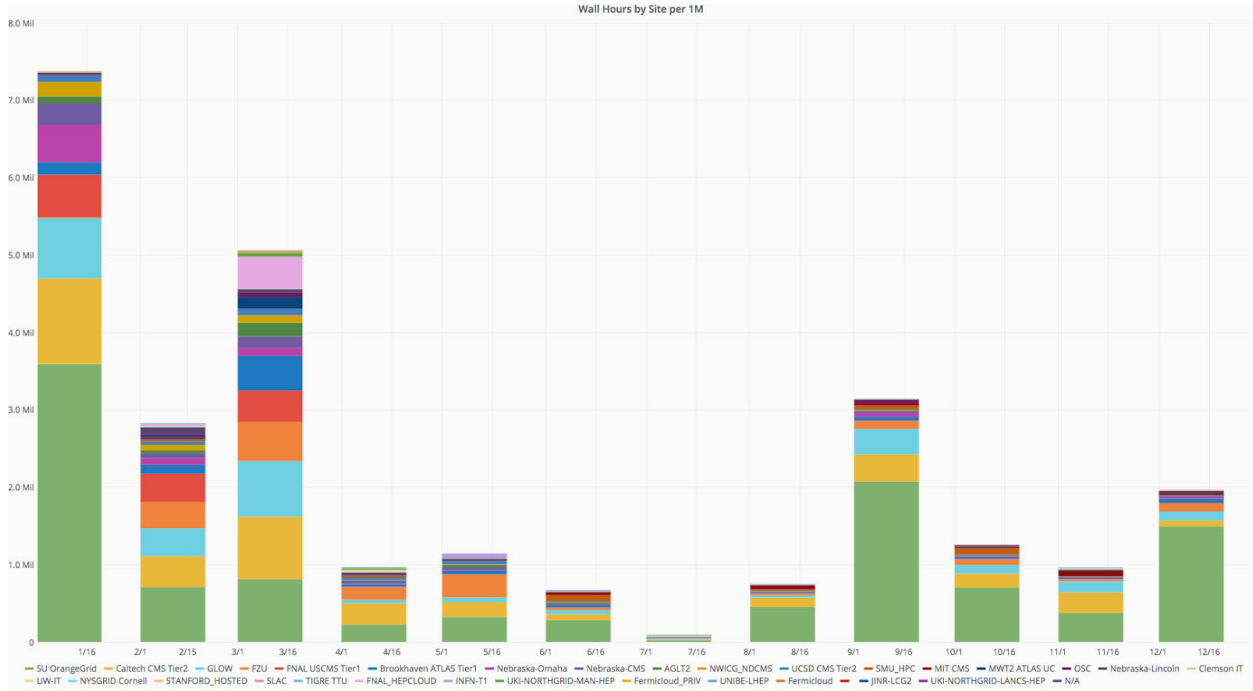


Figure 9: Opportunistic wall hours used by FIFE experiments during 2016 by remote site

### 2.3.1 NOvA

The NOvA experiment is currently the flagship neutrino experiment at Fermilab with the goal of precision measurements of neutrino oscillations, determination of the neutrino mass hierarchy, and sensitivity to the phase of charge-parity violation in neutrino oscillations. The NOvA experiment consists of a near detector at Fermilab and a far detector located more than 500 miles away in northern Minnesota. The detectors study neutrinos produced by the Fermilab Neutrino Main Injector (NuMI) beamline.

NOvA has published results on electron neutrino disappearance, muon neutrino appearance, and a measurement of the neutrino mixing angle  $\theta_{23}$ . Opportunistic OSG resources were critical to completing the analyses in time for the Neutrino 2016 conference. In the past year, they have made extensive use of opportunistic computing on the OSG, using over 9 million CPU hours. NOvA also continues to make use of a dedicated high-performance computing (HPC) allocation at the Ohio Supercomputing Center. Due to past work by OSG staff on the job submission infrastructure, NOvA is able to seamlessly submit jobs to dedicated Fermilab resources, opportunistic OSG resources, and their HPC allocations.

NOvA has also been one of the early users of StashCache. Several of their simulation workflows require delivering large auxiliary files (hundreds of MB each) to each job, but each job can take a different subset of these files. That means that the hit rate on any local worker node cache (putting these files in CVMFS for example) will be very low across jobs. StashCache solves this problem by offering a POSIX access method to the end user, while actual file access is done behind the scenes via XRootD sent to one of several regional caches around the country. The XRootD redirection can also be done to directly access an experiment's dedicated storage elements at certain sites.

### 2.3.2 MicroBooNE

MicroBooNE Experiment is a liquid argon time projection chamber (LArTPC) that is part of the Fermilab short-baseline neutrino program. It has been taking data since October, 2015, and presented its first results in 2016.

MicroBooNE had certain parts of its detector simulation that required up to 7 GB of memory, quite a bit more than the 2 GB per CPU offered by most sites. While that requirement can be met on Fermilab's GPGrid through partitionable slots, early projections were that GPGrid alone would not have been able to meet MicroBooNE's schedule. Fortunately, OSG was able to step in and provide some high-memory job slots through remote sites, including three European sites that were new to supporting FIFE experiments: University of Bern, University of Lancaster, and University of Manchester. All three sites were able to be ramped up and into full production for MicroBooNE within a few weeks, with Lancaster and Manchester taking only one week. These sites, along with Hyak at the University of Washington, provided approximately 107,000 CPU hours to MicroBooNE for their high-memory simulation jobs during the critical phases of conference result preparation beginning in March 2016, and concluding with the first results presented at the Neutrino 2016 conference in July. Figure 10 shows the breakdown of CPU hours for MicroBooNE at the University of Manchester (green), University of Bern (yellow), and University of Washington (blue) over this time period. These sites in particular provided critical support to MicroBooNE for running memory-intensive simulations.

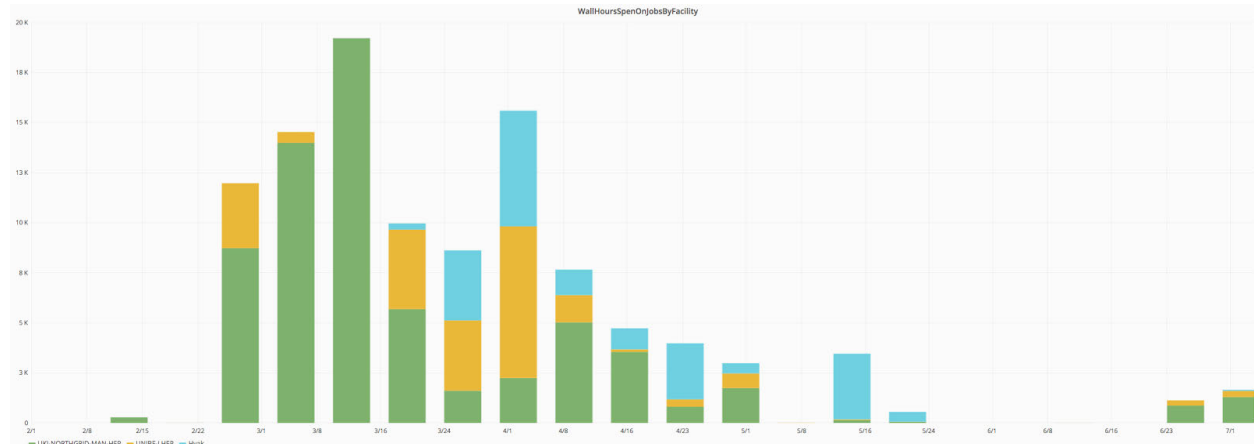


Figure 10: Wall hours for the MicroBooNE experiment from February through July, 2016

### 2.3.3 MINOS+

The Main Injector Neutrino OSCillation experiment (MINOS) is designed to study neutrino oscillations using a neutrino beam from Fermilab to the Soudan Mine in Minnesota. MINOS+ was an extension of the MINOS experiment, and completed data taking in 2016. MINOS/MINOS+ produced several recent results on topics such as neutrino properties, limits on sterile neutrino oscillations, and limits on large extra dimensions.

A MINOS+ collaborator at the University of Texas obtained an allocation on Stampede cluster at the Texas Advanced Computing Center. By setting things up so that the allocation was also available as an XSEDE allocation, he was able to get access to it via the standard OSG GlideinWMS factories. In turn, that meant there was no additional work that had to be done in terms of job submission infrastructure, and it was also easy to share the allocation with other MINOS members as needed.

### 2.3.4 Mu2e

The Mu2e experiment is designed to search for lepton flavor violation via the decay of a muon to an electron. Data taking is currently expected to commence in approximately 2022, but in 2016 Mu2e faced a DOE Critical Decision 3 (CD-3) review. The experiment needed to perform an extensive computing campaign to optimize the beam and detector designs. The computing resources required for the campaign were well beyond Mu2e's resources at Fermilab, and Mu2e ended up began a successful effort to run this campaign using primarily opportunistic OSG resources, becoming the fourth-largest VO to consume resources in 2015. These trends continued in 2016 with Mu2e consuming approximately 39 million CPU hours, of which over 18 million were on opportunistic sites on the OSG. The work paid off during the DOE review, with Mu2e being granted full CD-3 approval and being fully funded for the next phases of design and construction in FY17.

### 2.3.5 DUNE/protoDUNE

The Deep Underground Neutrino Experiment (DUNE) is a planned neutrino beam experiment that will become the centerpiece of the Fermilab neutrino physics program. There will be a near detector at Fermilab and a far detector at the Sanford Underground Research Laboratory in South Dakota. Current plans call for construction and data-taking to commence in 2018 and after 2023, respectively. In the near term, a prototype experiment called protoDUNE is under construction and will begin taking data in 2018. protoDUNE will serve as a test bed for several technologies under consideration for use in the final DUNE apparatus.

During 2016, DUNE made significant strides in all phases of the program, including attracting new international collaborators, refining its computing model, and running a large amount of studies for beam optimization.

Several laboratories and universities outside of the US wish to provide computing resources to DUNE as part of their overall contributions to the experiment. Some of these sites already have experience supporting LHC experiments. Even so, different sites will have their own choices of local batch systems and scheduling policies, and transparently integrating these systems in these early stages of the experiment can be extremely challenging. Additionally, with protoDUNE being located at CERN, it will be necessary to integrate CERN's computing infrastructure into a cohesive framework.

The OSG infrastructure naturally lends itself to such an environment. By building on the successful experiences of NOvA and MicroBooNE in commissioning European sites, it should be very easy for new sites to begin supporting DUNE computing. Indeed, this experience had already paid off in early 2017, with Imperial College London and Institute of Physics (FZU) in Prague now supporting DUNE jobs submitted through the Fermilab GlideinWMS frontend. In the case of FZU, which was already running NOvA jobs, DUNE support was in full production in less than one day.

### 2.3.6 SeaQuest

SeaQuest is a fixed-target experiment at Fermilab that uses Drell-Yan processes to study nuclear structure. Prior to 2016, SeaQuest had done only a single brief period of opportunistic OSG job submission. During 2016 they were able to run nearly 600,000 opportunistic hours across nine different OSG sites. While this is a small total relative to some of the larger VOs on OSG, it does represent nearly 25% of SeaQuest's total wall hours in 2016, demonstrating that OSG can provide a significant boost to VOs of all sizes.

## 2.4 Nuclear Physics

The past year has seen further growth of OSG use for nuclear physics beyond the traditional Heavy Ion communities at RHIC and the LHC. The following are particularly noteworthy example stories.

The Solenoidal Tracker at RHIC (STAR) collaboration has continued to make use of the OSG fabric to run their simulations, and has also recently shifted to perform their data production campaign on the grid. The addition of the Dubna site (a 1,000-core pledge at first) has recently showed an end-to-end workflow efficiency as high as 97% with the result brought back to the central Tier-0 center at BNL. A noticeable activity however has been for STAR to shift their attention to the use of HPC and especially, the use of NERSC/Cori resources. This work was presented at the Computing in High Energy and Nuclear Physics (CHEP) 2016 conference<sup>1</sup> where not only a 99% CPU utilization efficiency was showed but an end-to-end workflow efficiency in excess of 95%. While simulation processing on HPC was attempted by a few experiments before, this first in the field real data reconstruction was enabled thanks to the reliable OSG software stack. As a result, the STAR experiment has been awarded an allocation of 25 million hours at NERSC/Cori, the totality of which will be processed via an OSG interface and steered from BNL. The use of remote resources by the experiment, enabled by the OSG, represents a boost of 33% of its local resources. The STAR experiment has also approached the high-energy physics community to define a program of work for future years where HPC resources would be seamlessly integrated to the OSG fabric and the experiences from all sides integrated into a single vision of a super-facility empowered by the OSG.

Along with STAR, another long-time user of OSG resources — A Large Ion Collider Experiment (ALICE) — has continued to run at about 1 million hours per year. Also, the OSG has seen new activity from RHIC and BNL's Electron-Ion Collider (EIC). First, the sPHENIX collaboration, having their science case endorsed through DOE review, has made use of OSG resources at the level of 6 million hours to perform further detector research and development simulations. 5 trillion collision events were simulated with a reported 99% efficiency. The EIC research and development group has made modest use of OSG resources so far, but have started to investigate the opportunistic use of cycles. This is in anticipation that many future experiments (in planning, but not yet funded by the agencies) will have limited computing resources of their own. Once again, the resources offered by the OSG offered a unique opportunity to speed up the delivery of a scientific case for an EIC by allowing complex and computational challenging simulations to be performed.

Professor Steffen Bass (Duke University) has further expanded his group's use of OSG. At 15 million hours, he is the third largest single-PI user on OSG within the last year<sup>2</sup>. Unlike the nuclear experimental programs, the heavy ion theory community does not typically benefit from having dedicated resources, and the OSG appeared to be a superb opportunity for carrying an ambitious and challenging physics program as well as an attractive match for the way the community works. Focused on study of the formation and properties of quark-gluon plasma (QGP), this community has considerable computing requirements to perform 2D hydrodynamics as well as to move to 3D hydrodynamics, which would increase their computational needs by an order of magnitude while unfolding uncharted domain of science discovery to date. This work is estimated to require up to 1 billion CPU hours per year within 5 years.

OSG representatives attended the Thomas Jefferson National Accelerator Facility (JLab) workshop on the Future Trends in Nuclear Physics Computing (March 16–18, 2016) to discuss possible collaborations between OSG and JLab. As a result, the OSG User Support team held a workshop at JLab on May 17–19, 2017, that attracted 41 students and post-docs from 12 institutions engaged in science at JLab. Also, the OSG Technology Investigations team worked through the needs of GlueX for a production infrastructure to operate at scale on OSG. This led to a scalability evaluation of HTCondor file transfer as underpinning for the GlueX Monte Carlo production workflow. OSG demonstrated that HTCondor file transfer was

---

<sup>1</sup> <https://indico.cern.ch/event/505613/contributions/2227375/> “STAR Data Production at NERSC/Cori, an adaptable Docker container approach for HPC”

<sup>2</sup> <http://www.opensciencegrid.org/nuclear-physics-and-computer-science-meet-on-the-osg/>

sufficient for the task and helped JLab deploy a submission host that achieves the operational scale tested during this evaluation. This was completed in May, 2017. Ongoing projects with JLab include integration of multiple clusters at GlueX institutions into OSG for use by GlueX, adoption of Singularity by GlueX and JLab, and deployment of an XRootD data federation to simplify GlueX data access from GlueX institutional computing resources. We expect these ongoing projects to continue throughout 2017, and possibly into 2018 before they are all completed.

## 2.5 Laser Interferometer Gravitational-Wave Observatory (LIGO)

Following the groundbreaking detection of gravitational waves announced in early 2016, on June 16, 2016, LIGO scientists announced their second direct observation of gravitational waves from a pair of coalescing black holes. Gravitational waves are one of the newest and most exciting frontiers in physics and astronomy. LIGO is the world's leading facility with the goal of detecting gravitational waves from astrophysical sources. LIGO aims to test the General Theory of Relativity in the domain of highly nonlinear dynamic gravity and open a completely new observational window on the universe that fundamentally differs from that provided by electromagnetic or particle astronomy. Gravitational-wave observations will provide answers to some of the outstanding questions about the nature of gravity and the high-energy universe, including: (i) Do short hard gamma-ray bursts come from the merger of two neutron stars or the merger of a neutron star and a black hole? (ii) What causes the shock revival in the core-collapse of massive stars? (iii) What is the equation of state of matter at nuclear pressures and densities? (iv) What is the mass distribution of black holes in the universe and do they "have no hair"? (v) Are observed gravitational waves consistent with those predicted by General Relativity? Gravitational-wave observations are uniquely suited to explore these and many other outstanding questions in strong field gravity and high-energy astrophysics. Construction of the Advanced LIGO detectors is now complete and, when these detectors reach design sensitivity in approximately 2018, they will be an order of magnitude more sensitive than the first-generation detectors.

Compact binary coalescence (CBC) is the most promising source of gravitational waves for Advanced LIGO. The inspiral and merger of a binary containing stellar-mass compact objects (neutron stars and black holes) generates gravitational waves that sweep upward in frequency and amplitude through the sensitive band of Advanced LIGO. Compact binary coalescence searches with LIGO consist of four stages: (i) initial analysis of LIGO data to determine detector performance and tune the parameters of the search pipeline; (ii) full analysis of the data set with the final search parameters to detect signals and measure the false alarm rate of detection candidates; (iii) reanalyzing the data with the addition of simulated signals; and (iv) estimating the parameters of any detected signals.

The CBC workflow requires significant computing and data transfer resources. The runs done on OSG in 2016 required over 16 million CPU core-hours; approximately 15% (12%) of these hours utilized Comet and Stampede. The total volume of unique LIGO data analyzed was 10 TB but the workflow required over 1 PB of data to be read from storage. Up to 19,000 cores were used to support LIGO as shown in Figure 11; this resulted in a peak data transfer rate of approximately 10 Gbps. The graph below shows the CPU hours and per-site breakdown of LIGO usage in 2016.

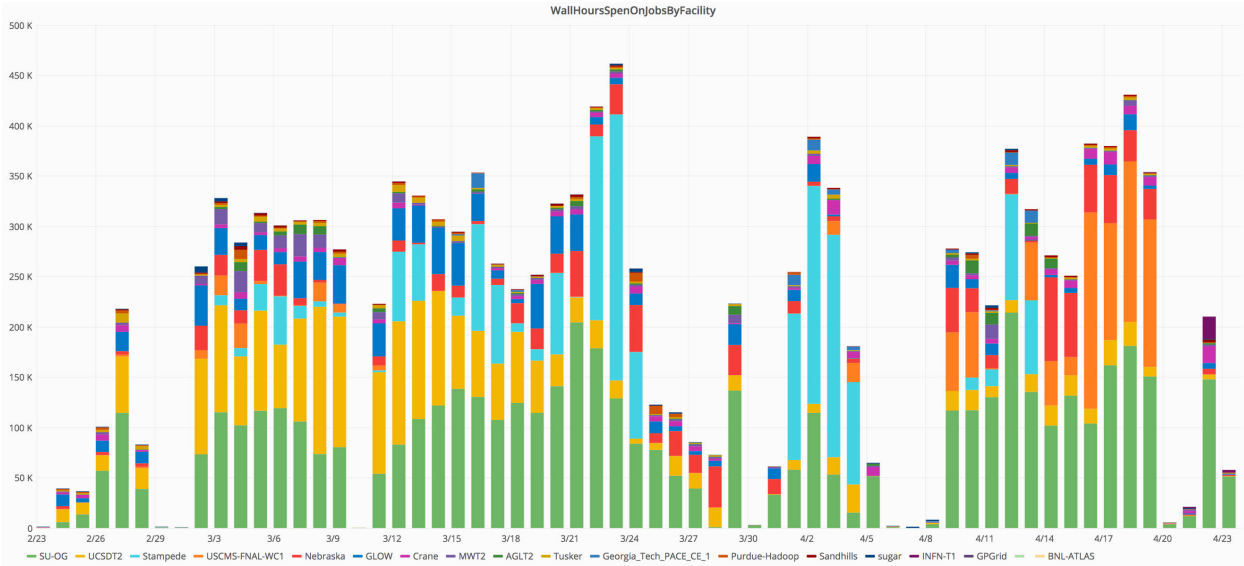


Figure 11: LIGO Usage of OSG

In 2017, LIGO plans to utilize the same approach to run the CBC workflow to analyze the Observation Run 2 data.

In addition to converting LIGO pipelines to run on the OSG, LIGO is integrating opportunistic computing resources from its collaborators by leveraging the OSG to provide the appropriate middleware to access these sites. The OSG has enabled LIGO to easily harness resources it was previously unable to use without major one-off systems integration effort customized to each site. The resources that LIGO has been able to efficiently use for the first time via OSG include Georgia Tech, OrangeGrid at Syracuse University, SciNet in Canada, and Virgo collaboration allocations at European data centers (e.g., CNAF, Lyon, Nikhef, Polgraw). Pilot efforts are underway to access Blue Waters at the National Center for Supercomputing Applications (NCSA) at the University of Illinois at Urbana-Champaign as well.

To run LIGO's CBC pipeline on the OSG, a few technical and organizational challenges had to be solved:

- **Help make the CBC pipeline portable.** The underlying scientific software, PyCBC, and the workflow management software, Pegasus, already have several considerations for portability. For the missing worker node software dependencies, such as GCC, we have provided LIGO with access to the OSG Application Software Installation Service (OASIS) service.
- **Making LIGO data available across the OSG.** LIGO has two types of data: calibration data (publicly accessible) and detector readouts (private). The calibration data is relatively small and read by each job, making it a perfect fit for OASIS. The detector data was staged to an opportunistic storage area at the US CMS Nebraska Tier-2 site using the LIGO data replicator. To access the data, LIGO jobs directly downloaded the files from the Nebraska GridFTP and/or XRootD servers. Access rates peaked at 10 Gbps, illustrating the utility of 100 Gbps WAN connectivity.
- **Getting LIGO access to OSG resources.** Working with the OSG User Support team, we contacted multiple sites to enable opportunistic access. Unlike many OSG VOs, the privacy concerns of LIGO data required us to manually verify there was a separate user account for LIGO jobs. In total, about 15 sites were configured for access.

- **Transparently allocating computing resources.** Each site that enabled LIGO access is unique; to keep the project manageable, they must be accessed in a similar manner. For this, we used GlideinWMS to build an HTCondor pool out of dedicated, OSG opportunistic, and XSEDE allocation-based resources (namely, Comet and Stampede). With the minimum number of changes outlined above, LIGO was able to perform their analysis with the same workflow management tool (Pegasus). To highlight the level of transparency of using OSG, we note runs were done by both professors and students.
- **Executing XSEDE allocations on XD resources via OSG.** LIGO provided an initial use case for incorporating the use of XSEDE Resource Allocations Committee (XRAC) allocations of XD resources (particularly, Stampede) into OSG resource provisioning. This started simply — hand-submitting individual batch jobs that unpacked to large 1024-core glide-ins and explicitly specifying a single XD project ID. By the end of the year, OSG incorporated this into our automated factory submissions, passing the XD project ID transparently across the infrastructure. This allows LIGO to use all their resources from a single job submission point at Syracuse University.

## 2.6 IceCube

IceCube is a neutrino detector built at the South Pole by instrumenting about a cubic kilometer of ice with 5,160 light sensors. The detector started taking data in 2006 and it is expected to operate for at least 20 years. It was designed and developed by an international collaboration that currently includes 300 people from 47 institutions in 12 countries that collectively participate in the research program.

IceCube’s discovery of an astrophysical neutrino flux in 2013 has confirmed cosmic neutrinos as essential astronomical messengers. IceCube is the first instrument that measures the properties of this astrophysical neutrino flux, and constrains its origin. The prospects for astronomy are extraordinary, with IceCube observations indicating a more prominent than anticipated role of proton acceleration relative to electrons. See *Neutrinos and cosmic rays observed by IceCube* (2017, the IceCube Collaboration) for an overview of recent findings from the analysis of IceCube data, and their implications on our understanding of cosmic rays.

IceCube uses a mixture of resources to run data processing, analysis and simulation jobs. A dedicated cluster at the University of Wisconsin–Madison serves as the collaboration main analysis facility, with about 7,500 CPU cores and 400 GPUs. This central facility only accounts for about 50% of the resources. Various mechanisms are then used to harness the power of a large and heterogeneous pool of distributed resources. All of these mechanisms make use of HTCondor, therefore presenting users a single consistent interface to all these resources. This setup is an excellent example of OSG’s mantra to submit locally, and run globally.

First, jobs can use HTCondor’s flocking mechanism to access HTCondor pools managed by various groups at Wisconsin. One of these pools, operated by the Center for High Throughput Computing (CHTC), is in turn part of the OSG GlideinWMS infrastructure and provides access to IceCube grid sites in Canada and Europe as well as to opportunistic OSG sites via the GLOW Virtual Organization. In 2016, IceCube used about 8 million CPU hours through the OSG GlideinWMS, and an additional 8 million CPU hours via direct HTCondor flocking to non-IceCube UW clusters.

Several of the IceCube collaborating institutions have access to local campus computing resources. However, many of these do not provide a grid interface but just local submission capabilities. In order to enable homogeneous and efficient access to these resources, IceCube has developed pyGlidein, a collection of python scripts designed to launch HTCondor glide-ins. The scripts help to shield the user

from the complexity of submitting to a collection of heterogeneous sites and make all IceCube resources look like a single large pool. pyGlidein is used to access dedicated IceCube sites in Canada, Europe, the US, and Japan.

In 2016, IceCube received an XSEDE allocation to run simulations in a number of GPU-capable supercomputers. This allocation also included 3.9 million CPU hours in the OSG, which was transparently added to the pool of available resources for IceCube simulations by means of the pyGlidein system.

The flexibility of the pyGlidein system has also enabled IceCube to implement fine-grained scheduling policies such as prioritization of specific groups within the collaboration in specific resources. This feature has been successfully implemented for accessing the large cluster operated by CHTC.

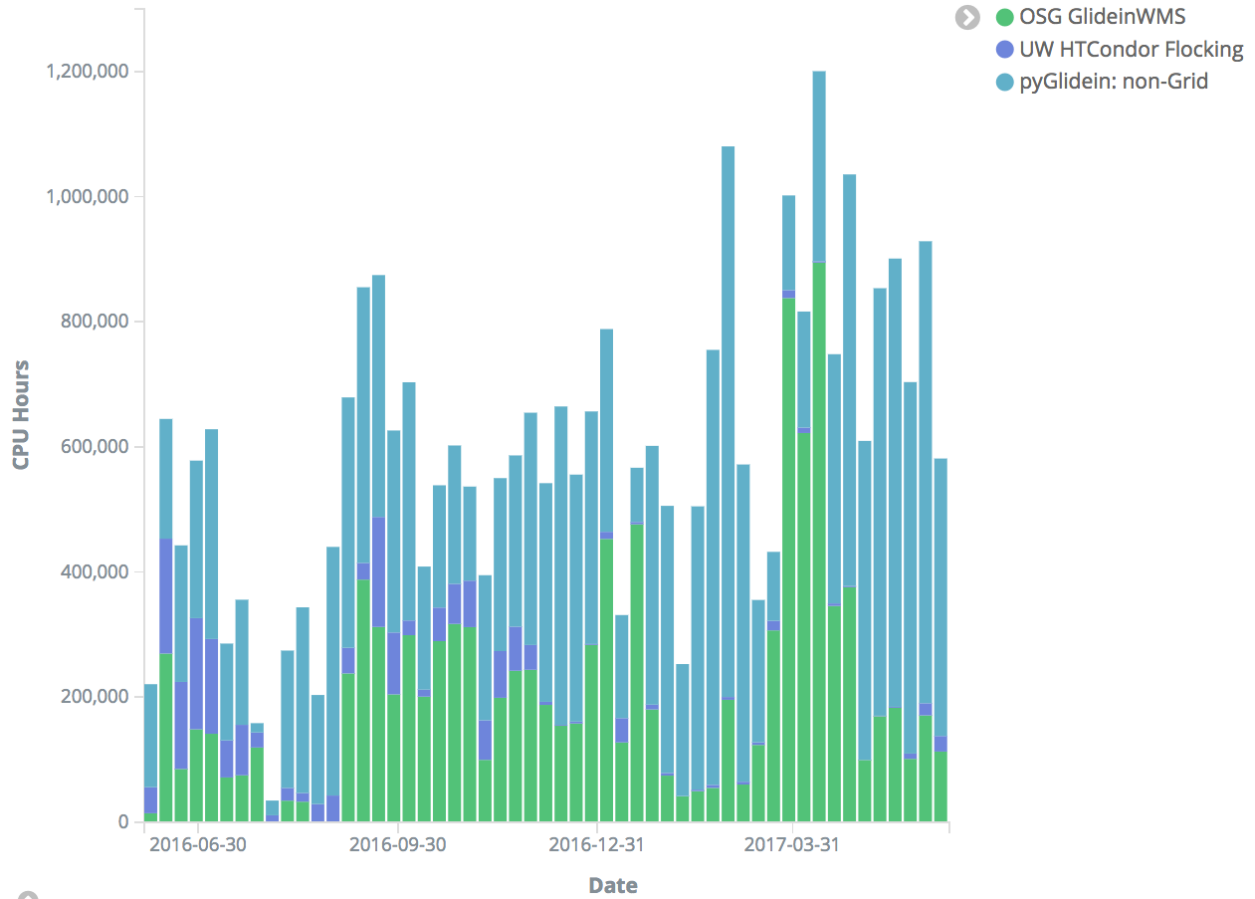


Figure 12: IceCube CPU hours per week by access method

Figure 12 shows the CPU hours used per week during the last year via the three different federation mechanisms: OSG GlideinWMS, pyGlidein, and HTCondor flocking.

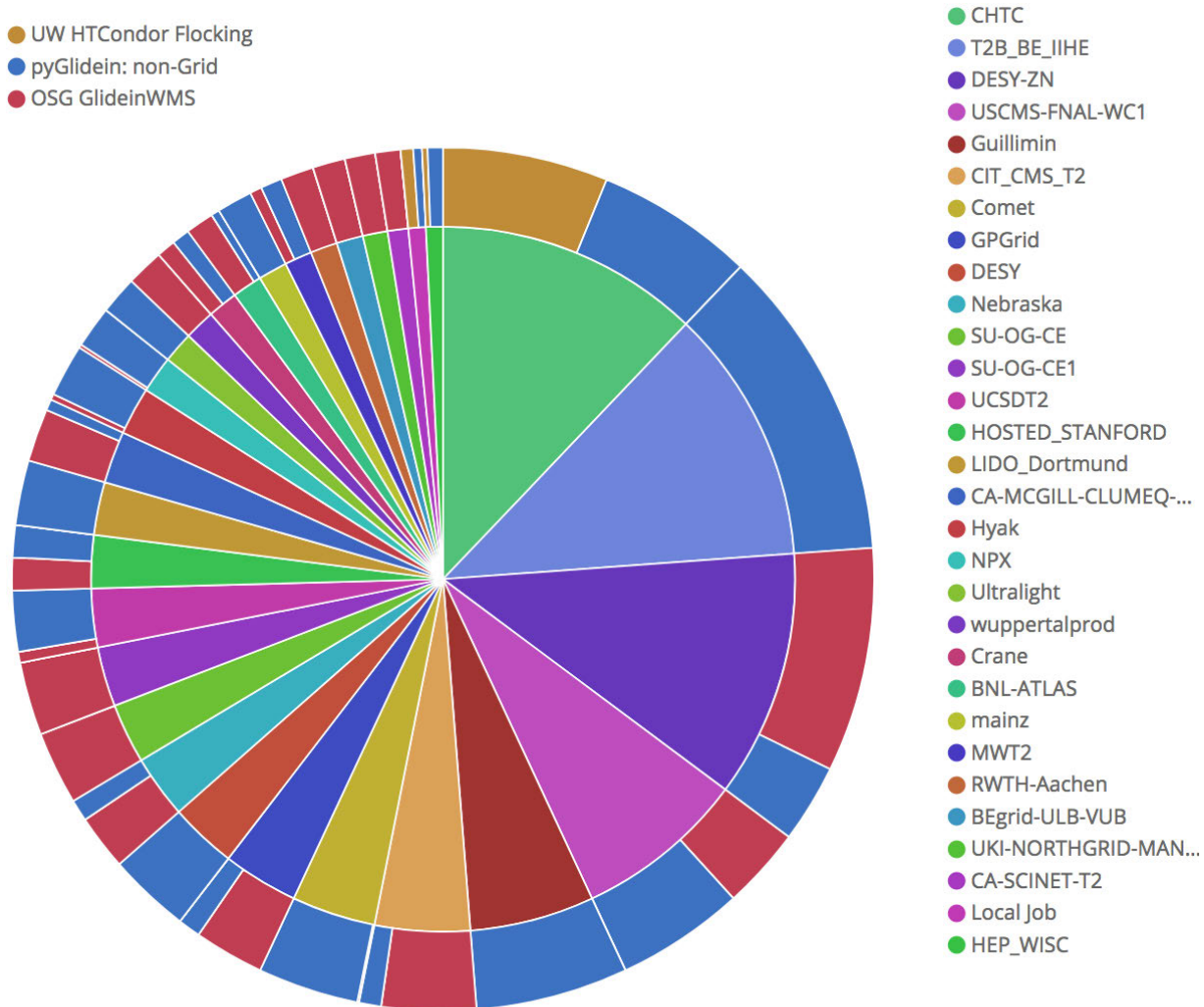


Figure 13: Distribution of IceCube CPU hours by site and access method

Figure 13 shows a pie chart distribution of the above CPU hours per site and per federation mechanism. This pie chart shows the power of DHTC in general, and OSG in particular:

- The largest single contribution accounts for only 20% of the total of more than 11 million hours.
- OSG enables IceCube to operate internationally, with very sizeable contributions from multiple locations in Germany (DESY, Aachen, Dortmund), Canada (McGill), Belgium (IIHE), and the UK. Some of these international contributions come from clusters that are not part of the LHC infrastructure. OSG is thus integrating internationally beyond just the LHC.
- OSG enables IceCube to operate transparently across XSEDE allocations, institutional collaborators worldwide, and opportunistic resources at both LHC sites as well as non-LHC sites. The XSEDE allocations span multiple XD resources.

## 2.7 Astronomy

In addition to LIGO and IceCube, the OSG provides critical support to a wide variety of experiments within the Cosmic Frontier. These include dark matter detection, dark energy studies, gamma ray astronomy, gravitational wave astronomy, and high-energy cosmic ray and neutrino studies. In this section, we highlight a few experiments and their achievements.

### 2.7.1 AMS

The Alpha Magnetic Spectrometer (AMS) is a particle physics experiment hosted on the International Space Station, designed to measure electrons, protons, and ions (e.g., iron and helium), along with, and importantly, their anti-particles. Its science goals include searches for cosmic anti-matter, dark matter annihilation, and precision cosmic ray measurements. From installation in 2011 through December 2016, AMS collected over 90 billion cosmic rays, 16.5 million electrons, 1.08 million positrons, 3.7 billion helium events, and even a handful of anti-helium events. They have seen several unexpected results in their data, notably a clear excess in the positron energy spectrum above 10 GeV, shown in Figure 14 (red indicates positron energy flux as a function of energy, green indicates the expected flux distribution from background collisions of cosmic rays and the interstellar medium, and dark red indicates the predicted flux for a physical model with a dark matter component). This is a very interesting and important result since some dark matter models predict such an excess. Other unexpected results include that the proton flux cannot be described by a simple power law function, as GWAS generally assumed, and that the proton spectral index appears to be momentum-dependent, again contrary to previous assumptions.

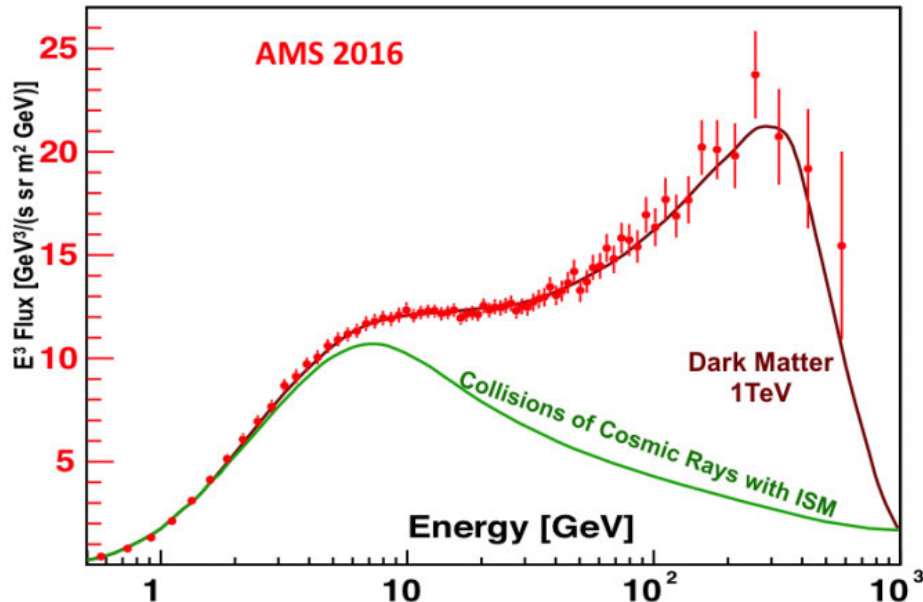


Figure 14: AMS positron energy flux

To meet the computing requirements of all of these results, AMS continued the successful use of OSG resources begun in 2015 and described in last year's OSG report. AMS has access to a wide variety of sites through a submission host at Massachusetts Institute of Technology (MIT), which also connects to non-OSG grid resources. During 2016, AMS used 20.7 million wall hours on OSG sites via its MIT submit host. These hours were important for calculating the p-value of their positron excess over the expected background, and for setting confidence limits on alternative explanations of their excess.

## 2.7.2 DES

The Dark Energy Survey is a multi-year experiment designed for high-precision cosmology using four main probes of dark energy: supernovae, galaxy clusters, baryon acoustic oscillations, and weak gravitational lensing measurements. It makes use of the Dark Energy Camera mounted on the 4m Blanco Telescope at the Cerro Tololo Inter-American Observatory in Chile. DES has a wide variety of computing resources available to it, and its primary connection to opportunistic OSG sites is currently through the same job submission infrastructure used by the FIFE experiments. In late 2015 and early 2016, DES was regularly using OSG sites to provide additional processing power to complete its search for an optical counterpart to the first LIGO gravitational wave event. Using the same techniques, DES has performed optical follow-up on two additional LIGO triggers.

The same techniques used to perform searches for optical counterparts to gravitational wave sources can also be applied to searches for transient and moving objects. Last year DES published a discovery of a dwarf planet that is currently the second-most distant object known in our solar system. These techniques, along with opportunistic OSG resources, are also being used in the ongoing DES search for the hypothetical Planet Nine. DES is also in the process of preparing additional analyses to run on OSG resources, including the opportunistic use of GPU clusters. StashCache, accessed via CVMFS, will also play an increased role within DES during 2017.

## 2.7.3 South Pole Telescope

The South Pole Telescope (SPT) project uses the cosmic microwave background (CMB) to uncover some of the most important features of our universe and the physics that govern it. The SPT is a 10m telescope located at the NSF's Amundsen-Scott South Pole station, the best site on Earth for microwave observations, and is optimized for sensitive, high-resolution measurements of the CMB. It is funded jointly by NSF and the Department of Energy (DOE).

Since the deployment of the SPT in 2007, the SPT team has completed two large surveys: 1) the 2500-square-degree SPT-SZ survey (2007–2011), and 2) the 500-square-degree SPTpol survey (2012–2016). The SPT-SZ and SPTpol observations have led to groundbreaking results that have moved the field of CMB research forward in significant ways. These results include the first galaxy clusters discovered using the Sunyaev-Zel'dovich (SZ) effect and the first detection of the elusive “B-mode” pattern in the polarization of the CMB. SPTpol and SPT-3G, discussed below, are DOE Cosmic Frontier experiments.

The third-generation camera for SPT, SPT-3G, was deployed during Austral summer 2016–17 (first light January 30, 2017) and will deliver a large improvement in sensitivity over the already impressive SPT-SZ and SPTpol surveys. This increase in sensitivity comes from two technological advances: an improved wide-field optical design that allows more than twice as many optical elements in the focal plane, and pixels that are sensitive to multiple observing bands in a single detector element. The sensitivity of the SPT-3G receiver will lead to precise constraints on the sum of the neutrino masses and potentially deliver a detection of the primordial B-mode signal from a background of gravitational waves from the epoch of inflation.

The significant advances in sensitivity delivered by the SPT-3G receiver come primarily from increasing the number of detectors at the focal plane of the telescope. With this comes a concomitant increase in the requirements for data storage and computing needs. For a 5-year run time, an estimated 1.2 PB of storage and 150 million CPU hours are required. The OSG group at the University of Chicago deployed a new data analysis and storage infrastructure at both the South Pole and at the University of Chicago for the SPT-3G collaboration.

At the South Pole, OSG deployed new hardware consisting of a hypervisor for experimental control and access to analysis resources, two analysis servers, one hot spare that can act as either an analysis machine or the hypervisor, and two storage servers with about 200 TB (about one season's worth of raw data) capacity each. The existing computing resources from SPTpol and SPT-SZ were tied into the new hardware and are used as additional analysis machines. To deploy the new hardware and perform the initial set-up, a staff member of ATLAS Midwest Tier 2 (MWT2) travelled to the South Pole.

The upgrades to the infrastructure at the University of Chicago were equally extensive. OSG deployed two new dedicated job submission and data analysis nodes that allow job submission to OSG and to the local MWT2 resources with higher opportunistic priority. To facilitate distribution of software, OSG also set up a CVMFS repository server and added an OASIS sub-repository for SPT.

With the increase in data rate, a new data storage needed to be deployed as well. At the moment, SPT has 150 TB allocated on the OSG Stash file system located at MWT2. This is meant as a primary storage location for the roughly 40 TB coming from the South Pole via satellite in the first year and user data. Future expansions to the OSG Stash storage system are planned to accommodate the data coming from pole via satellite and being hand-carried back from South Pole (about 200 TB/year). OSG has also set up a data management infrastructure for data ingestion, automatic backup, and data distribution across the OSG. MWT2 has set up a server that is dedicated for ingesting data from United States Antarctic Program (USAP) servers in Denver to the OSG Stash and automate backup to National Energy Research Scientific Computing Center's (NERSC) High Performance Storage System. For data distribution to OSG, MWT2 has set up two GridFTP doors for OSG Stash.

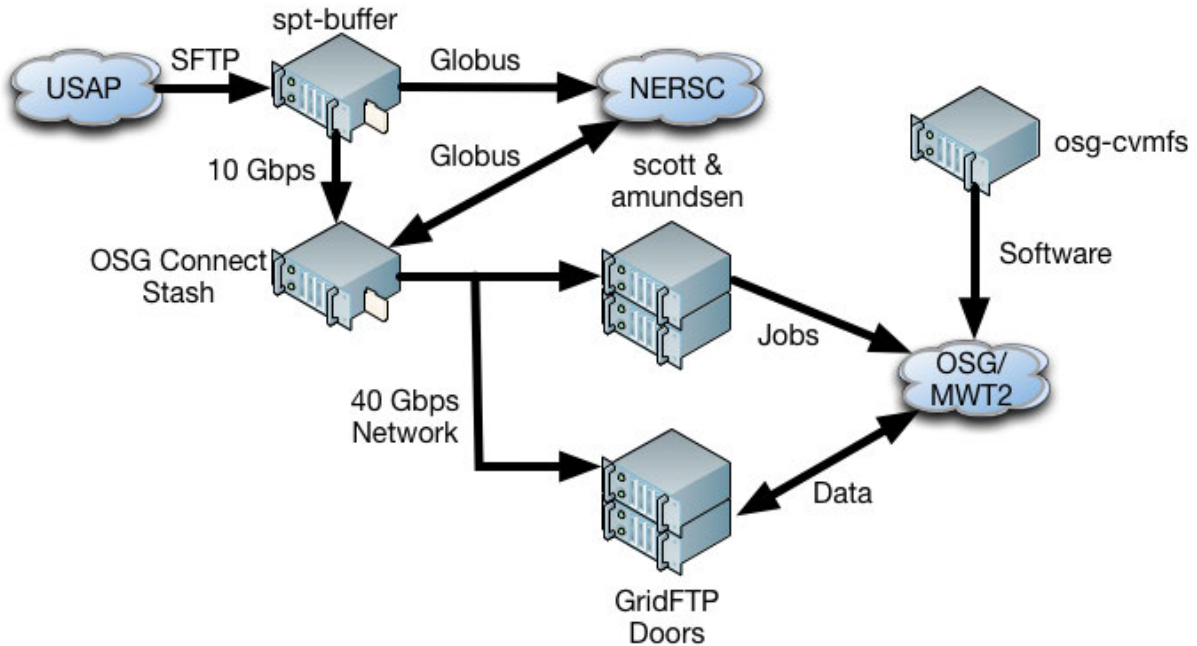


Figure 15: Overview of the SPT infrastructure setup at MWT2

This new data analysis framework and storage framework and infrastructure will allow SPT to be the first CMB experiment to extensively use the OSG, or grid computing of any kind, for their processing and storage needs. This is a proof-of-concept for computing models used by current and future CMB

experiments. This is particularly important for the future CMB-S4 experiment, which is expected to generate a factor of 50 more data than SPT3G and will require large amounts of computing resources.

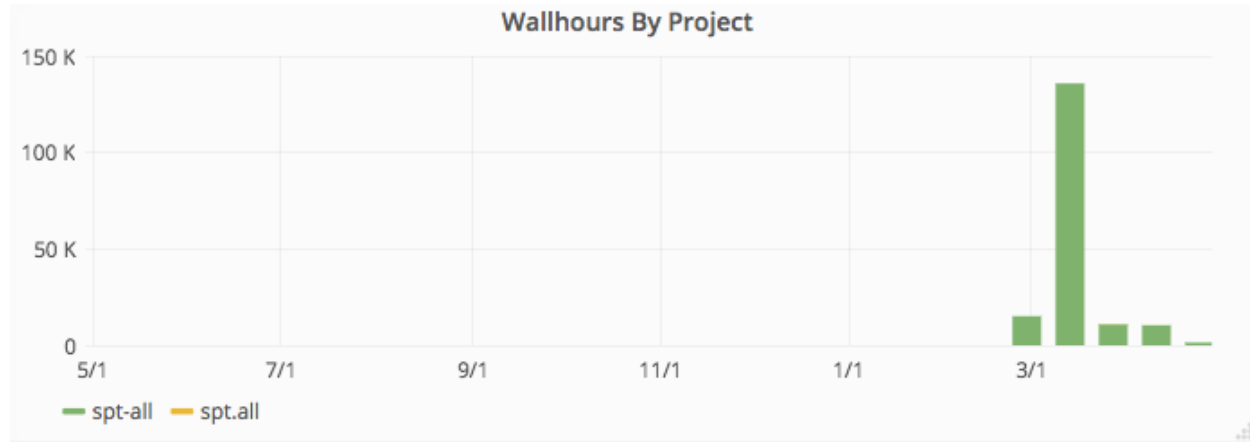


Figure 16: South Pole Telescope OSG usage from May, 2016, through May, 2017

#### 2.7.4 VERITAS

Imaging Atmospheric Cherenkov Telescopes (IACTs), like VERITAS, are ideal for studying point-like and moderately extended very high-energy (greater than 100 GeV) gamma ray sources. VERITAS consists of an array of four optical telescopes in southern Arizona and aims to observe the nanosecond-long flash of Cherenkov light produced by the charged particle products of the interaction of gamma rays with the atmosphere as they travel through the atmosphere. VERITAS is currently the most sensitive operational IACT above 100 GeV.

VERITAS has been making extensive use of OSG for their new Monte Carlo production needs. This work focuses on high energy (greater than 10 TeV) events, improved detector response simulation, and adding simulation of the night sky as a background. These changes and improvements require of 10 million CPU hours and 400 TB of storage.

OSG has been helping VERITAS with both the need for more computational and storage resources. VERITAS is currently storing over 120 TB of their simulation output on the OSG Stash storage service. With help from OSG, VERITAS was able to use the Pegasus workflow manager to produce their entire Monte Carlo chain from gamma-ray interaction simulation to final data products.

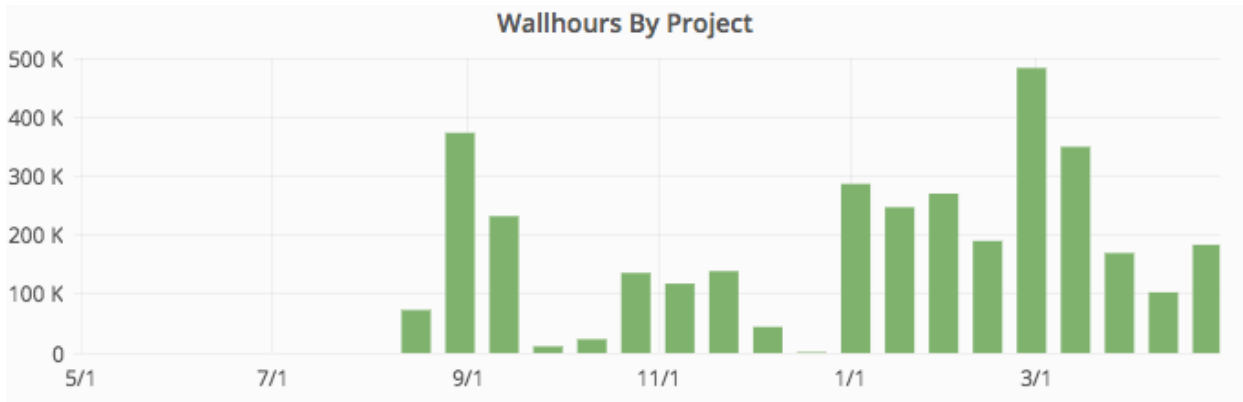


Figure 17: VERITAS OSG usage from May, 2016, through May, 2017

### 2.7.5 XENON1T

The XENON1T collaboration aims to uncover a crucial piece of our understanding of the universe through the direct detection of Weakly Interacting Massive Particles (WIMPs), a proposed dark matter particle, by their interaction with ordinary matter in a specialized, low-background detector. XENON1T is the third phase of the XENON experimental program and features a 2-ton dual-phase liquid xenon time projection chamber (LXe TPC) as target for dark matter. XENON1T is the largest LXe TPC ever built. The larger mass and the lower radioactive background reached in its central 1-ton volume are expected to lead to a world-leading sensitivity for WIMP-like dark matter particles. Beyond WIMPs, the extremely low background condition makes XENON1T sensitive to a variety of other dark matter models, spanning from Axion-like particles to hidden photons. The detector has operated since last quarter of 2016, and it is presently acquiring data for its science run. XENON1T released results from its first 34.2 days of science run in May 2017, achieving the world's best sensitivity for direct WIMP detection over a large WIMP mass range. Like its predecessors XENON10 and XENON100, it is located at the Gran Sasso Underground Laboratory (LNGS) in Italy.

The increases in the detector and fiducial volume, the use of active shielding from outside backgrounds, changes to the detector readout and triggering, and the need to produce 10 times the experimental lifetime in Monte Carlo simulation have dramatically increased the data rate and processing requirements compared to the predecessors. The OSG user group has had a significant part in establishing a data management system, integrate the various computing resources into one interface, and data processing and Monte Carlo simulation production framework for the XENON1T collaboration.

One of the main tasks for the OSG group has been setting up and maintaining a data management system for XENON1T. The main requirement was to efficiently connect a number of data storage allocations at various collaborating institutions across Europe and the US through a single interface. To do so, the OSG group set up a XENON1T-specific version of the ATLAS data management system, Rucio. The main objective of this system is to allow XENON1T to efficiently transfer data from the experimental site at LNGS to permanent storage locations in Europe and Israel and temporary storage location in the US for processing on OSG and campus computing resources independent of file transfer protocol and allow for reliable file transfers between sites.

XENON1T's Rucio instance manages six storage locations: LNGS; National Institute for Subatomic Physics (NIKHEF) in Amsterdam, Netherlands; Centre de calcul de Institut national de physique de nucléaire et de physique des particules (CCIN2P3) in Lyon, France; Weizmann Institute of Science in Tel

Aviv, Israel; OSG Stash in Chicago; and University of Chicago's Research Computing Center. These storage locations constitute nearly 800 TB of available storage of which over 450 TB are currently used. These 450 TB are comprised of over 7,000 data sets with over 450,000 individual files. To facilitate the movement between the various endpoints OSG has worked with the XENON collaboration and the LHC Open Network Environment to allow LNGS, NIKHEF, CCIN2P3, and OSG Stash to use the dedicated transatlantic link for data movement between the various sites. Additionally, MWT2's ATLAS collaborators that the US ATLAS Tier-1 center at Brookhaven National Laboratory have allowed XENON1T to use ATLAS's US-based File Transfer Service (FTS) to allow for reliable, monitored, and automatic transfer between sites. The OSG group also provides continues maintenance and monitoring of the Rucio service and the availability of and network performance between the various storage elements.

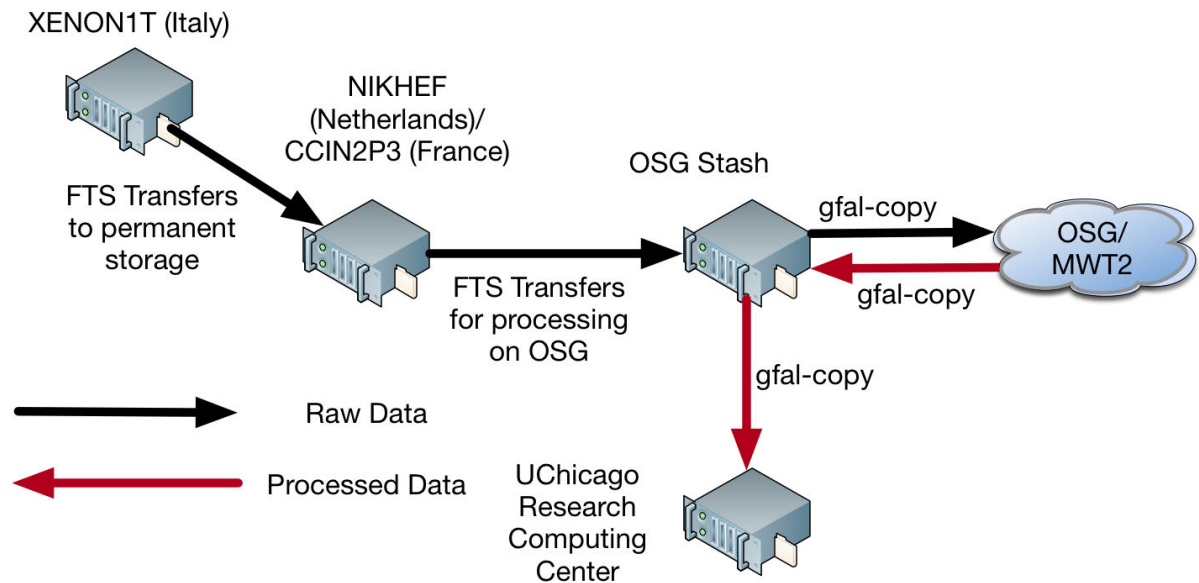


Figure 18: XENON1T data flow for data processing from LNGS to OSG

The OSG Stash storage service is the main storage location for XENON1T data in the US. It is meant as a data store for data to be processed on the available US compute resource. As part of this, the OSG group had to add GridFTP access to the OSG Stash service, which is currently shared with SPT and VERITAS. XENON1T is currently occupying nearly 300 TB in OSG Stash. After the successful use of OSG Stash, the University of Chicago XENON group decided to invest in dedicated storage on OSG Stash. The OSG group at is currently moving XENON's data to this dedicated storage.

The second major task OSG has been involved in with the XENON1T collaboration is establishing a single point of submission to all available compute resources through the OSG interface. XENON1T has been able to leverage compute resources at OSG sites including MWT2, campus clusters such as the University of Chicago's Research Computing Center, NSF-funded HPC centers such as San Diego Supercomputer Center's (SDSC) Comet through an allocation of OSG co-PI Frank Würthwein, and European Grid Infrastructure (EGI) sites such as CCIN2P3, through a single interface. To make all of these resources available from a single job submission point, the OSG had to work closely with several stakeholders across the US and Europe. They are working closely with SDSC staff to leverage Comet's Virtual Cluster for OSG users. Similarly, they are working with ATLAS collaborators at the EGI site CCIN2P3 to allow XENON to submit transparently to EGI. Future plans are to allow submission to

NIKHEF as well. To ease the distribution of XENON1T’s software across all the various sites, OSG set up a CVMFS repository server and added an OASIS sub-repository.

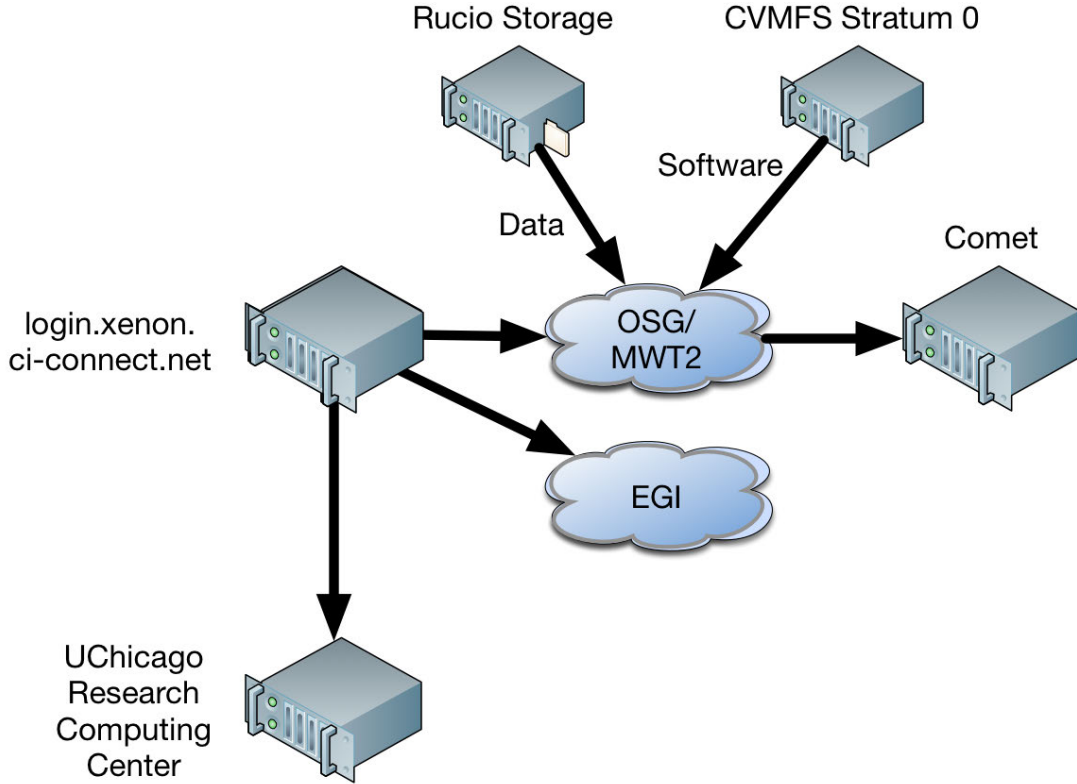


Figure 19: XENON1T compute resources and access methods

The third major task has been to aid the XENON1T collaboration in creating data processing and Monte Carlo simulation production workflows. This work has allowed XENON1T to leverage their broad resources successfully for data processing and Monte Carlo production, move their data processing from dedicated campus cluster resources to OSG, and automate their data processing workflow. The data processing workflow is based on HTCondor’s DAGMan, while the Monte Carlo workflow is based on the Pegasus workflow manager. The different approaches were taken because of the ability of Pegasus to submit to the EGI sites independently and because of the higher interdependence between jobs in the Monte Carlo workflow.

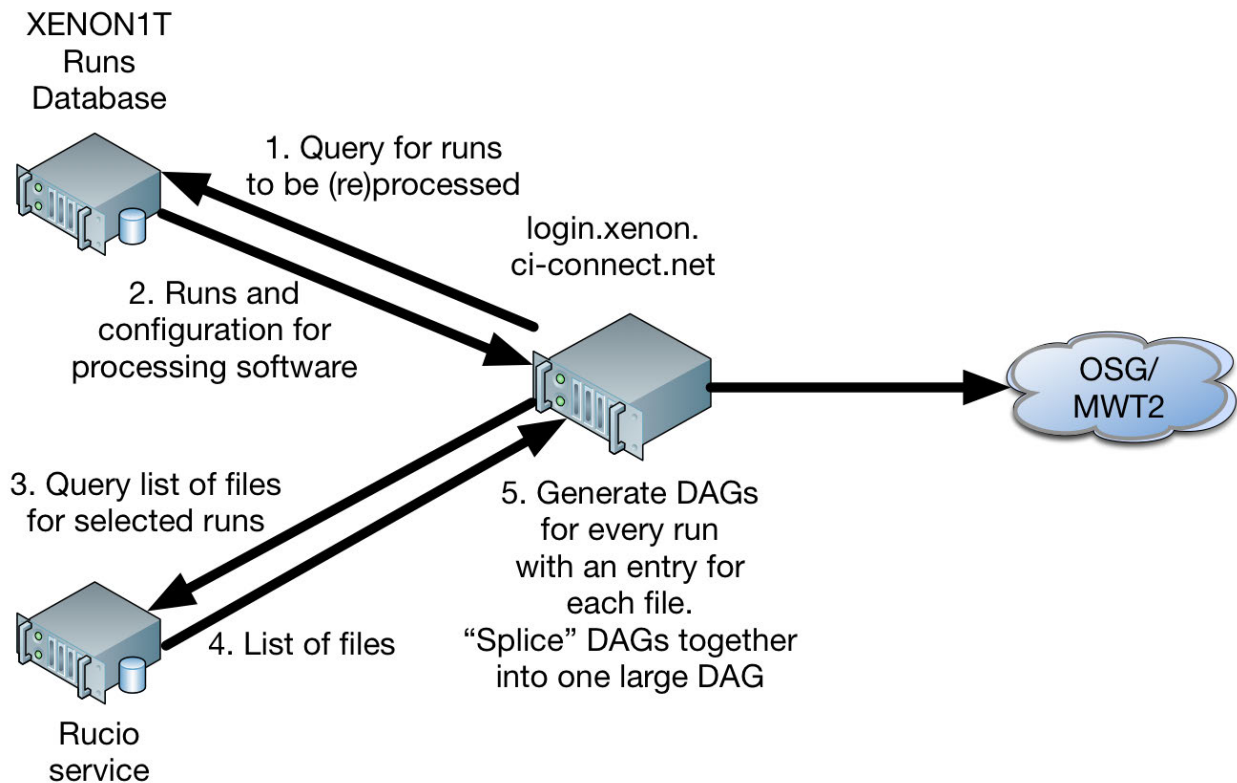


Figure 20: XENON1T data processing workflow

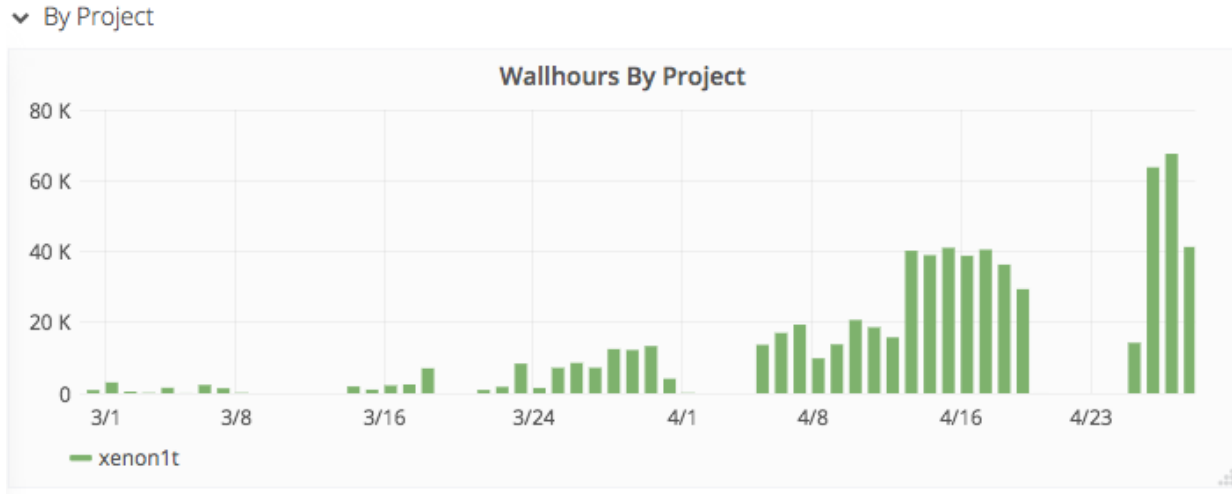


Figure 21: XENON1T wall hours used on Comet

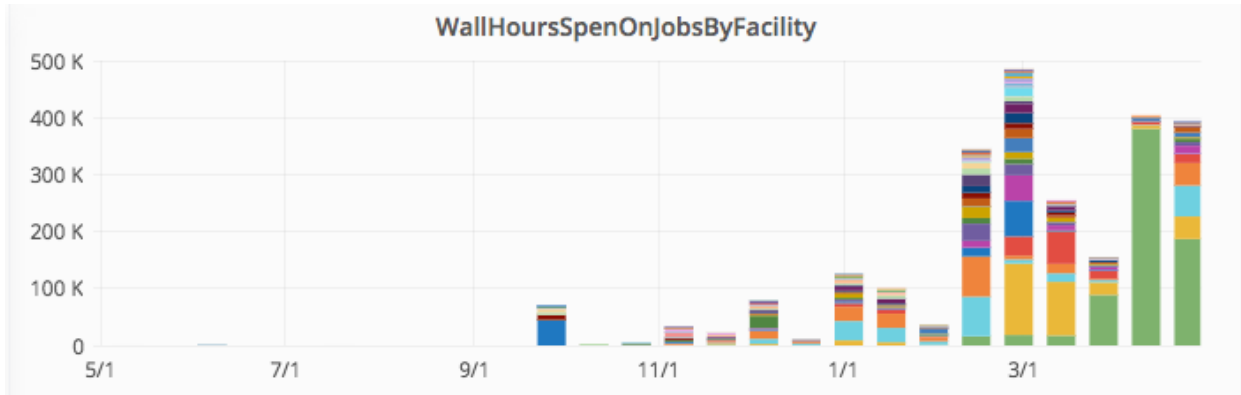


Figure 22: XENON1T OSG usage from May 2016 through April 2017

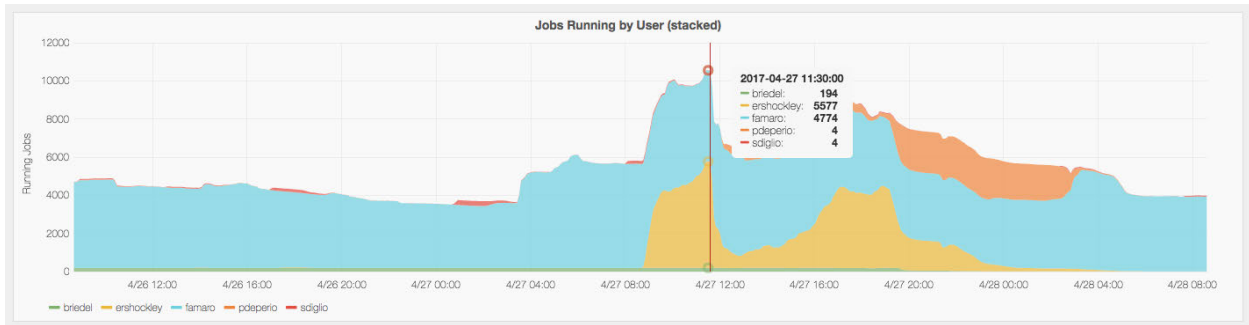


Figure 23: XENON1T using more than 10,000 cores simultaneously

## 2.8 Campus Researchers

The OSG leverages its geographic and institutional diversity to bring distributed high-throughput computing (DHTC) to a broad and growing cross-section of US researchers. Individual researchers typically do not bring computing resources to contribute to OSG. The OSG team assists these researchers in adapting their applications to run in the DHTC environment, helps them get access to OSG for submitting their jobs, and supports them in completing their research computation.

Other VOs such as GLOW (the Grid Laboratory of Wisconsin), HCC (the Holland Computing Center), and the SBGrid (Structural Biology Grid at Harvard Medical School) support researchers within their communities. Researchers not already affiliated with an existing OSG community gain access to DHTC via the OSG Open Community.

### 2.8.1 OSG Open Community

The OSG continues to increase access to DHTC resources for US-based researchers. Members of the OSG consortium aggregate their resources to provide computing for their experiments and make unused resources available to other OSG members; these shared compute cycles are referred to as opportunistic cycles. We operate the OSG VO that does not own any computing resources, and its primary purpose is to harvest opportunistic cycles. This VO serves as the backbone for what we call the OSG Open Community. It provides access to DHTC for US researchers who are not already members of any other existing community active on OSG.

The OSG is a powerful sharing ecosystem. There can be a steep learning curve for those not already familiar with DHTC. To lower the barrier of entry, we have built an infrastructure that shields the user from the complexities of the grid. This infrastructure is depicted in Figure 24. Different organizations may use different entry points while participating in the OSG Open Community. The OSG provisioning services are implemented using HTCondor GlideinWMS software.

## How does the OSG work?

There are four ways to access the OSG:

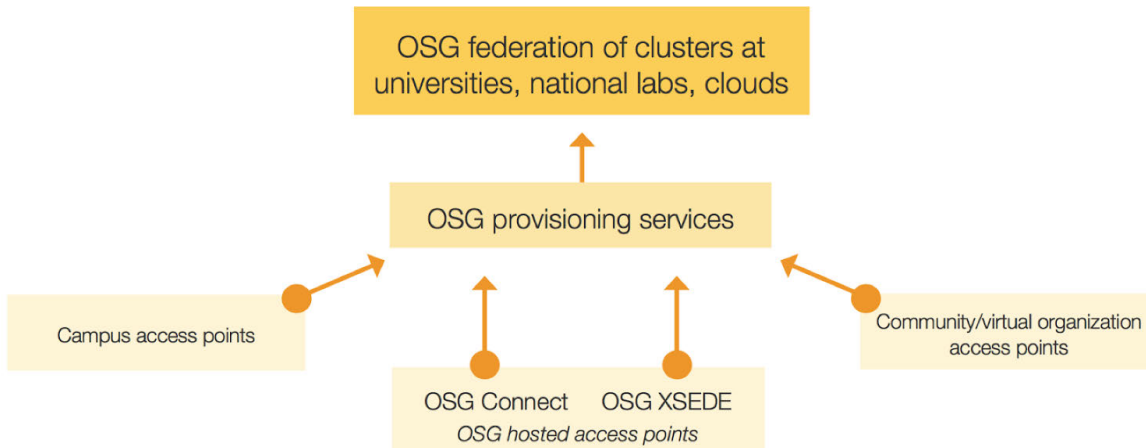


Figure 24: OSG access points

The needs of stakeholders vary. For individual users we provide three methods: the OSG Connect service provides easy-to-use login access based on their campus credentials; through XSEDE; and legacy users continue to use OSG via the OSG-Direct login host. For research groups, experimental collaborations, and campuses who want to administer their own login nodes for their users, we provide a bulk connection through dedicated login nodes. An example of each type of stakeholder is the Baker Lab at the University of Washington, the LIGO collaboration, Clemson University, and University of California San Diego, respectively.

Figure 25 and Figure 26 show resource usage by field of science for researchers accessing the open facility using OSG-hosted access points — OSG Connect and OSG XSEDE — for the past year.

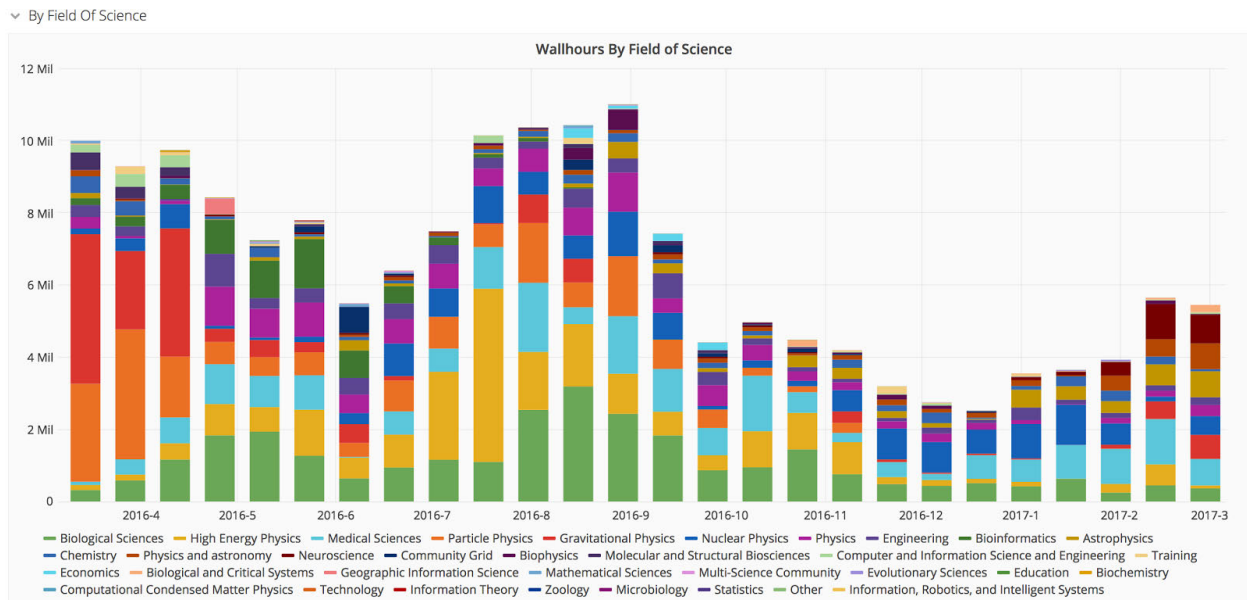


Figure 25: History of OSG CPU resource usage via OSG Connect and XSEDE by field of science

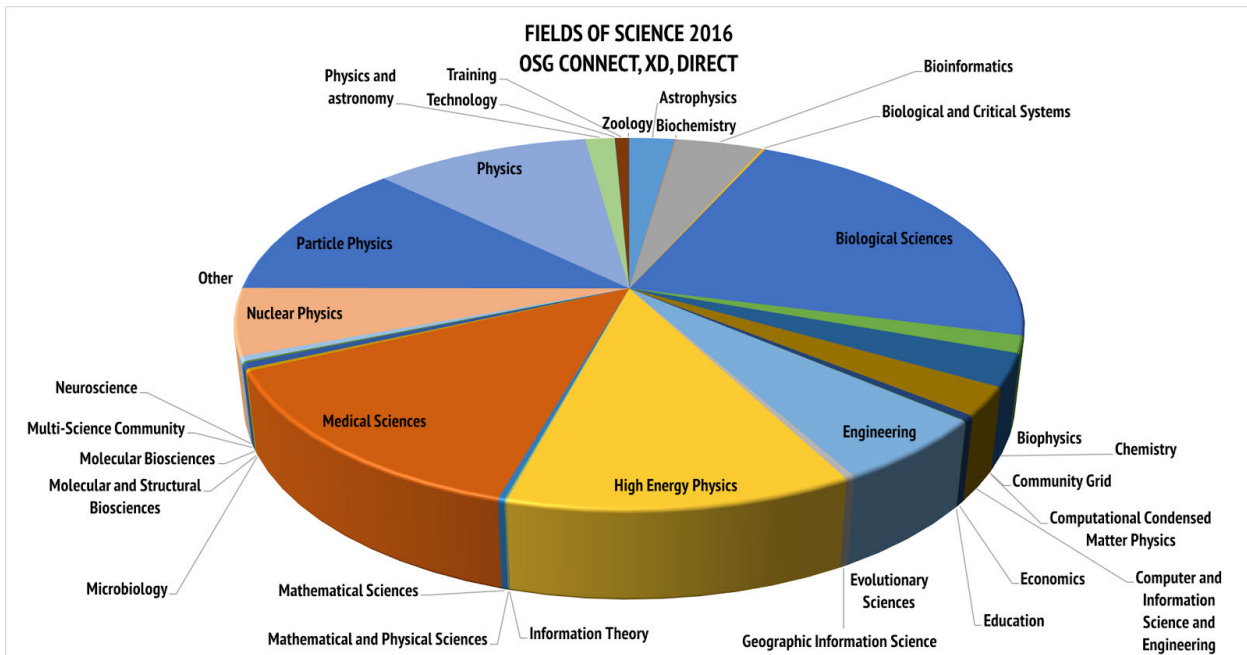


Figure 26: Breakdown of OSG CPU resource usage via OSG Connect, XSEDE, and Direct

### 2.8.2 Active Projects using the OSG Virtual Organization

Over the last year, 132 groups have utilized the OSG VO. These groups are diverse in terms of their research work and resource utilization. Figure 27 shows the number of active projects by field of science over the last year.

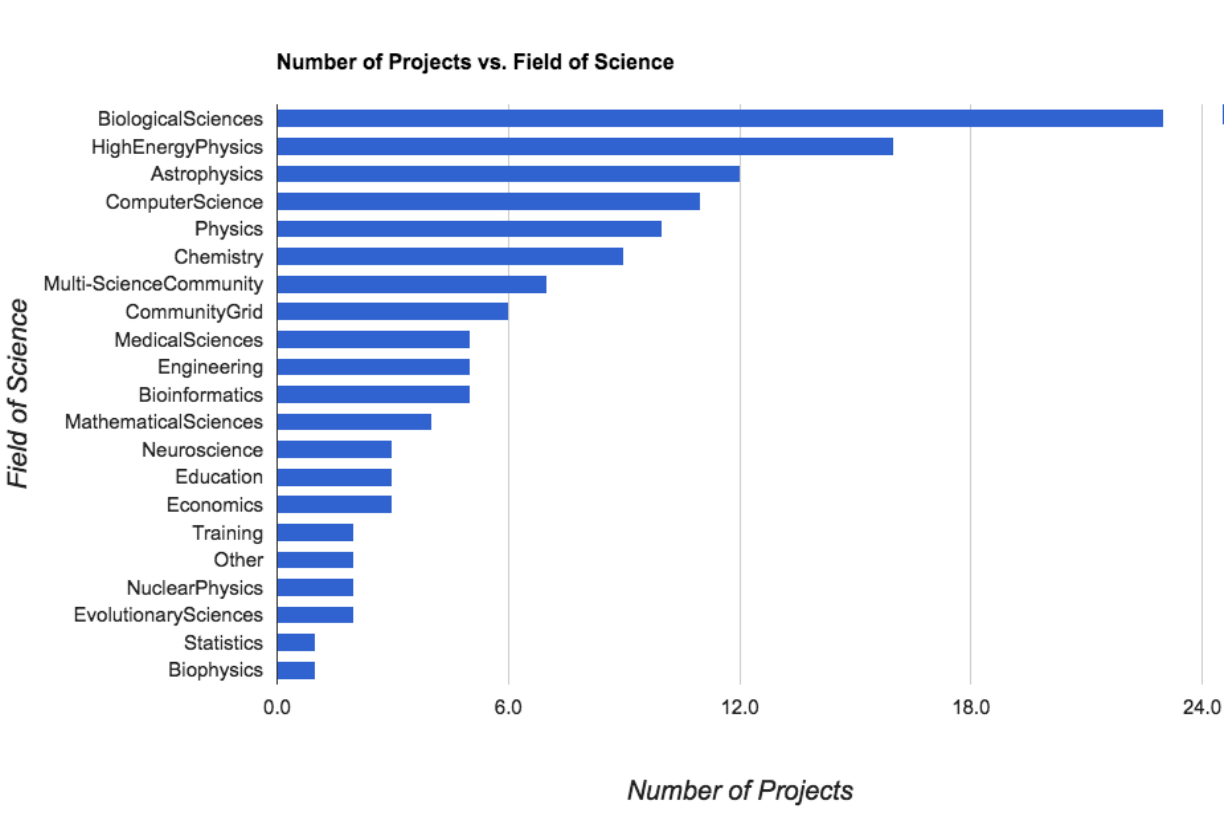


Figure 27: Active projects using the OSG VO by field of science

Table 1 lists the usage of wall hours by research project over the last year (the last column shows wall hours; *Mil* is million, and *K* is thousand). The usage of wall hours varies among the groups: 26 groups consumed more than a million wall hours, 56 groups consumed between a million and 10,000 wall hours, and the remaining 50 groups consumed less than 10,000 wall hours.

**Table 1: OSG usage in past year for OSG Connect, Direct, and XSEDE access points**

Project Name	PI Name	Institution	Field of Science	CPU walltime (hours)
TG-IBN130001	Donald Krieger	University of Pittsburgh	Medical Sciences	23.39 Mil
SPLINTER	Samy Meroueh	Indiana University	Medical Sciences	20.80 Mil
Duke-QGP	Steffen A. Bass	Duke University	Nuclear Physics	15.34 Mil
CpDarkMatterSimulation	Christoph Paus	MIT	High Energy Physics	13.99 Mil
AMS	Baosong Shan	MIT	High Energy Physics	10.31 Mil
IceCube (including TG-PHY150040)	Francis Halzen	University of Wisconsin	Astrophysics	8.97 Mil

FutureColliders	Sergei Chekanov	Argonne National Lab	High Energy Physics	8.68 Mil
z2dqmcmc	Snir Gazit	University of California Berkeley	Physics	8.28 Mil
SourceCoding	David Mitchell	New Mexico State University	Engineering	8.13 Mil
LIGO	Peter F. Couvares	California Institute of Technology	Physics	6.53 Mil
IBN130001-Plus	Donald Krieger	University of Pittsburgh	Neuroscience	6.06 Mil
seq2fun	Peter Freddolino	University of Michigan	Bioinformatics	4.61 Mil
BioGraph	Alex Feltus	Clemson University	Biological Sciences	3.56 Mil
VERITAS	Nepomuk Otte	Georgia Institute of Technology	Astrophysics	3.29 Mil
AlGDock	David Minh	Illinois Institute of Technology	Chemistry	2.76 Mil
UNLberf	Jean-Jack M. Riethoven	University of Nebraska-Lincoln	Biological Sciences	2.31 Mil
XENON1T	Luca Grandi	University of Chicago	Astrophysics	2.21 Mil
PRTH	Endre Takacs	Clemson University	Physics	2.16 Mil
HCCLocalSubmit	David Swanson	University of Nebraska	Community Grid	2.09 Mil
maesSwigmodels	Ariella Gladstein	University of Arizona	Evolutionary Sciences	1.97 Mil
DetectorDesign	John Strologas	University of New Mexico	Medical Sciences	1.96 Mil
molcryst	Olexandr Isayev	University of North Carolina at Chapel Hill	Chemistry	1.39 Mil
PainDrugs	Pei Tang	University of Pittsburgh	Medical Sciences	1.23 Mil
PreBioEvo	J. Woods Halley	University of Minnesota	Biophysics	1.11 Mil
atlas-org-uchicago	Robert William Gardner Jr	University of Chicago	High Energy Physics	1.01 Mil
EvolSims	Oana Carja	University of Pennsylvania	Biological Sciences	987.37 K
ConnectTrain	Robert William Gardner Jr	University of Chicago	Training	964.11 K

CombinedPS	Ozkan Celik	Colorado School of Mines	Biological Sciences	838.72 K
DemandSC	Fernando Luco	Texas A&M	Economics	758.72K
selfassembly	Eddie Tysoe	University of Wisconsin Milwaukee	Chemistry	611.42 K
nicesims	Nathan Kaib	University of Oklahoma	Astrophysics	581.26 K
EIC	Tobias Toll	Brookhaven National Laboratory	High Energy Physics	540.17 K
EvoProtDrug	Milo Lin	UT Southwestern	Biological Sciences	535.59 K
atlas-org-utexas	Robert William Gardner Jr	University of Texas - Austin	High Energy Physics	529.13 K
TG-GEO150003	Jon Pelletier	University of Arizona	Engineering	424.88 K
TG-AST150044	Jennifer Lotz	Space Telescope Science Institute	Astrophysics	402.47 K
TG-CHE140110	John Stubbs	University of New England	Chemistry	369.00 K
TG-MCB150090	Emiliano Brini	SUNY at Stony Brook	Biological Sciences	310.10 K
OSG-Staff	Chander Sehgal	Fermilab	Computer Science	300.37 K
TG-AST150033	Juliette Becker	University of Michigan	Astrophysics	297.60 K
Perchlorate	Justin M Hutchison	University of Illinois	Engineering	259.83 K
lftsim	Joel Giedt	Rensselaer Polytechnic Institute	High Energy Physics	226.43 K
NSNM	Vadim Apalkov	Georgia State University	Physics	198.25 K
SouthPoleTelescope	John Carlstrom	University of Chicago	Astrophysics	192.45 K
SysBioEdu	Stephen Ficklin	Washington State University	Biological Sciences	178.91 K
microphases	Patrick Charbonneau	Duke University	Chemistry	174.43 K
LiuLab	Kevin Jensen Liu	Michigan State University	Bioinformatics	147.48 K
DeerDisease	Lene Jung Kjaer	Southern Illinois University	Biological Sciences	146.24 K
uchicago	Robert William Gardner Jr	University of Chicago	Multi-Science Community	139.38 K

TG-AST150012	Gregory Snyder	Space Telescope Science Institute	Mathematical Sciences	137.40 K
TG-AST160036	James Davenport	Western Washington University	Astrophysics	137.39 K
duke-boolnet	Daniel Gauthier	Duke University	Physics	133.18 K
TG-CCR140028	Shantenu Jha	Rutgers, the State University of New Jersey	Computer Science	121.97 K
fluidsim	Erkan Tuzel	Worcester Polytechnic Institute	Physics	121.66 K
unleppass	Adam Caprez	University of Nebraska - Lincoln	Bioinformatics	117.96 K
TG-CHE140098	Paul Siders	University of Minnesota, Duluth	Chemistry	113.66 K
KORDrugdiscov	David Toth	Centre College	Chemistry	85.85 K
GeoTunnel	Elena Guardincerri	Las Alamos National Lab	Nuclear Physics	72.94 K
TG-AST150046	Suzanne Hawley	University of Washington	Physics	70.91 K
holosim	Allan Strand	College of Charleston	Biological Sciences	69.44 K
TG-PHY160031	Nepomuk Otte	Georgia Institute of Technology	Mathematical Sciences	66.89 K
TG-AST160046	Leslie Hebb	Hobart and William Smith Colleges	Physics	60.48 K
UserSchool2015	Tim Cartwright	University of Wisconsin - Madison	Education	58.04 K
TG-MCB160027	Yang Zhang	University of Michigan	Biological Sciences	57.71 K
AtlasConnect	Robert William Gardner Jr	University of Chicago	High Energy Physics	49.60 K
AmorphousOrder	Patrick Charbonneau	Duke University	Chemistry	46.41 K
NSLS2ID	Dean Andrew Hidas	Brookhaven National Laboratory	High Energy Physics	40.63 K
ContinuousIntegration	Robert William Gardner Jr	University of Chicago	Engineering	36.55 K
TG-MCB160069	Edward O'Brien	Pennsylvania State University	Biological Sciences	35.87K
TG-MCB160192	Samuel Thompson	University of California, San Francisco	Biological Sciences	35.06 K

freesurfer	Donald Krieger	University of Pittsburgh	Neuroscience	33.10 K
duke-CMT	Harold U. Baranger	Duke University	Physics	32.20 K
atlas-org-harvard	Robert William Gardner Jr	Harvard University	High Energy Physics	31.10 K
SFCphases	Paul Siders	University of Minnesota Duluth	Chemistry	28.64 K
TDAstats	David Meyer	University of California San Diego	Mathematical Sciences	27.14 K
TG-AST170008	Stephanie Hamilton	University of Michigan	Astrophysics	24.28 K
mab	Vivek Farias	Massachusetts Institute of Technology	Computer Science	22.82 K
TG-TRA130030	Neranjan Edirisinghe Pathirannehelage	Georgia State University	Mathematical Sciences	21.31 K
TG-MCB060061N	Jeffry D. Madura	Duquesne University	Biological Sciences	17.58 K
MS-EinDRC	Jacob Pessin	Albert Einstein College of Medicine	Medical Sciences	16.78 K
PCFOSGUCSD	Frank Wuerthein	University of California San Diego	Physics	13.49 K
EDFCHT	Jianghao Chu	UC Riverside	Economics	11.99 K
TG-TRA140043	Igor Yakushin	Pennsylvania State University	Computer Science	8.97 K
Paniceae-trans	Jacob Washburn	University of Missouri	Biological Sciences	7.23 K
ERVmodels	Fabricia Nascimento	University of Oxford	Biological Sciences	4.54 K
TrappedOrbits	Kathryne J Daniel	Bryn Mawr College	Astrophysics	2.87 K
atlas-org-fresnostate	Harinder Singh Bawa	Fresno State University	High Energy Physics	2.64 K
hABCNWHI	Yvonne Chan	Iolani School	Biological Sciences	2.51 K
duke-SWC-Duke15	Mark R. DeLong	University of Chicago	Multi-Science Community	2.02 K
UserSchool2016	Tim Cartwright	University of Wisconsin Madison	Education	1.39 K
EmpModNatGas	Ashley Vissing	University of Chicago	Economics	1.25 K
EHEC	Chuck Kaspar	University of Wisconsin-Madison	Biological Sciences	< 1K

TCGAPartCorr	Chad Shaw	Baylor College of Medicine	Bioinformatics	< 1K
KickstarterDataAnalysis	Feng Bill Shi	University of Chicago	Statistics	< 1K
CentaurSim	Nathan Kaib	Northwestern University	Astrophysics	< 1K
RIT	Stanislaw P. Radziszowski	Rochester Institute of Technology	Computer Science	< 1K
TRNG	Asia Aljahdali	Florida State University	Computer Science	< 1K
atlas-org-anl	Robert William Gardner Jr	Argonne National Laboratory	High Energy Physics	< 1K
RicePhenomics	Harkamal Walia	University of Nebraska Lincoln	Biological Sciences	< 1K
CometCloud	Javier Diaz-Montes	Rutgers	Computer Science	< 1K
Clemson	Marcin Ziolkowski	Clemson University	Multi-Science Community	< 1K
HTCC	Rob Quick	Indiana University	Community Grid	< 1K
atlas-org-osu	Robert William Gardner Jr	The Ohio State University	High Energy Physics	< 1K
SBGrid	Piotr Sliz	Harvard Medical School	Biological Sciences	< 1K
duke-campus	Tom Milledge	Duke University	Community Grid	< 1K
DataTrieste	Rob Quick	International Center for Theoretical Physics	Multi-Science Community	< 1K
TG-MCB140268	Graziano Vernizzi	Siena College	Biological Sciences	< 1K
REDTOP	Corrado Gatto	Fermi National Accelerator Lab	High Energy Physics	< 1K
AfricanSchool	Rob Quick	Indiana University	Education	< 1K
Swift	Michael Wilde	University of Chicago	Computer Science	< 1K
GTConvertHTC	Mehmet Belgin	Georgia Tech	Multi-Science Community	< 1K
atlas-org-slac	Robert William Gardner Jr	SLAC National Accelerator Laboratory	High Energy Physics	< 1K
duke-bgswgs	Hai Yan	Duke University	Bioinformatics	< 1K
TG-TRA100004	Andrew Ruether	Swarthmore College	Training	< 1K
UserSchool2014	Tim Cartwright	OSG	Multi-Science Community	< 1K

cms-org-nd	Kevin Lannon	University of Notre Dame	High Energy Physics	< 1K
AdHocComm	Trevor Santarra	University of California Santa Cruz	Computer Science	< 1K
OSGOpsTrain	Rob Quick	Open Science Grid	Community Grid	< 1K
MaizeAminoAcids	Timothy M Beissinger	University of Missouri	Evolutionary Sciences	< 1K
RADICAL	Shantenu Jha	Rutgers University	Computer Science	< 1K
TG-STA110011S	Stephen McNally	University of Tennessee, Knoxville	Other	< 1K
PTMC	Derek Dolney	University of Pennsylvania	Molecular and Structural Biosciences	< 1K
duke-duke-campus	Tom Milledge	Duke University	Community Grid	< 1K
TG-TRA120004	Rob Lane	Columbia University in the City of New York	Other	< 1K
NeurOscillation	Bradley Voytek	University of California San Diego	Neuroscience	< 1K
TG-MCB090174	Shantenu Jha	Rutgers, the State University of New Jersey	Biological Sciences	< 1K
TG-IRI160006	Victor Hazlewood	National Institute for Computational Sciences	Engineering	< 1K
idTrackerParallel	Andrew Ruether	Swarthmore College	Biological Sciences	< 1K
StanfordRCC	Ruth Marinshaw	Stanford University	Community Grid	< 1K
SciSim	Amit Goel	University of Central Florida	Multi-Science Community	< 1K
srccoding	Joerg Kliewer	New Jersey Institute of Technology	Computer Science	< 1K

### 2.8.3 Center for High Throughput Computing (University of Wisconsin–Madison)

Established in 2006, the Center for High Throughput Computing (CHTC) at the University of Wisconsin at Madison (UW–Madison) serves as the campus's centralized research computing center, supporting multiple on-campus clusters for distributed high-throughput computing, as well as a cluster dedicated to high-performance computing. These campus resources provided roughly 321 million CPU hours during the 2016 calendar year. As an active member of the OSG, the CHTC provided an additional 34 million CPU hours to campus researchers via the OSG in 2016. Together, HTCondor developers and other CHTC staff support other on-campus cluster administrators. The CHTC employs a team of Research Computing Facilitators who provide consulting, resource/personnel matchmaking, and support to enable scholarly

discoveries through computing. Facilitators and other campus staff also represent UW–Madison’s participation in the NSF-funded Advanced Cyberinfrastructure–Research and Education Facilitators (ACI-REF) project. All standard CHTC resources and services are provided to UW–Madison researchers and collaborators at no charge, but with buy-in opportunities for groups needing priority access to specific, local hardware. Located in the Department of Computer Sciences, CHTC is funded by grants from the National Science Foundation (NSF) and Department of Energy (DOE), and by various UW–Madison funding efforts.

#### 2.8.4 Holland Computing Center (University of Nebraska–Lincoln)

The Holland Computing Center (HCC) at the University of Nebraska (NU) provides advanced computing, storage, and networking resources to researchers in the NU system and statewide, as well as their associated collaborators worldwide. HCC is managed by the Office of Research and Economic Development at the University of Nebraska–Lincoln and is funded by grants from the NSF, the National Institutes of Health, and by various NU funding sources. HCC maintains several on-campus clusters for high performance as well as distributed high throughput computing, including a Tier-2 site for the US CMS project. All of these HCC resources, when they are idle, are shared opportunistically with OSG users.

During 2016, HCC resources provided 67.4 million CPU hours to OSG VOs, 19.8 million opportunistically. HCC researchers that benefited from the OSG besides high energy physicists included several bioinformatics researchers, including one (Shu) who presented his work at the annual OSG All Hands Meeting in March 2017. Several HCC faculty and staff work closely with OSG to advance its mission, including contributing to outreach activities such as Software Carpentry Workshops and OSG User School sessions that train users to use DHTC methods and technologies. HCC currently hosts the GRACC database for OSG accounting; Bockelman with HCC leads the OSG Technologies Area, and Swanson serves as OSG Council Chair.

## 3 The OSG Fabric of Services

### 3.1 Technology Investigations

The OSG Technology Area provides the OSG with a mechanism for medium- to long-term technology planning and evolution. This area helps our software and services consolidate into a high-quality, robust platform for DHTC. Over the last year, several long-term projects have come to fruition. Newly started projects have revolved around the theme of “simplify, simplify, simplify”: minimizing the maintenance and operational burden of OSG services. In this section, we highlight several areas with significant progress over the last year.

**Retire deprecated/obsoleted services:** Several of the OSG services were from the early “grid days” and did not reflect modern usage of the OSG, or were originally adopted to help support LHC Run 1. As part of a cross-cutting activity (with the Software and Production areas), we retired support for Globus GRAM (CE software; replaced by HTCondor-CE) and the BDII (information service software; replaced by the OSG Collector).

We made all the technical steps necessary for sites to retire SRM, GUMS, and VOMS Admin. We are actively collaborating with “pathfinder” sites and VOs to perform these retirements. These pieces of software have very different functionalities but share one important aspect: They are significant, externally-developed Java applications where OSG Software has taken up primary development. When the retirement is completed — estimated to be next year — this will represent significant decreased maintenance costs for OSG Software.

**Authorization overhaul:** OSG’s authorization system relies on mapping of individual user’s global identities (i.e., their grid certificate) to a specific site-local account. OSG is no longer used in this manner: Sites work at the VO level and users no longer need global identities, only VO identities, to use OSG services. Trust between users and sites is established via transitive trust with the VO. Authorizing VOs at sites is a far simpler task than authorizing individuals; we have begun the process of updating our software and documentation to reflect this fact. For example, instead of a user database with thousands of entries synchronized locally (as in GUMS), we only need a mapping from VO name to a Unix username. The latter can be done via a simple mapfile. This overhaul — expected to complete in the next project year — will minimize complexity of site deployments and be the technical mechanism to allow the retirement of GUMS. Eliminating GUMS, in turn, means we will no longer need the web services from VOMS Admin, allowing us to eliminate VOMS Admin support.

**OSG Storage and StashCache:** The caching-based data distribution infrastructure project, StashCache, was started in 2015 and saw its initial production use in 2016. The initial production use was for OSG VO users; during some weeks in early 2017, usage accounting recorded more than 1 petabyte of transfers per week through this infrastructure.

The StashCache infrastructure was augmented with a POSIX interface using the CVMFS/OASIS infrastructure developed in previous years. This significantly reduces the user adoption burden of the StashCache technology; the tradeoff is not every OSG site runs the requisite CVMFS release. Further work added an authenticated interface to CVMFS: This allows OSG to securely distribute LIGO data files, again easing the burden of using OSG for new LIGO users. The StashCache/CVMFS activity resulted in a paper at CHEP 2016; the LIGO use case was submitted as a paper to the Practice and Experience in Advanced Research Computing (PEARC) conference in 2017.

**Container Support:** The OSG is an admittedly heterogeneous environment — its compute resources consist of dozens of loosely-coordinated, independently-administered clusters. Throughout the OSG’s

lifetime, we have tried to discover the correct balance between hiding differences and exposing heterogeneity in the computing environment.

Historically, we have worked with users to help make portable applications, applications that have no dependency on the underlying operating system. While this is still the preferred approach, we have found that using containers has lessened the burden of portability for new users. This, hopefully, provides a simpler on-ramp to OSG.

The container system utilized is Singularity, from Lawrence Berkeley National Laboratory. Singularity originally focused on the needs of HPC admins (leading to significantly different design choices than Docker, for example): This has led to surprisingly quick adoption across OSG sites. The OSG VO added support for Singularity in mid-February 2017: since then, 17 million jobs have been started inside containers. Generally, 40–70% of cores available to the OSG opportunistic pool have Singularity enabled. CMS and FIFE have subsequently adopted the OSG integration for Singularity: CMS has the capability in production at five sites and has launched about 2.5 million jobs inside containers.

The integration of Singularity with CMS’s submission infrastructure allows CMS sites to drop support for gLExec; given that CMS is the only user of this tool, we will have the opportunity to drop support for gLExec in the next project year.

**New Accounting System (GRÅCC):** In early 2016, we had identified serious scalability issues with the centralized database components of our accounting system, Gratia. Its MySQL database scaled poorly, and all its central components were fundamentally tied to MySQL. We decided to redesign the central portions with two goals:

- De-couple functionality of each component, allowing any one to be replaced independently in the future.
- Drastically reduce the size of the project via use of industry components.

Both goals were met by our new project, GRÅCC. GRÅCC utilizes Elasticsearch for record storage, a standalone web-server to listen for new records, off-the-shelf dashboard tools (Grafana, Kibana), and a messaging bus (RabbitMQ) for all the components to communicate. By having a messaging bus in the design, incoming accounting records can be sent to multiple database back-ends (for example, the production database, a test database, and the tape archive). This solution was integrated together by the OSG Technology team and delivered into production at the end of the project year. While work remains to improve operations, the maintenance cost of accounting is down significantly and, using the NoSQL database Elasticsearch, we have more flexibility to improve records in the future.

### 3.2 Software

The OSG Software team produces an open source software distribution that underpins the technical platform of the OSG Production Grid and supports the operation of the production facility as well as end-user scientific applications. The Software team provides packaging and builds for software provided by developers across many spaces, from job schedulers to network storage solutions. The team also creates and maintains software tools that satisfy needs of the research computing community that are not met elsewhere. In some cases, this requires supporting tools critical to the scientific community that have otherwise been abandoned by the original developer. Further, the Software team integrates the components of the distribution, performs automated testing of the integrated software, and supports the software in production.

Ultimately, the mission of the Software team is to minimize the effort needed to manage the software that underlies DHTC. Thus, the team works closely with the OSG Technology, Release, Production, Security, and Operations teams, plus key stakeholders in the scientific community.

This year, the Software team focused on completing long-term migrations, most prominently the transition from Globus GRAM to HTCondor-CE. We ended support for the former while the latter saw new features including HTCondor-CE Bosco, a slimmer version that submits jobs over SSH, and HTCondor-CE View, which provides local job monitoring. The Software team also worked directly with stakeholders to ensure that their systems were compatible with the new HTCondor-CE information system.

In August, the Software team ended support for the old OSG 3.2 release series and Enterprise Linux (EL) 5 along with it. This aligned nicely with Red Hat's EL 5 support timeline, which is expected to end in early 2017, so most of our end-users had already migrated to a newer operating system version.

Meanwhile, our current release series saw completion of Java component support on EL 7 for the OSG software stack save for VOMS Admin, which was eventually abandoned after it was determined that there was no demand for it on EL 7. Also on EL 7, we added or improved upon systemd integration for some components, however this project is still in progress.

Reviewing the Software team's major goals for the year:

- **Routine updates and support.** In its central role, the Software team continued to support the careful growth of OSG sites and technical capabilities. During the year, the team added nine packages that were requested by end-users or were required for the health of the software stack, and out of over 400 completed work tickets, 146 were bugs, new features, or improvements. We also support sites as they install and configure software, handling dozens of support tickets per year; in particular, we helped sites such as Cancer Computer, University of Utah, and Rio de Janeiro State University add their resources to the OSG.
- **Support Security-Enhanced Linux (SELinux).** SELinux is a security layer that manages software permissions that is enabled by default on EL 7. To support the OSG community's migration to EL 7, the team had to ensure SELinux compatibility with the entire OSG software stack. After initial investigation, the scope of this project was greatly reduced as only a few upstream packages were affected. The extent of OSG Software team effort was limited to assisting upstream developers as necessary and adding the ability to enable SELinux in our automated test suite.
- **Madison Integrated Test Bed (ITB).** To better reflect the makeup of a site in the OSG today, the team redesigned and redeployed the core nodes of our ITB. Maintaining an up-to-date installation of our own software stack gives us insight into usability issues that would not normally make their way into bug reports.
- **Documentation renovations.** This year, the team focused on writing documentation for new software components as well as maintenance and cleanup of existing documentation; cleanup is a particularly important task since outdated documents contribute to noise in user search results. The large-scale projects, however, were put on hold as we explored modern replacements for the TWiki documentation. We eventually settled on a MkDocs implementation hosted on GitHub with the transition slated for this year.
- **Year 5 internal maintenance.** This year saw major changes to the team's key internal infrastructure, including a major version update to our Koji build system as well as a move to Git and GitHub for version control of OSG-owned software.

- **Improve automated testing.** The team maintains a software system to test the integrated software stack automatically every night and on demand. Over the past year, we improved our coverage by adding tests for the GSI-OpenSSH tools and the Slurm batch system, which is seeing increased adoption among OSG sites. The test suite itself was made to be more expressive with fine-grained controls that allow developers to manage test ordering and organize test environments into logical sets. Additionally, we implemented some continuous integration tests that provide quick and automatic feedback for any code changes.

In sum, the Software team continued to help the OSG grow its user base by supporting the OSG technical infrastructure and its range of technical capabilities through timely and effective updates of the OSG software stack.

Looking forward, the Software team will continue to deliver new and updated software with minimal disruption to the production facility and to respond briskly to user support requests, security updates, and critical bug fixes. Further, the team will introduce new technologies that will help enable the expected growth and diversity of the facility in coming years. A selection of key initiatives follows:

- Enable growth of OSG computing resources through a streamlined software stack. In OSG 3.4, the team expects to drop unsupported GRAM packages as well as releasing software that consolidates job authentication technologies, both of which will greatly reduce the size of the OSG CE and worker node clients.
- Enable greater diversity of users by supporting new technical capabilities such as Singularity, whose containers provide a uniform runtime environment for researchers.
- Improve quality of software releases by using the team's ITB site to test pre-releases of OSG software in a production-like environment.
- Support accounting infrastructure migrations to technologies designed specifically for the OSG such as the CE-collector information service and the GRACC accounting system.
- Support the growth of OSG computing by continuing to maintain integrated, well-tested, production-grade software and supporting sites with current and usable documentation.

### 3.3 Release Management

The OSG Release team performs a set of activities related to software releases: assessing the quality of software prior to release; defining the schedule and contents of software releases, based on demand for and readiness of software updates; and completing the technical steps of issuing software releases. Primarily, the team tests software and packaging changes from the Software team, employing both general regression tests (to check that pre-existing functionality is preserved) and specific tests of the changes (to check that the changes are effective). When possible, software is tested in environments that mimic production deployments, and, as needed, by real users with production-like resources. Accepted software changes are gathered into releases — usually once a month — which the team produces along with accompanying release notes. To fulfill its mission, the Release team works closely with the Technology, Software, Security, and Operations teams.

In the past year, the Release team made 20 software releases across two release series, averaging about 25 changes (varied in size) per release. Consistency was the team's primary focus throughout the year — in testing each change, in defining and creating releases, and in writing release notes. To achieve the consistency that OSG sites expect, the team maintained, updated, and followed a set of detailed internal processes. For manual testing, the team writes and maintains test recipes for various software components, and several recipes were added.

This year, we added data-only releases. Updates to certificate authorities and VO data do not always line up with our software release schedule. Using data-only releases gives up the flexibility to adopt these changes quickly. In addition, when the previous series is receiving security updates only, it is better to identify these updates as data-only. We made two releases identified as data-only releases this year. However, the last six releases of the OSG 3.2 series were essentially data-only releases.

To attempt to measure the effectiveness of the Release team on overall OSG software quality, this year the team tracked when acceptance tests failed, thereby requiring that software or packaging changes be fixed before use in production. During the year, ten changes — or roughly 3.3% of all changes — failed tests and were sent back to the Software team for rework. Certainly, catching these test failures improved the quality of production releases, as each one could have affected production users otherwise. But the significance of the changes and their failures varied considerably, from trivial to critical, leaving open the question of overall effect.

More generally, though, it is difficult to measure sources of quality (or lack thereof) in OSG software releases. Defects in the field are reported inconsistently and in many forums, including support tickets, emails, and phone calls. Further, identifying clear blame for each defect is challenging, as any particular change may be touched by many people and groups. Thus, the characterization of release quality is still anecdotal and qualitative. That said, the past year saw relatively few quality issues that were clearly attributable to failures or omissions by the Release team. For instance, no special releases were needed outside of the usual monthly schedule. This track record is a positive indicator for the Release team, but further tracking and metrics would help tease out the relationships between production failures and root causes.

### 3.4 Operations

The OSG Operations team provides the central point for operational support and coordination for the infrastructure needed to sustain the OSG ecosystem. OSG Operations publishes real-time status information about OSG resources; supports users, developers and system administrators; maintains critical grid infrastructure services; provides incident response; and acts as a communication hub. The goals of the OSG Operations group include: supporting and strengthening the autonomous OSG resources, building operational relationships with peer grids, providing reliable grid infrastructure services, ensuring timely action and tracking of operational issues, and assuring quick response to security incidents. During the last year, OSG Operations continued to provide the OSG with a reliable facility infrastructure and community support while at the same time adding and improving services to offer a more robust toolset to stakeholders.

OSG Operations actively supports US LHC activities and will continue to refine and improve our capabilities for these stakeholders. OSG Operations attends WLCG Operations meetings and face-to-face events when possible to assure strong communication between the OSG and WLCG Operations groups. OSG Operations was heavily involved in the Information Services Working Group of the Worldwide LHC Computing Grid which lead to the retirement of an obsolete Information Service and adoption of a new HTCondor Collector service. This led to a more efficient exchange of vital resource matchmaking information. We also actively track and push to resolution issues reported by the WLCG community by synchronizing our problem ticket systems. As OSG Operations supports the LHC data-taking phase, we continue to meet the high expectations for service reliability and stability of existing and new services.

The OSG Networking Datastore continued stable operation and a new Custom Mesh Configuration service was deployed based on development from the perfSONAR working group. Capacity was also increased on the OSG Network Datastore to deal with continual new data provided by perfSONAR probes. This service consists of an Apache Cassandra database and several data visualization frontends.

This service also publishes network statistics to CERN and the WLCG, providing a worldwide snapshot of networking within the LHC compute community.

OSG Operations also supported and maintained the OSG Certificate Authority which uses CILogon signing to issue user and service certificates. This is integrated with the OSG Information Management service.

During the last year, OSG Operations continued to provide and improve tools and services for the OSG. These include:

- Exceeded expectations for service availability and reliability as defined by Service Level Agreements.
- Continued to operate the OSG GlideinWMS factory, which is the primary submission infrastructure in OSG. During this reporting period OSG Operations concentrated on efficient usage on existing sites rather than growing the number of resources.

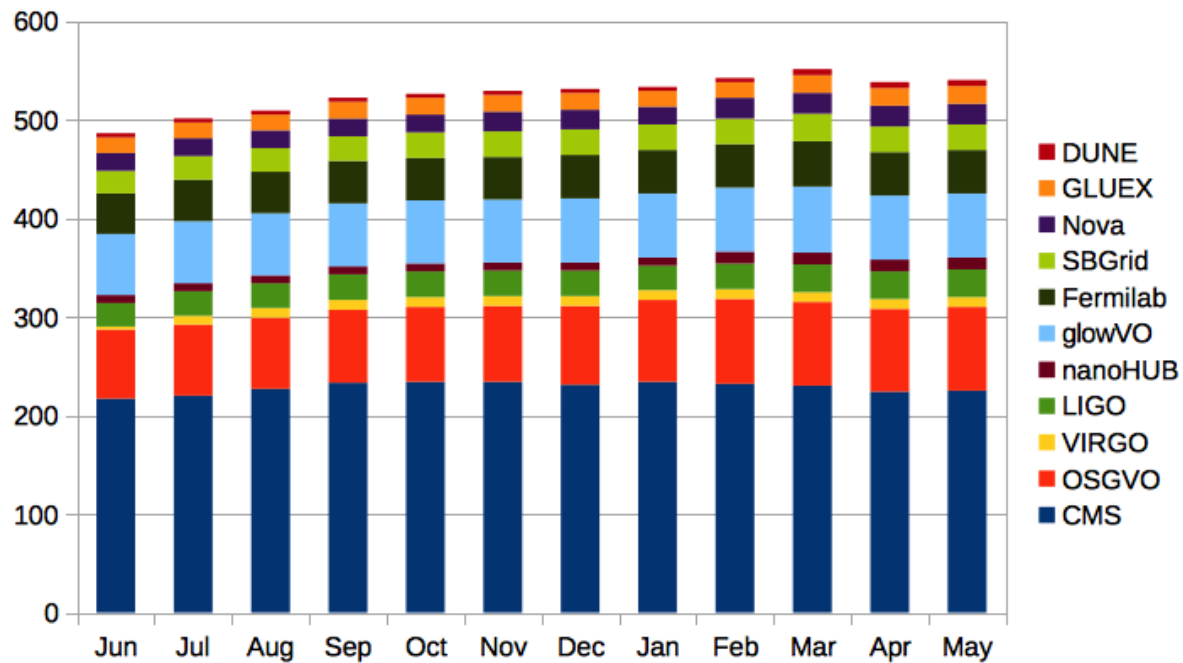


Figure 28: OSG GlideinWMS factory resources per virtual organization (VO)  
(VOs share resources so each resource may be counted more than once in this chart)

- Operated the OSG PKI Front-End service allowing users to request certificates via the OSG Information Management (OIM) service. OIM's administrative interface issues and tracks all certificate-related activities.
- Processed more than 289 million accounting job records and 1.37 billion transfer records totaling 122 PiB of data transfers in OSG.
- Transitioned from the Gratia accounting service to the new GRÅCC accounting service based on Elasticsearch and Grafana.
- Closed over 4,300 customer tickets.

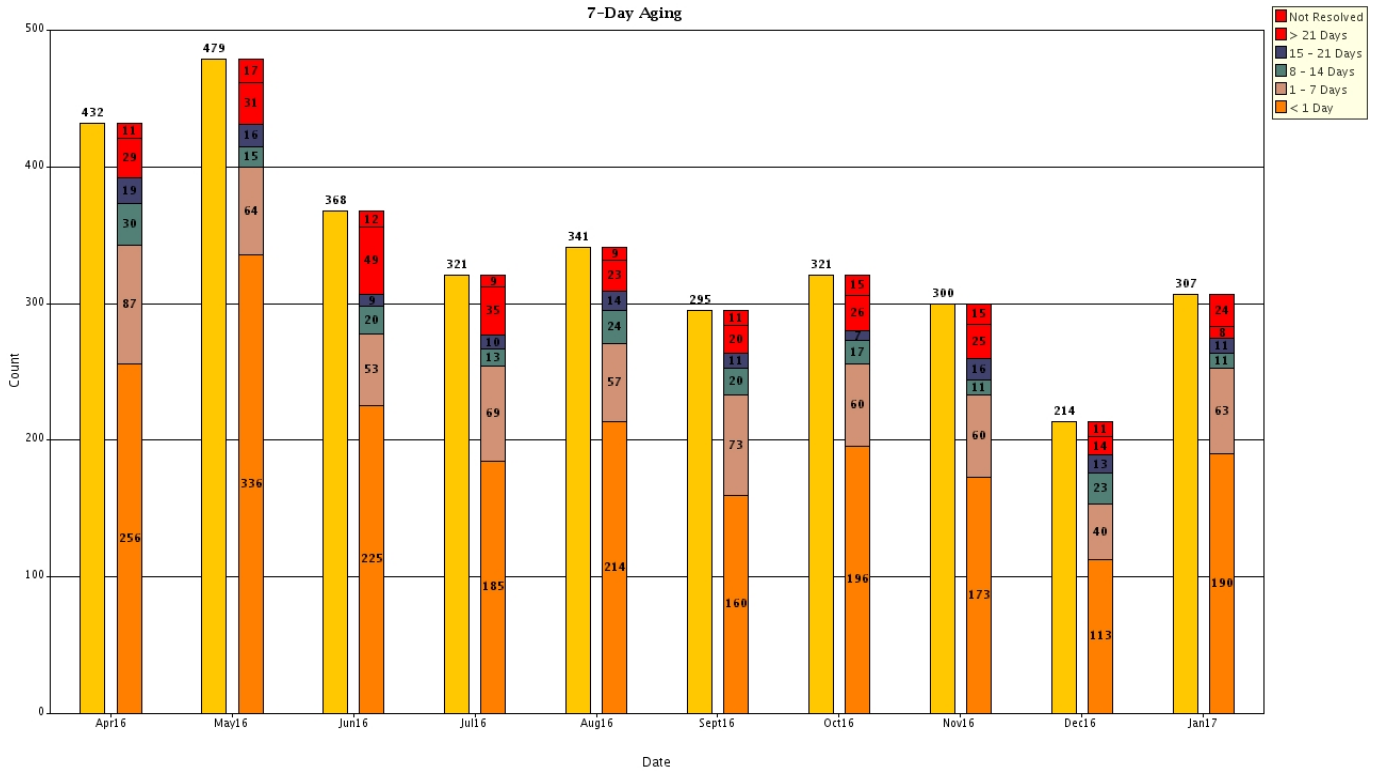


Figure 29: OSG monthly ticket activity, April 2016 through January 2017

- Continued our partnership with WLCG and EGI operations groups. This included working on change management for our shared services (ticketing, monitoring, and accounting) and attendance and presentations at major peering partner events.
- Began research on a single sign-on (SSO) solution for OSG operational and web services. This includes talking to several collaborators and is moving toward initial development partnering with CILogon 2.0.
- Began transitioning documentation from the Production and Operations TWiki sites to GitHub.
- Operated and participated in the implementation of:
  - perfSONAR, a network metric datastore. The GOC maintains the hardware for this service and operates multiple instances of data visualization and storage instances.

- StashCache, a global file system implemented using the XRootD protocol. Two instances forming a high availability pair serve as the redirector for this service.
  - HTCondor Collectors, a central HTCondor-CE information gathering component. These implement the collector component of an HTCondor compute element.
- We continued efforts to improve service availability via the completion of service upgrades:
  - Updated the operating system for all services running on Red Hat Enterprise Linux (RHEL) 5 to meet the end-of-support date (3/31/2017).
  - Updated the operating systems to latest RHEL7 versions and virtual machine host software to assure consistency of service environment.
  - Moved final legacy components from old software content system ([software.opensciencegrid.org](http://software.opensciencegrid.org)) to new system ([repo.opensciencegrid.org](http://repo.opensciencegrid.org)).
  - Continued to maintain high availability for the XD-Login submission node. Currently this service has over 2,400 registered users and operates at greater than 99% availability.
- Due to being late in the lifetime of the grant new hardware purchases were avoided if possible. However, we did update storage capacity for the OSG Network Datastore to allow collection for several more years of data.

### 3.5 Network Monitoring

Networks are fundamental to the use and operation of grid systems, yet they are treated as an external black box in grid operations, with no awareness of the network state and no possibility to manage or prioritize traffic to optimize the performance and efficiency of the overall grid system. During this fifth year of the OSG networking area, we made the OSG networking services production while continuing to integrate network monitoring into OSG (in much the same way as storage systems and clusters have been) to deliver an ensemble-system capable of robustly serving scientists using OSG.

The goal of this OSG network activity is to define a set of services and functionality which transform the current best effort networks into a managed component of the OSG. Our intent is to enable OSG to become the source of needed network metrics for OSG sites and for our partners (like WLCG). Over time, we intend to augment the OSG software stack with a monitored, managed network component, building upon the tools and framework already existing or planned in OSG wherever appropriate and extending those capabilities as required.

The primary goal for Year 5 in network monitoring was to put our network datastore service into production and begin to integrate analysis and alerting on network metrics. Building upon our work in year 4 to instrument grid sites with OSG and WLCG we have worked to deliver a robust way to gather, store and serve the various network metrics the infrastructure was capable of providing.

During Year 5 we have some very specific goals for OSG Networking.

1. Maintain / update the OSG networking services / documentation.
2. Reach out to non-WLCG OSG sites; and integrate those interested:
  - a. Advertise that OSG is ready to help sites with networking issues via OSG web pages, targeted email (cyberinfrastructure list, perfSONAR user list, etc.), and via interactions with sites at conferences and meetings.

- b. Encourage as many NSF CC\*xxx sites as possible to integrate their perfSONAR instances into OSG networking; OSG provides them a mesh-configuration and gathers their data.
  - c. Provide standalone mesh-configuration tool for use by campuses and VOs.
- 3. OSG will create a network alerting service to find obvious network problems:
  - a. This will involve the creation of a suitable analysis pipeline such that perfSONAR data can be analyzed on a timescale of every 1–2 hours.
  - b. Obvious problems include significant decrease in bandwidth between a source and destination or continuing significant packet loss along a path or correlated with a specific site.
  - c. Actual alerts will be issued by GOC staff based upon alarms they receive.
- 4. Enable automated alerting (email, SMS) on well identified alarms.
  - a. This was a stretch goal for the year but we feel we can deliver some capability here.
  - b. Requires accurate, synchronized mapping of sites to contacts.
  - c. Tunable pattern of alerts (e.g., 1 alert, wait 1 day and alert if problem continues, then every 3 days until fixed).

As of April, 2017, we have 249 registered, active perfSONAR instances worldwide which we track with daily updates at [http://grid-monitoring.cern.ch/perfsonar\\_coverage.txt](http://grid-monitoring.cern.ch/perfsonar_coverage.txt). Each of these instances is controlled centrally via OSG’s mesh-configuration service (see <https://meshconfig.grid.iu.edu/>), which defines the tests to be carried out. The test metrics are gathered by OSG using perfSONAR RSV probes which feed the data into the OSG Network Datastore and publish those metrics into a message queueing system hosted at CERN. We have ATLAS and LHCb clients consuming the OSG datastore metrics to use for problem diagnosis and higher-level decision support workflow planning. We are developing tools and infrastructure to take the next step and support alarming and alerting on network issues.

Summary status for each of the goals follows.

- Goal 1: Maintain / update the OSG networking services / documentation—Ongoing
  - Ongoing updates to OSG documentation—incremental updates all year
  - Service evolution, minor updates—incremental updates all year
  - Hardware for OSG (doubled storage)—completed April 25, 2017
  - Mesh-Config Administrator (MCA) standalone package—completed April 30, 2017
- Goal 2: Reach out to non-WLCG OSG sites; Integrate those interested —Dec 1, 2016: delayed
  - Outreach is dependent on both MCA (see above) and perfSONAR 4.0 which was released 6 months later than expected (mid- April 2017)
  - We have continued to advertise OSG network services in many venues.
  - New milestone is to undertake a recruitment campaign in summer 2017.
- Goal 3: OSG will create a network alerting service to find “obvious” network problems.
  - Network alerting service prototype was finished in Fall 2016

- Using our perfSONAR metrics we scan all of a site's source-destination paths looking for packet-loss above a threshold and produce a continually updating alarm table.

We also have progress to report on our stretch goal:

- Goal 4: Enable automated alerting (email, SMS) on well identified alarms.
  - Network alerting service prototype was finished in December 2016.
  - We have developed a service that will alert users via email when sites they are monitoring appear in the “alarm” table (Goal 3).

There are a few related activities to report progress in. One of the most important items to note is that we have used the OSG perfSONAR monitoring infrastructure to identify and fix network problems involving a number of OSG institutions as well as globally for sites and networks of importance to OSG members. Both ATLAS and LHCb continue to use the data OSG is gathering as input to their distributed infrastructure management systems. Details of both efforts and related OSG work are documented in the 2017 International Committee on Future Accelerators, Sub-Committee on International Connectivity network monitoring report at [http://icfa-scic.web.cern.ch/ICFA-SCIC/documents/ICFASCIC2017\\_MonitoringGroupReport.pdf](http://icfa-scic.web.cern.ch/ICFA-SCIC/documents/ICFASCIC2017_MonitoringGroupReport.pdf)

Some further information on the new version of the mesh-configuration software used by OSG to organize and control the set of network tests carried out by the perfSONAR instances. OSG networking with the help of Soichi Hayashi/IU finished an easily installable version called MCA. The original version was built into the OSG OIM and MyOSG deployments which had a number of shortcomings: it depended upon a complicated, large software infrastructure which couldn't practically be deployed anywhere else and it was not easy to update or modify the software capabilities. The new release supports easy installation outside of OSG and will allow OSG campuses and virtual organizations to deploy and manage their own perfSONAR network monitoring instances. As of May 2017, the OSG test instance (<https://meshconfig-itb.grid.iu.edu>) is running the new MCA and the replacement of the production instance will be transitioned to <https://meshconfig.grid.iu.edu> before June 2017.

Last thing to note is that the release of perfSONAR 4.0 included many new features and a re-architecting of the toolkit itself. This meant that OSG needed to update its monitoring systems. We choose to upgrade our OMD/check\_mk instances to instead use the newly developed Experiments Testing Framework (ETF) from WLCG. We have implemented and tested “etf\_ps” to replace our existing monitoring. Details are at <https://hub.docker.com/r/mbabik/etf/>

We have a number of challenges in our network monitoring work. The network datastore service that is run by OSG is a much more complicated service than is typically deployed by OSG operations and this has led to some issues when problems arise. We originally followed the perfSONAR developers and used esmond as the long-term archive for our network metrics. esmond, a combination of PostgreSQL and Cassandra, has been problematic to maintain and easily use for analyzing our data. Now that perfSONAR 4.0 is released and noting that it includes RabbitMQ (a message queuing system) it may be possible to re-architect how OSG gathers, distributes and makes available network metrics.

Another ongoing challenge is to keep the almost 250 perfSONAR servers updated, secured, and functional. Related to this we have updated and improved our extensive monitoring of the end-sites to help us identify problems and aid end-sites in quickly resolving them but it still is somewhat people-time intensive to maintain proper operations.

For next year, we want to improve our ability to exploit analytics on the gathered network metrics, improve the data acquisition and storage, and augment the alerting system we have prototyped. During

Year 5 we focused solely on finding problems via packet-loss but there are many additional signatures of network problems and bottleneck identification possible with the rich dataset we are continually acquiring. As noted above, the new perfSONAR 4.0 release provides us with an opportunity to re-architect how data is acquired and made available for use via OSG. We intend to explore using the RabbitMQ capability of each node to publish data to OSG and store that data in Elasticsearch rather than esmond. This should have two immediate benefits: 1) the data should be accessible in minutes, rather than tens of minutes and 2) the data will be directly accessible for analytics. The self-subscription model for alerts seems to be practical, and we will augment the basic system we have with additional options for end-users, network managers, and site-admins to customize the type and frequency of alerts they will receive. A primary metric of success will be the change in the number of problems (alerts) we generate, indicating that real network issues are being identified and fixed.

## 3.6 Security

The OSG is incredibly diverse in its resources, geography, and user base, presenting complex challenges with regard to cybersecurity. OSG's Cybersecurity Team is tasked with enabling OSG's mission by providing security expertise and support to OSG's operational systems and distributed software. This involves ensuring that resource providers and users can take leverage their institutional cybersecurity resources.

### 3.6.1 Overview

The primary areas of OSG's Cybersecurity Team activity are:

- To work with other teams in evaluating and planning new features or other systems changes that may impact security;
- To provide services to support the security of OSG, such as certificate bundling, and an annual risk assessment; and
- To provide incident and vulnerability response support for OSG.

Additionally, the OSG Cybersecurity Team undertook the following special projects in Year 5:

- Handoff of cybersecurity leadership from Fermilab to Indiana University
- Move the CVMFS master key to a hardware security module
- Assist the Technology Area in establishing a secure mechanism for automated host cert issuance
- Create a proof-of-concept process for static analysis of OSG software
- Perform a comprehensive review of OSG's security program

### 3.6.2 Security Process

OSG implements integrated security management, the notion that primary responsibility for security rests with those managing systems, software, and processes within OSG. The OSG Cybersecurity Team acts as a resource to these groups, aiding in risk awareness, controls implementation, remediation of problems, and consulting with teams to provide them with security expertise for their work. The Cybersecurity Team reports, internally and externally, on OSG security matters, ensuring that stakeholders can make informed cybersecurity risk decisions. Finally, the team coordinates with XSEDE, WLCCG, EGI, REN-ISAC, and others to share threat information to stay on top of the evolving security needs of the OSG.

### 3.6.3 Certificate Bundling

Maintaining releases of OSG's certificate authority (CA) bundle, which is based on the Interoperable Global Trust Federation (IGTF) bundle, is essential to the security of the grid because it enables OSG resources to accurately identify trusted hosts, and know when a certificate has been revoked (for example, due to compromise). Previously, certificate bundles took a great deal of manpower to generate (a full day or more each month). This year, OSG Cybersecurity Team began to automate the bundling process, bringing down the time to a few hours. We expect the time to be less than an hour within a year of continued development.

### 3.6.4 Risk Assessment

OSG Cybersecurity produced a risk assessment this year identifying cybersecurity risks throughout the project based on input from Area Coordinators and their staff.

### 3.6.5 Incident and Vulnerability Response

The need for incident and vulnerability response in OSG has increased significantly in Year 5 compared to the previous year. The Cybersecurity Team attributes this to increased awareness of OSG's security needs as well as more active pursuit of vulnerabilities in many software packages relied on by OSG.

### 3.6.6 Vulnerability Comparison

**Table 2: OSG vulnerability incidents**

Vulnerability found in:	Year 4	Year 5
Operating System	0	1
Libraries	4	6
Grid Software	2	5
<b>TOTAL:</b>	<b>6</b>	<b>12</b>

### 3.6.7 Incident Comparison

#### Security Incidents in Year 4 (2):

Security issue with HDFS installations at US-CMS T2 sites. The report was received from WLCG Security Officer Romain Wartel on May 9th, early morning. CERN was contacted over the weekend by a third party, regarding a number of exposed CMS Hadoop instances.

Denial-of-Service attack against opensciencegrid.org website.

#### Security Incidents in Year 5 (3):

Denial-of-Service attack against GOC ticket system.

OSG website was defaced to advertise “cheap fake oakley sunglasses”.

A security incident was detected at CLUSTER.USTC.CN. There was no impact on grid resources since these machines were not in the same network as grid nodes. A keylogger was also installed, recording some login credentials. Access to AGLT2 and U. Michigan machines using stolen credentials were discovered.

### 3.6.8 Other Goals

Knowledge transfer for the handoff of Cybersecurity Team leadership from Fermilab to Indiana University was accomplished this year by improving documentation and automation for Cybersecurity Team functions and resources, retaining some of the previous-year staff going forward, and a temporary overlap in duties between the outgoing and incoming Information Security Officers. By employing this combination of strategies, we have been able to ensure a smooth hand-off with a minimum of disruption for OSG.

Testing of YubiKey 4 modules for managing SSL certificates is complete, and YubiKeys are about to be deployed to protect the CVMFS master key from potential compromise. Previously, OSG used a “load, unload” scheme to reduce the time window in which the master key was exposed to Internet-connected servers. However, this strategy has its faults: Primarily, that it still leaves the master signing key open to theft if a server vulnerability is found before or during its use. Once the key is stored only on the YubiKey modules, someone breaking into one of the relevant servers could at most cause something to be signed with the CVFMS master key, but not obtain the key itself. Thus, any malicious signatures could only be created while an attacker controlled the server, and OSG could safely continue use of the key, knowing it has not been taken by the attacker because it was never present on the server. This is the primary advantage of storing the key only in an external, USB-connected security device.

The Cybersecurity Team and Technology Area continue to work together on the host certificate issuance problem, and hope to have a proof-of-concept solution ready to begin final testing and deployment in Year 6.

The Cybersecurity Team has established a process for applying static analysis techniques to software relied upon by OSG (both internally developed and externally developed software). Initial results of static analysis have been provided to relevant developers for feedback and remediation. Outcomes from this proof-of-concept analysis project may be used to design a continuous software assurance procedure for OSG should it be deemed useful.

A comprehensive review of the OSG Security Program was performed by the incoming Information Security Officer. It will be presented, along with recommendations, at the upcoming OSG Area Coordinators’ meeting in preparation for Year 6.

## 3.7 Production Support

The area of production support is dedicated to providing access to DHTC to communities and organizations above the scale of individual researchers (who are supported by the OSG User Support and Campus Grids Area) and also increasing the availability and access to opportunistic resources. Furthermore, production support provides guidance and oversight in the process of onboarding new sites to the OSG.

The availability of opportunistic computing cycles is potentially challenging as the computing needs of ATLAS and CMS, whose sites constitute a majority of OSG resources, increase with Run 2 of the LHC beginning in 2015. As seen in

Table 3, total opportunistic computing on the OSG has again increased, although the pace of increase is somewhat smaller (note that mu2e usage only shows non-Fermilab, and thus opportunistic, sites).

**Table 3: OSG opportunistic usage and trends**

Virtual Organization	2012	2013	2014	2015	2016
osg	3,168,025	47,931,106	97,138,495	125,607,605	159,463,159
glow	16,924,657	15,896,802	23,284,533	29,181,727	34,147,653
engage	18,610,782	7,673,167	1,680,835	-	-
sbgrid	2,271,005	4,194,011	2,558,253	3,392,649	1,266,146
hcc	5,017,649	3,693,243	639,626	356,084	2,749,174
gluex	5,257,905	106,317	4,941,831	65,481	110,850
mu2e	-	-	-	46,226,574	18,259,145
<b>Total Hours</b>	<b>51,250,023</b>	<b>79,494,646</b>	<b>130,243,573</b>	<b>204,830,120</b>	<b>215,996,127</b>
Annual growth rate	51%	55%	64%	57%	5%

In 2016, we continued to focus on adding new sites to the OSG that are not used, and to optimize and increase opportunistic access to existing sites. In 2016–2017, we added six university sites which contribute resources to the OSG resource pool, and are continuing to expand this pool in 2017. The development of the OSG Hosted-CE infrastructure has greatly simplified this task and should enable additional sites to participate in the OSG that otherwise might not due to insufficient support resources.

We also continue to support all VOs in efforts to increase their use of OSG services, including both dedicated and opportunistic computing resources. One of the most significant new trends in 2016 was a marked increase in opportunistic resource consumption by both ATLAS and CMS. As the largest two VOs, they each control a large fraction of OSG resources, and opportunistic running has not been a significant priority for them in the past. As this has become a larger priority for both experiment, their opportunistic resource usage does create a noticeable effect on opportunistic resource availability. Overall opportunistic hours were still increasing across the OSG throughout 2016, but during the last few months of 2016, VOs that typically use a significant amount of opportunistic resources saw their overall totals drop. After the release of LHC results for the 2017 winter conferences, opportunistic hours for non-LHC VOs resumed their increase. We expect to see similar spikes for the LHC VOs when they are engaged in conference-result preparation for both the summer and winter conference seasons.

The Mu2e Collaboration at Fermilab, a proposed experiment designed to make precision muon-to-electron conversion measurements, has continued their highly successful use of opportunistic cycles that began in spring 2015. By the end of 2015, Mu2e was the fourth largest VO on the OSG by overall production. During 2016, Mu2e consumed over 40 million payload wall hours, with over 60% of those coming from resources outside of Fermilab. This dramatic increase in resources allowed Mu2e to meet all of their stretch computing goals in 2016 and contributed heavily to their receipt of full CD-3 approval from the DOE in July, 2016.

In late 2015 and early 2016, OSG staff members also worked with the Dark Energy Survey (DES) experiment to port a computational workflow intended to perform searches for electromagnetic counterparts to LIGO triggers. This framework requires utilization of tens of thousands of cores in approximately 12 hours and was successfully exercised during the observation of LIGO’s first gravity wave event. This same work was also extended to the transient object search framework that led to discovery of a dwarf planet, and to the ongoing search for the hypothetical Planet Nine. The AMS experiment on the International Space Station had a very successful compute run on the OSG in 2016, consuming over 20 million CPU hours.

In addition to supporting sites and communities seeking to provide and access opportunistic resources, we also enabled access to dedicated computing resources by means of OSG infrastructure and tools to VOs who seek them. In particular, collaborations whose primary computing footprint is in existing OSG sites but are seeking access to resources outside of North America have taken advantage of this by connecting those resources to the wider OSG infrastructure (as ATLAS and CMS have from their inception). In particular, the NOvA experiment at Fermilab has connected resources in both the Czech Republic and Russia to their OSG-enabled submission infrastructure, while the MicroBooNE experiment has done so with resources in Switzerland and the UK. We are currently engaged in commissioning support for the DUNE experiment at several sites in the UK. The IceCube experiment is now also able to access some dedicated resources in Europe. In addition to laboratory or university resources, some experiments also have access to allocation-based High-Performance Computing resources such as the EXtreme Science and Engineering Discovery Environment (XSEDE), and national supercomputers such as NERSC. Both the CMS and MINOS+ experiments have successfully tested submitting jobs to their allocations on the Stampede cluster at the Texas Advanced Computing Center (part of XSEDE) via the standard OSG software submission infrastructure.

Production support has also re-engaged with two VOs that had previously used OSG but had run very little in recent years. The LSST VO has re-established some job submission infrastructure and is flocking jobs to the OSG user pool, and the GlueX experiment is ramping up for a large production run when their upgraded detector resumes operations in summer 2017. GlueX is pursuing multiple strategies at once with OSG. We completed deployment and validation of a submission point at JLab in support of production operations for GlueX. We are engaging with multiple GlueX institutions to make their clusters available for GlueX via OSG, and thus also to production processing of jobs submitted from the JLab submission point. And we started discussions of deploying an XRootD data federation such that GlueX collaborators can access GlueX data at JLab conveniently from their home institutions.

Last year saw tremendous progress in the effort to overhaul the OSG accounting tools, especially in the user interface. These tools also report usage information to WLCG and XSEDE. The new system, known as GRACC, transitioned to production in April 2017.

### 3.8 User Support and Campus Grids

The OSG User Support team consists of staff from the University of Chicago, University of Southern California (USC) Information Sciences Institute (ISI), and the University of Nebraska. The primary goal of the user support team is to make sure that researchers are comfortable utilizing DHTC resources. To achieve this goal, the support team engages researcher groups in multiple ways:

- Interaction through a helpdesk system via web-submission, email and an online chat service.
- Creation of articles and training materials that serve as useful reference material for novice and advanced users.

- Installation and maintenance of application software packages and libraries which are distributed via OASIS to OSG sites and accessed using an OSG-tailored “modules” command so as to maintain a uniformity of environment across OSG sites.
- Consultation with researchers to help adapt workflows to the distributed environment of the OSG.
- Consultation with campus research IT organizations to provide guidance for connecting campus HPC resources to the OSG.
- “Facilitation for facilitators”, for example providing guidance to ACI-REF teams to access the DHTC environment of the OSG, through either dedicated webinars or delivery of sessions at the OSG User School.

In the past year, we deployed a help desk system to help managing support for a diverse user community in terms of institution, science domain, and workflow type. Figure 30 shows the breakdown for user support issues over a year from March 1, 2016, to March 1, 2017. During this time 1,123 support issues were resolved by the team. During the weekly team meetings, the support team reviews the system collected details and averages for response time, first response time, time to resolution, and so on. Some of these statistics are skewed by large numbers resulting from a few tickets that required additional effort and time from the support team to set up the software or workflow for the users. Support metrics for the year:

- 1,089 issues submitted
- 1,123 issues resolved (34 from previous periods)
- First response time average: 4 hours and 41 minutes
- Average resolution time: 43 hours
- Issues resolved on first contact: 65%
- Issues resolved within SLA limits: 83%

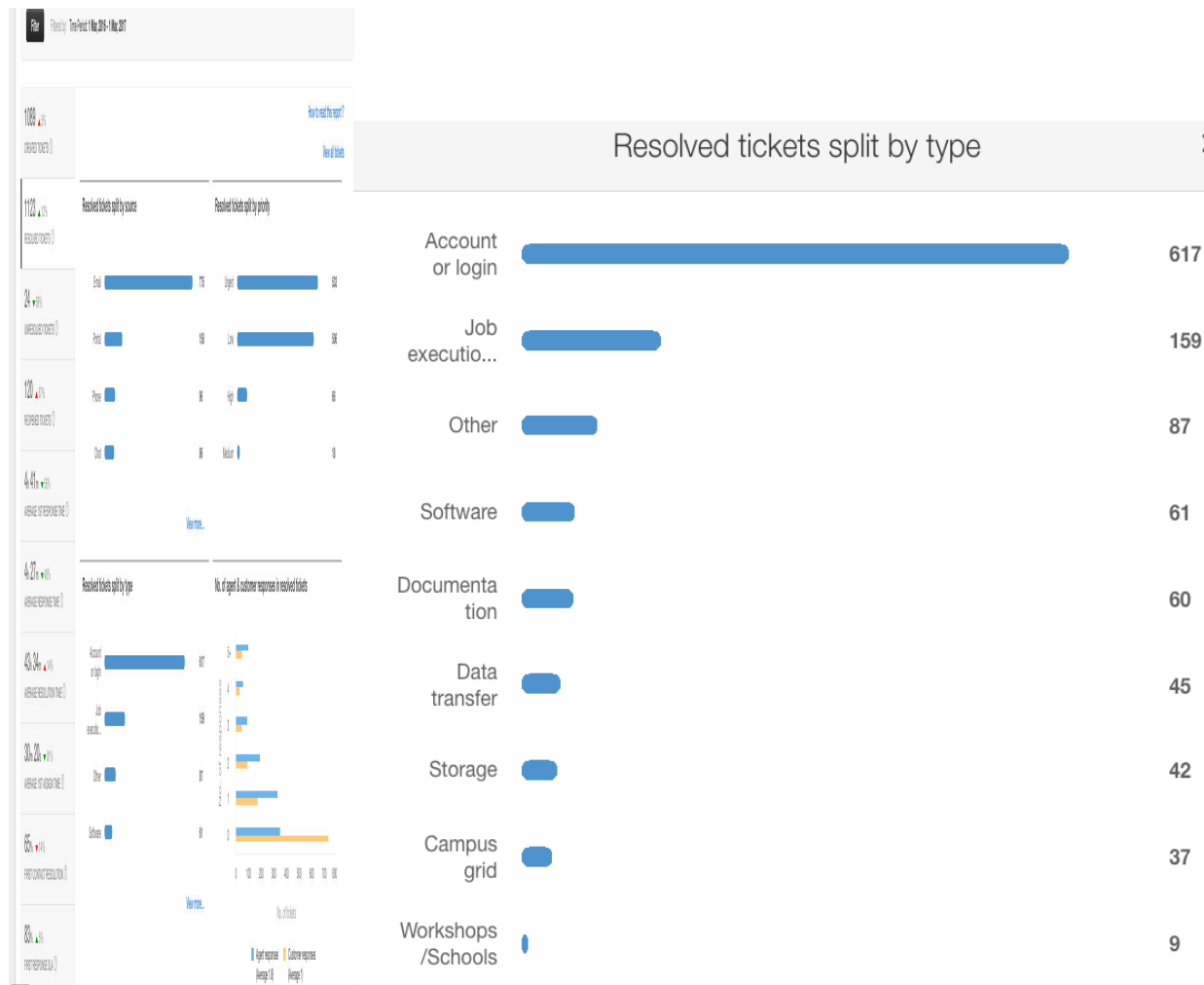


Figure 30: OSG user support metrics

The helpdesk ticketing system allows users to provide feedback on a resolved ticket. In the past year, 82 users provided feedback on their experience with the ticket support. Most users said that their user support experiences were positive (90% positive, 10% neutral, and no negative feedback as shown in Figure 31).

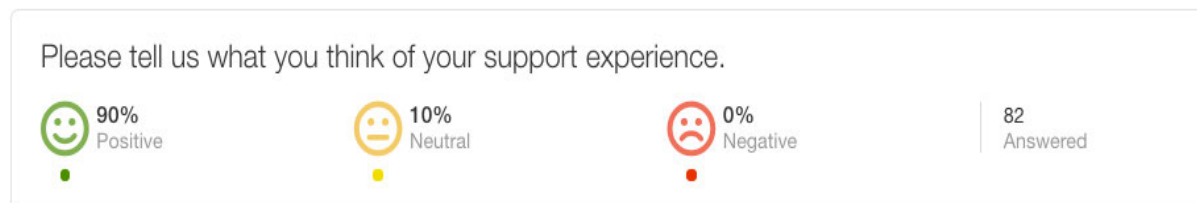


Figure 31: OSG user support feedback results

### 3.8.1 Support for the XSEDE User Community

Since April, 2012, the OSG has been operating as high-throughput XD service provider (SP) to the XSEDE community. OSG pledged 2 million service units per quarter, and individual PIs could submit allocation proposals via the XRAC process. OSG then operated an XD-login infrastructure accessible via the XSEDE web portal just like any other XSEDE SP. However, in contrast to a normal SP, OSG does not restrict the total hours a PI is allowed to consume. During 2016, OSG provided 32 million hours as XD SP to the XSEDE community via 29 projects.

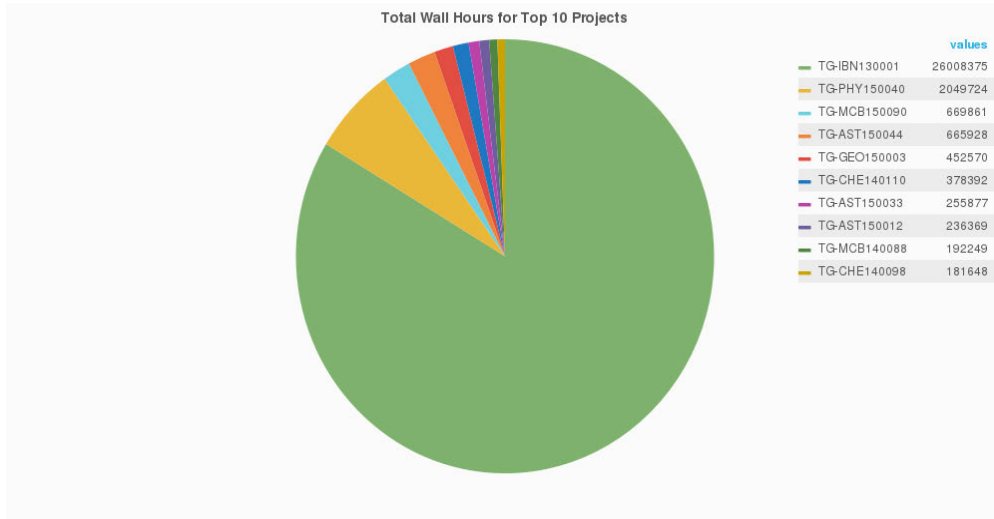


Figure 32: Top 10 XSEDE projects on OSG

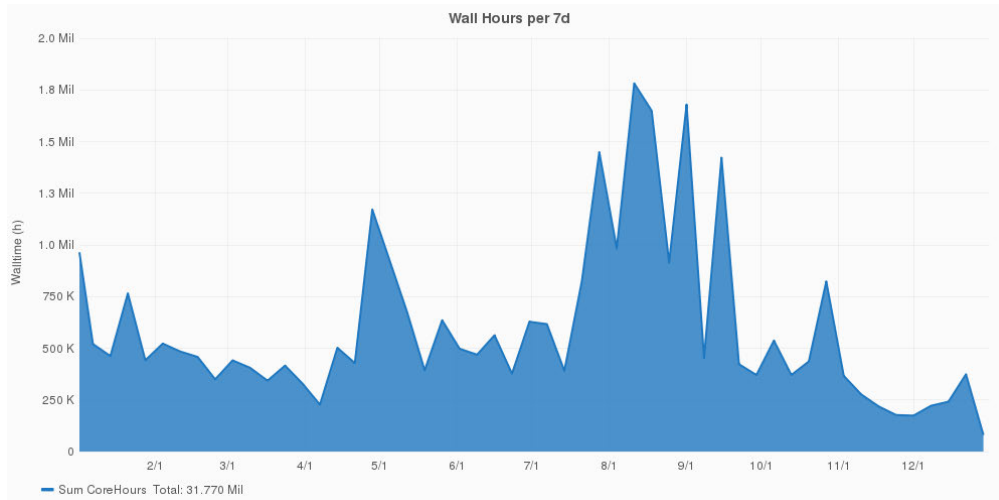


Figure 33: OSG XSEDE wall hours per week

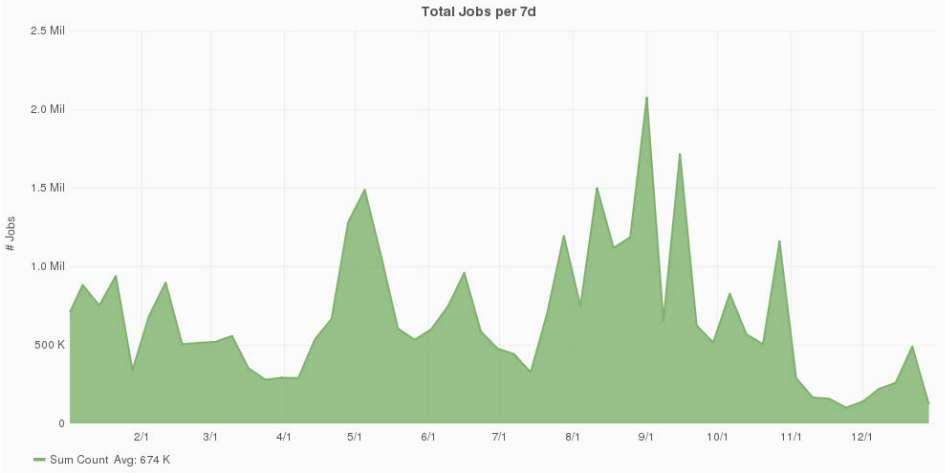


Figure 34: Number of OSG XSEDE jobs per week, showing variability of workloads

During 2015, OSG started two additional interactions with the XD program in support of the XSEDE user community. First, we allowed seamless integration of OSG SP allocations into the local submission infrastructure of customers following our principle of “submit locally, run globally”. Second, we allowed seamless integration of XSEDE allocations on other SPs to be serviced via OSG interfaces. The first two XD SPs where this was done are Comet and Stampede, as described previously in this report.

As a result of these additions, we now support seamlessly integrated operations of local, OSG, and XD resources allowing the use of multiple XD resources as part of a single workflow. For example, a single PI could now run a workflow that starts with some preprocessing locally, dispatching some part of the workflow for simulation on the Comet GPUs, and another on the Intel Phis at Stampede, only to assemble the outputs of both for further processing on OSG, and archive the results back locally. At present, none of the science we support is quite this complex in their workflows. However, IceCube has presently XSEDE allocations at two different XD resources, and a third allocation on OSG. Some of these allocations include GPUs, others do not. All of these resources are used in combination with resources at their home institution, UW–Madison, as well as at collaborating institutions in Europe. The entirety of this diverse pool of resources is accessed via OSG interfaces.

We expect this kind of operations increasingly to become the norm. For example, XENON1T, a liquid xenon direct dark matter detection experiment at Gran Sasso, Italy, that is jointly funded by NSF and European agencies, has resources in Europe, University of Chicago, and a Comet allocation, and is starting to use all of these resources via OSG; see details about this project below. We expect LIGO, SBGrid, and GLOW/CHTC to follow this trajectory.

### 3.8.2 New User Facilitation Model

The top priority of the User Support team is to aid new users in getting accustomed to DHTC principles. Designing a workflow or porting over an established workflow is frequently an obstacle for researchers new to OSG. To better facilitate newcomers, we have strengthened and expanded our on-boarding process. The document *Facilitation in the OSG Context* details a four-step orientation process that accompanies each account creation. The most significant changes made to the previous on-boarding procedure are:

- A two-part consultation with the new user

The initial consultation functions primarily to confirm the user's identity and get an overview of their research goals, expectations from OSG, and any known job requirements. The second consultation will be arranged a couple weeks to a month after the account is created (depending on the needs of the researcher) and will be more in-depth. It is meant to help the user troubleshoot and find creative solutions to any roadblocks they have encountered using OSG.

- Tracking of user engagements

Facilitating users well requires us to have as much possible background information and knowledge about each researcher's scientific goals and computing needs. To this end, user engagements are to be tracked for each account and used to develop rich and detailed user profiles.

### 3.8.3 Workshops and Training Events

The user support team organized a hands-on workshop entitled "Basics of High Throughput Computing and OSG Connect" at the University of California San Diego (UCSD) in March, 2017 (<https://swc-osg-workshop.github.io/2017-03-09-UCSD-AHM/>). The curriculum of the workshop was focused on DHTC principles. As part of this workshop, a brief demo on the job submission to AWS via condor\_annex was shown. It allows the OSG user to harness the power of cloud computing from a OSG login host. There were around 25 participants from science and engineering disciplines. The UCSD workshop was well received by the participants.

### 3.8.4 Support for Container Workflows

The User Support and Technology Investigation teams have been the driving forces to get widespread Singularity container support on OSG. The Software team packaged Singularity into an easy to install RPM. Compared to Docker (for example), Singularity is very lightweight with only a single RPM, no daemons, and no special privileges required to run containers. For these reasons, Singularity is a great choice for supporting containers on OSG.

The OSG VO's approach is now to run all jobs through containers on sites which have Singularity installed. Each job is started within a dedicated container for that job only. There is no sharing of containers between the jobs. This approach was purposefully chosen so when user wants to run a custom image, the same approach is taken with the only change being that we load a custom container instead of the default one. Default images are provided for CentOS 6 and CentOS 7.

Container images are distributed via CVMFS. A new repository, /cvmfs/singularity.opensciencegrid.org/, was created and a tool was implemented to sync a list of images from DockerHub. Images are downloaded, and extracted as directories and files onto the file system serving the CVMFS repository. The resulting file system tree can be given as a container to Singularity. A major benefit is that when a container is started, only parts of the full image needs to be loaded. For example, suppose a user wants to run a simple Linux echo command. Singularity will only have to read the directory entries for / and /bin (where echo is installed) and the echo binary. This is a small number of KB or MB, compared to the multiple GB if the image was one large file.

DockerHub was chosen due to the large number of existing container images published there. The Docker images are easily converted to Singularity images. In the future, the CVMFS sync tool could support importing container images of other formats.

In a distributed system like OSG, testing and validation of the compute nodes are very important to ensure trouble-free user job execution. With the introduction of Singularity, we had to improve this testing even more as more container execution brought new failure points. This testing takes place in each glide-

in's periodic advertising script. Every 5 minutes, this script is run, and the new tests validates the site's Singularity install, that the image distribution over CVMFS looks correct, and that simple Singularity containers can execute. If all the tests pass, a flag is provided to the job wrapper that the site is validated and that the job wrapper can start running containers.

To date, we have run 17 million Singularity containers. The following two graphs (Figure 35 and Figure 36) show the number of container instances per day and what percent of all jobs run in containers. The fluctuations are due to not all OSG sites supporting Singularity and when Singularity sites are more or less busy, it shows up in these graphs. The trend is still increasing with the last couple of weeks, more than 50% of jobs at any given time have run via Singularity.

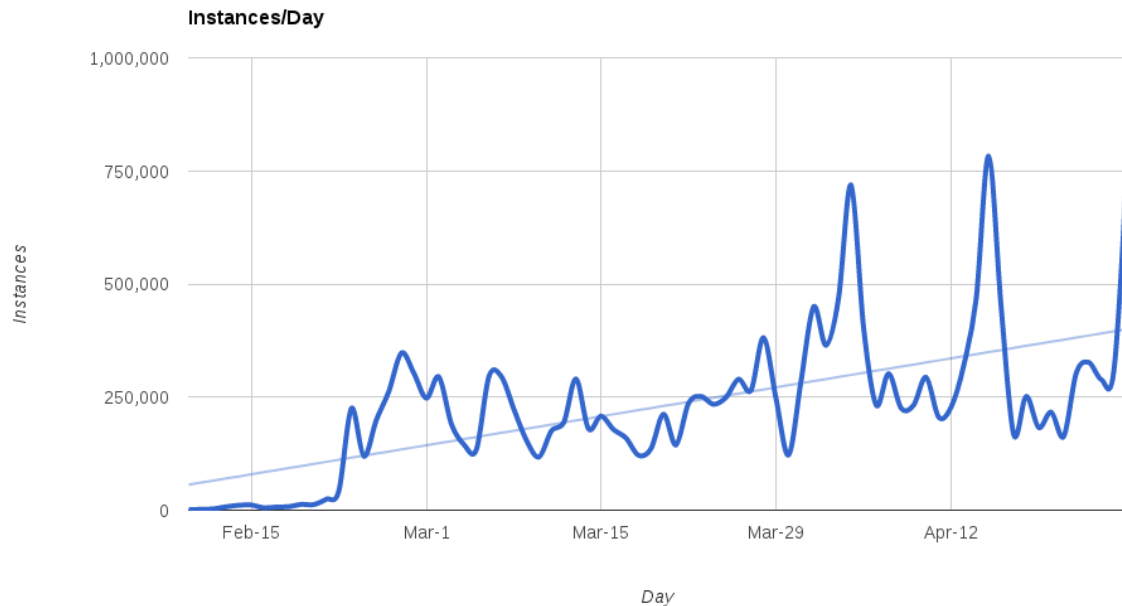


Figure 35: Number of OSG Singularity container instances executed per day

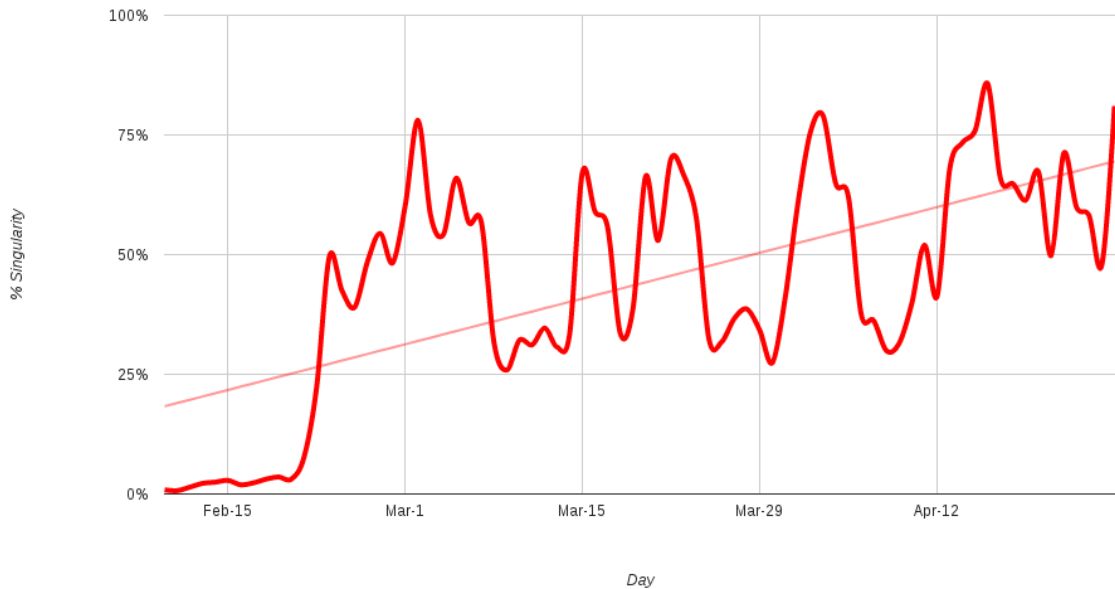


Figure 36: Percent of OSG jobs running inside of Singularity containers

### 3.8.5 Hosted Compute Elements

Running an OSG site has historically required fairly significant contributions of time and effort from the hosting institution. Staff at the institutions need to learn to install, configure, maintain, and troubleshoot the software in the OSG stack. This can sometimes require a significant investment of time and effort. In addition, without adequate training of backup personnel, the departure of a single staff member can result in an institution's site going down due to a lack of expertise. Even when an institution devotes the time and effort to contribute computing resources to OSG, it can take weeks or even longer for staff at the site to configure the OSG software to allow jobs from OSG users to successfully run at their site.

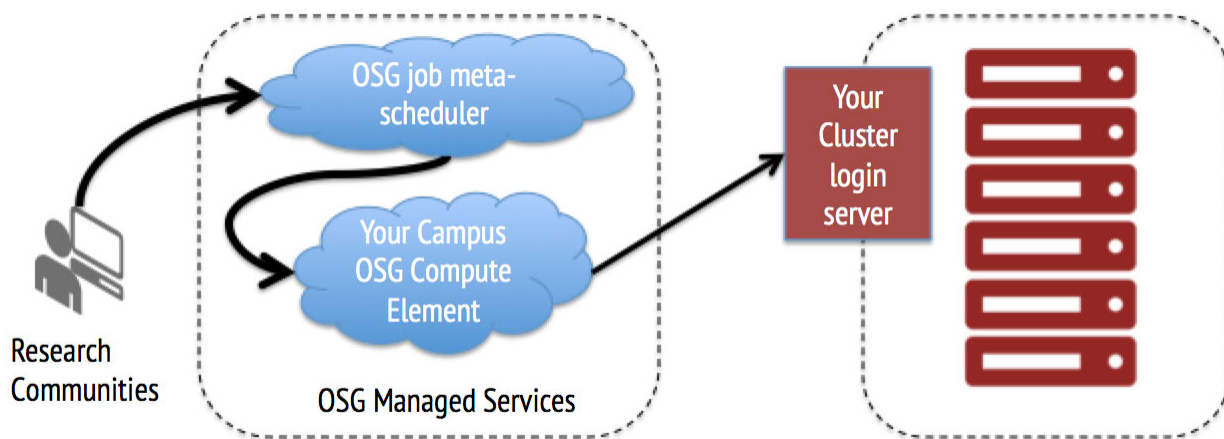


Figure 37: Services managed by OSG reduce the required effort needed at resource endpoints

For sites that simply want to contribute computational cycles, OSG has developed a hosted compute element (CE) that allows institutions to start contributing to OSG much sooner and to reduce training and

effort required for their staff. The hosted CE solution involves OSG staff installing and configuring a managed CE that will accept incoming jobs. The CE then submits the jobs to the institution's cluster using SSH. Staff at the institution contributing to OSG only needs to setup a SSH account that allows job submissions to the institution's cluster. OSG staff handle the management of the OSG related software and troubleshooting of any OSG related problems. This reduces the effort required from the contributing institution's staff to that required to support any other user of the institution's cluster. Likewise, the contributing institution's staff does not need any additional training or expertise since OSG staff members handle the management of the OSG related software.

In the last six months, the hosted CE approach has been used to several sites to OSG. The first site added was the Proclus cluster at Stanford. After an initial discussion with the director of research computing at Stanford, the Proclus cluster was contributing cycles to OSG within two weeks.

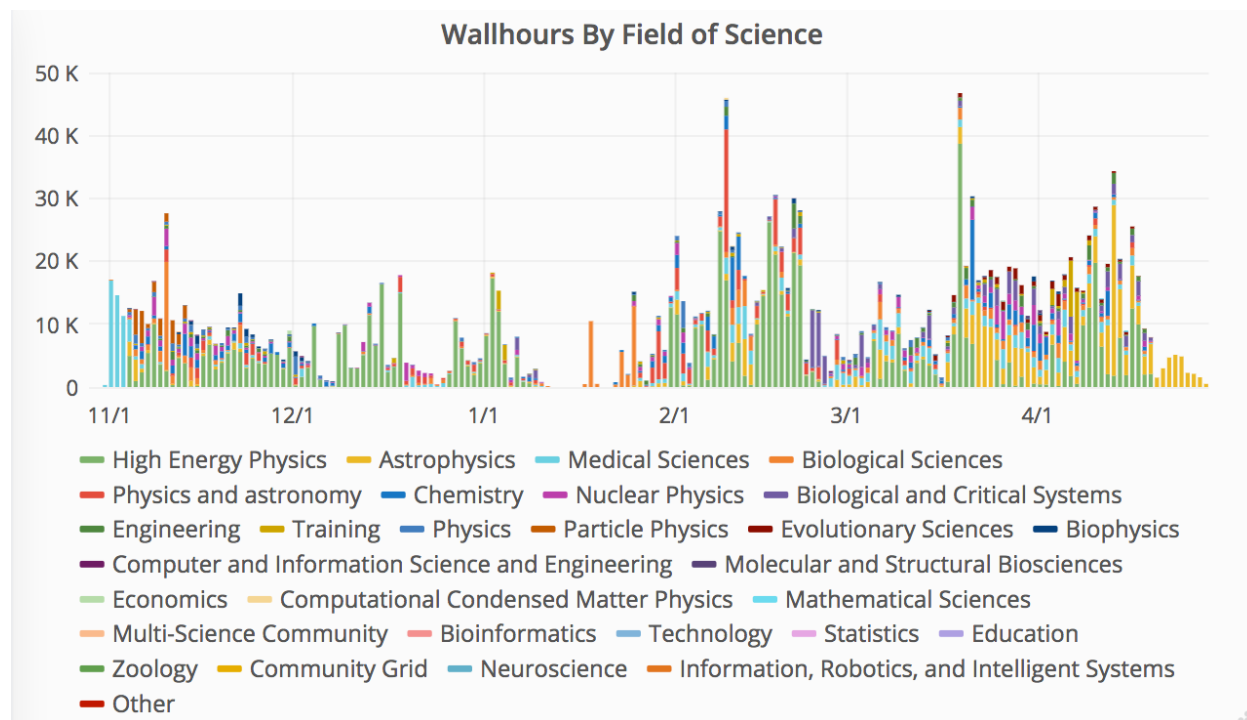


Figure 38: Fields of science supported by the Proclus Cluster at Stanford University

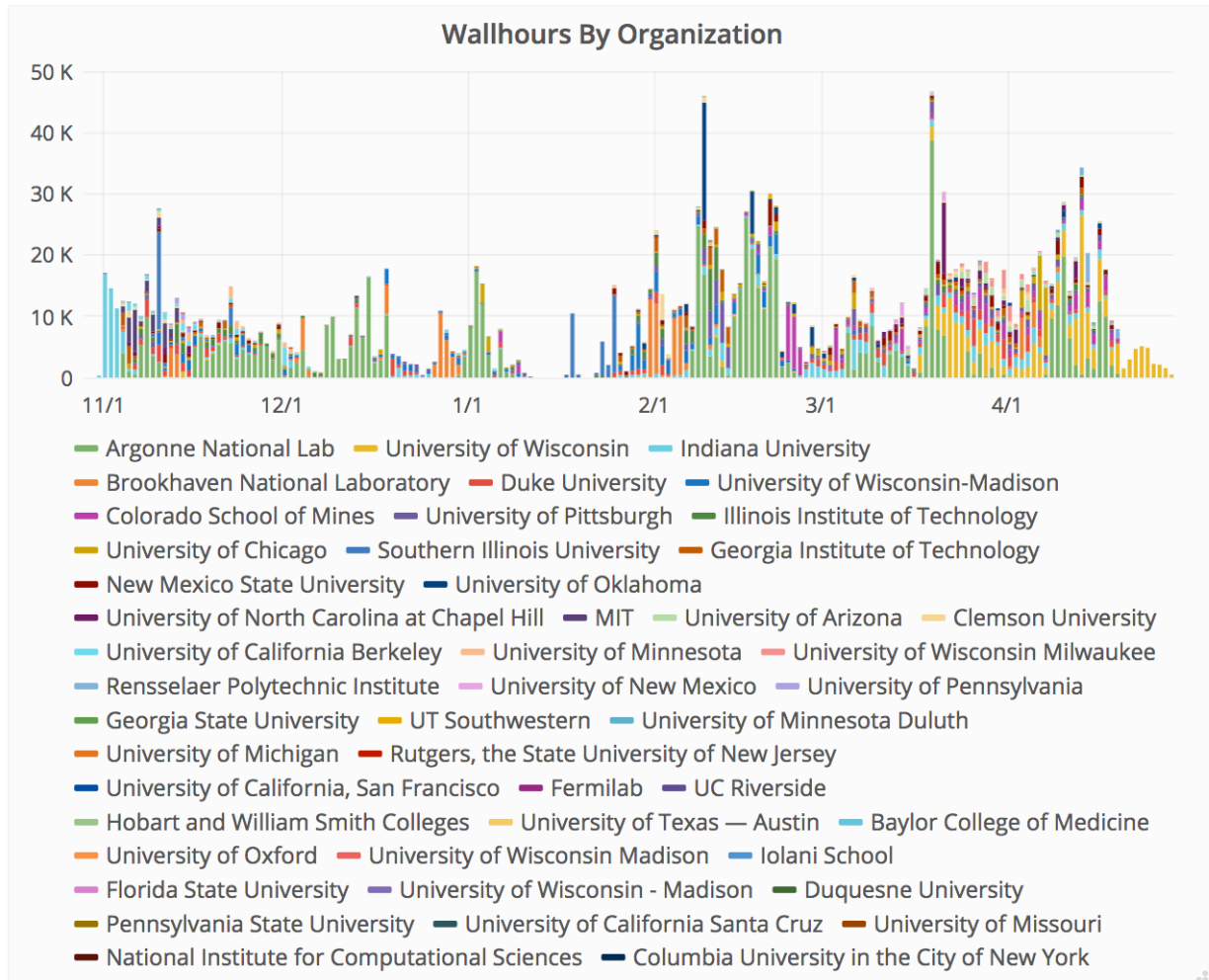


Figure 39: Institutions supported by the Proclus Cluster and Stanford University

Since then, the Proclus cluster has contributed over 2.1 million CPU hours to OSG. In addition, Proclus has contributed to over 31 fields of science and 64 institutions (Figure 38 and Figure 39). The Proclus cluster has consistently been in the top 15 contributors to OSG while requiring minimal ongoing effort from the Proclus administrators or OSG staff.

The second cluster contributing to OSG using this approach is Oklahoma State University's (OSU) Cowboy Cluster. This cluster was added at the end of February after a conversation with Dana Brunson, the Assistant Vice President for Research Cyberinfrastructure and Director, of the OSU High Performance Computing Center. Building on experience in setting up the Proclus cluster for Stanford University, the Cowboy cluster was contributing to OSG within a week. The effort required to configure and maintain the hosted CE for the Cowboy cluster has also been fairly minimal.

Based on experiences over the last six months in adding sites to OSG using the hosted CE approach, this is a viable method to allow institutions to quickly and simply contribute computational resources to OSG. The efforts required on the parts of institutional staff and OSG staff to setup, configure, and maintain a hosted CE have been minimal and have provided OSG with significant additional computational resources.

### 3.8.6 Supporting Community Software in OASIS

The OSG Application Software Installation Service (OASIS) is an OSG-run deployment of the CernVM File System (CVMFS). The User Support team has created a distributed software modules system that uses the OASIS system to provide users with a consistent way to access software that they need for their workflows. The distributed software modules system is deliberately modeled after the modules system used by many HPC systems including those provided by XSEDE. The distributed software modules system allows users to utilize the same commands (e.g., module load R/3.1.1) that they use on their native HPC environment to gain access to the software that they use. Using the distributed software modules system makes user jobs somewhat less portable, as the worker node must have CVMFS available (approximately 90% of OSG worker nodes). However, it decreases the barrier of entry for users starting on the OSG and has proven to be popular.

The distributed software modules system initially provided all the applicable software listed in the XSEDE campus bridging software repository. Over time it has grown to incorporate new software based on user requests. Users can open a support ticket requesting the addition of software that they need and the user support team can usually add the software to the system within 2–3 days. This allows users avoid the often complicated and technically challenging task of compiling, installing, and distributing their software in a heterogeneous environment like OSG. Once a user’s software has been added to the distributed software modules system, a single command in the user’s job makes their software available. An overwhelming majority of OSG Connect users utilize distributed software modules to run their workflows. In addition, other users of OSG have taken advantage of this system to run workflows. These users include users from the Center for High Throughput Computing at UW–Madison, users using XSEDE allocations through the XSEDE-OSG submit nodes, and OSG VOs. For the current distributed software modules environment, there are 284 modules available containing 130 GB of software, which has been used approximately 120 million times in 2016.

### 3.8.7 FSurf: A FreeSurfer Production Service

FreeSurfer is a widely used software suite for analysis of human brain magnetic resonance imaging (MRI) scans. It has been used for studying human brain anatomy in a variety of contexts such as exploring the neurophysiology of depression, examining possible anatomical differences involved in attention deficit hyperactivity disorder (ADHD), and studying autism. FreeSurfer can take 16–24 hours to analyze a single subject’s MRI scan. Thus, users without access to a large cluster or with large numbers of scans to analyze may need to wait weeks in order to do simple analysis of their data.

The User Support team has created a service called FSurf that allows FreeSurfer users to use the capabilities of OSG in order to process large number of scans. Users will be able to use the FSurf service using a simple command line interface. This means that users will not have to learn how to run FreeSurfer in a distributed environment. In addition, using the FSurf service allows users to gain the ability to start processing their scans more quickly than if they had to gain access to OSG through traditional means. The FSurf service supports several versions of FreeSurfer (5.1, 5.3, 6.0) and a variety of different methods of running FreeSurfer. It also automatically breaks up the FreeSurfer workflow into discrete chunks and parallelizes the workflow when possible in order to optimize the workflow’s execution on OSG.



Figure 40: User-accessible plot of OSG FSurf workflows currently running

The FSurf service has been extensively tested over the last several months. In addition, automated tests are run weekly to verify that the various workflow types can run successfully. Users can see the workflows that the service is currently running on the web (Figure 40). The service has seen increasing user interest and uptake since the last major release and the User Support team is in discussions with several groups regarding the adoption of the service by these groups.

## 4 Project, Consortium, and Partners

### 4.1 Project Institutions

The OSG Project was jointly enabled by the following institutions:

**Table 4: OSG project funded institutions**

Institution	Key Contributions
University of Wisconsin–Madison	PI, Release, Software
Brookhaven National Laboratory	Co-PI, Technology investigations, Release, Production support
Fermi National Accelerator Laboratory	Co-PI, Security, Production support, Operations, Project management
Indiana University	Operations, Communications
University of California San Diego	Co-PI, Executive Director, Operations, Software
University of Chicago	User support, XSEDE liaison (XRAC), Campus grids, Operations, Software
University of Illinois and NCSA	Security
University of Michigan	Network monitoring
University of Nebraska–Lincoln	Technology investigations, Software, Campus grids
University of Southern California Information Sciences Institute	User support, XSEDE liaison, Campus grids

### 4.2 OSG Council and Consortium

The OSG Council had two face-to-face and two phone meetings in the covered period. By the end of 2016, the Council consisted of the following individuals: Mike Norman, UCSD/SDSC; Kenneth Bloom, CMS; Kaushik De, ATLAS; Don Krieger, University of Pittsburgh Brain Trauma Research Center; Stefan Hoeche, SLAC; Jérôme Lauret, STAR; Craig Stewart, Indiana University; Rob Gardner, University of Chicago and Globus; Horst Severini, DOSAR; Miron Livny, University of Wisconsin–Madison and HTCondor; Eric Lançon, BNL; Paul Avery, University of Florida; Panagiotis Spentzouris, Fermilab; David Swanson, University of Nebraska Holland Computing Center (elected Chair). Ruth Pordes stepped down as Chair and from the Council due to retirement. Discussions concerning detailed plans for the immediate and long-term future of the OSG dominated the agendas, with all members endorsing the need for a strong OSG and the strategies to move forward in a new budgetary arrangement. Council matters are recorded at <https://opencswencegrid.github.io/council/>.

## 5 Education, Communications, and Other Outreach

The OSG reaches out to a wide variety of domain scientists and others who are interested in the state-of-the-art in large scale distributed computing for scholarly work. OSG staff offer targeted educational opportunities; provide regular communications about technology updates, service changes, and research highlights; and perform other forms of outreach to the community.

### 5.1 Education

OSG Education provides training opportunities for domain science users and new OSG staff. Training events are a form of outreach activity to the science community, helping to engage students, faculty, and researchers in the OSG infrastructure with the goal of transforming their scholarly work through the use of high throughput computing.

The **OSG User School 2016** in late July was the seventh annual offering of a training program for current and potential domain science users. The goal of the School is to help participants learn to use distributed high throughput computing, locally or across the grid, as a tool for doing their research.

This year, there were a large number of applicants (103), from which 55 participants were selected, coming from 31 institutions and such diverse fields as physics, chemistry, biology, engineering, plant and soil sciences, animal sciences, earth sciences, medicine, statistics, and economics. Through lectures, many hands-on exercises, and even live-action role-play, participants learned how to run science applications on distributed resources (locally and on OSG), build complex workflows, manage large and distributed data, and turn scientific computing challenges into appropriately sized and scaled workflows that are ready for real-world use. OSG staff and affiliates served as the instructors, and as a special and highly motivating event, four UW–Madison researchers came and talked about how using high-throughput computing has transformed their own scholarly work.

Again this year, participants rated the School very highly, and they seemed eager to apply what they learned to their own research. Instructors followed up with participants afterward to see how they are applying what was learned and to help them obtain resources at their own institutions or on OSG. As one simple measure of effectiveness, two participants from the School presented science results that relied on OSG at the OSG All Hands Meeting in March 2017.

Every year, the OSG School evolves to stay current with OSG technology and to freshen pedagogy and materials. This year most of the changes were relatively minor, with the greatest changes affecting the section on dealing with Big Data, an ever-evolving topic. The School will continue to improve for 2017, based on feedback from participants and changes within OSG.

OSG was also invited to send instructional assistance to the **CODATA/RDA Summer School for Research Data Science for Low- and Middle-Income Countries**, this course gathered students and staff from organizations worldwide to teach a foundational course in open science, data management, visualization, and research cyber infrastructures.

This summer school session gathered 70 students and more than a dozen experts in Trieste, Italy, at the International Center for Theoretical Physics (ICTP) for 2 weeks in August. The cyberinfrastructure session utilized the OSG open facility to teach the concepts of batch and distributed computing using HTCondor and the OSG Connect submission nodes. OSG User Support contributed heavily in making a training facility available for use during the school. This added to the emphasis of Open Science which was the cornerstone of the summer school by making the point that all resources (not only data) are part of the Open Science picture.

OSG has been invited to two international summer schools in this series in 2017, another in Trieste in July and a second in Sao Paulo again in association with ICTP.

The final school that OSG was involved in was the 2016 iteration of the **African School of Fundamental Physics and Applications**. This three-week school hosted students from many countries all over Africa and the Middle East. The school uses a combination of lectures, hands-on exercises, and computing workshops to advance the capacity of physics and their applications in Africa.

This school hosted approximately 70 students in Kigali, Rwanda, at the University of Rwanda. The final portion of this school was a workshop to introduce the students to the concepts of DHTC and show them how these concepts are applied to the work that is done in the area of high-energy physics. A team of instructors from the Distributed Organization for Scientific and Academic Research (DOSAR) traveled to Kigali to lead students through this workshop. OSG Connect was leveraged as a means of working through tutorials with the students.

DOSAR is currently working to submit a grant to ensure that OSG is involved in the 2018 school in Namibia.

## 5.2 Communications

The OSG Communications group is tasked with publishing information about the people benefiting from OSG, especially in research. They maintain an active web presence with new information updated regularly to help people engage with the OSG. They also take on special communication tasks such as the one requested by the OSG Executive Director to produce handout materials for Supercomputing 16 that highlighted OSG's involvement in winning two Top Supercomputing Achievement awards from HPCWire.

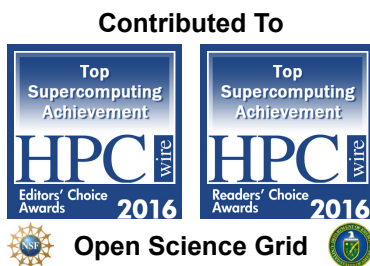


Figure 41: OSG Top Supercomputing Achievement awards from HPCWire

The Communications Area Coordinator position was split away from the Operations Coordinator position in the past year to better help focus the area effort. Kyle Gross was appointed as the Communications Area Coordinator in November, 2016.

Communications efforts in OSG is currently 0.5 FTE at Indiana University: 0.25 FTE for the writing of the monthly Research Highlights, and another 0.25 FTE for the Communications Area Coordinator, publication of the research highlights, as well as other periodic communications needed by the Project.

Support continued for the OSG web presence including the main site at [www.opensciencegrid.org](http://www.opensciencegrid.org) and our user-focused websites [users.opensciencegrid.org](http://users.opensciencegrid.org) and [support.opensciencegrid.org](http://support.opensciencegrid.org).

Routine communication of operational events is handled by OSG Operations and keeps stakeholders aware of the state of the OSG along with communicating important software updates, security patches, and community-building events. These operational communications are logged at [osggoc.blogspot.com](http://osggoc.blogspot.com).

There are also occasional special requests for operational communications such as aid with communication (via email and Twitter) for the OSG User School and announcements for tangential projects such as RDA and PEARC17. So, in addition to regular research highlights, the OSG Communication team is responsive to special requests and often handles several in a year.

A key output is short descriptions of science accomplished on OSG called Research Highlights. These research highlights are available at <http://www.opensciencegrid.org/news/research-highlights-list/>. The titles of the highlights since the last annual report are:

- [ATLAS and BNL Bring Amazon EC2 Online](#) (2/1/2016)
- [OSG Year-End Operations Update](#) (2/1/2016)
- [OSG Helps LIGO Scientists Confirm Einstein's Unproven Theory](#) (2/16/2016)
- [SBGrid Uses the OSG to Accelerate Structural Biology Research](#) (2/23/2016)
- [Where Did All the Antimatter Go?](#) (7/12/2016)
- [Update on the Brain Trauma Research Center](#) (8/29/2016)
- [OSG Council Member Stefan Höche Receives IUPAP Young Scientist Prize](#) (9/30/2016)
- [OSG Receives HPCwire's 'Top Supercomputing Achievement' Awards](#) (11/15/2016)
- [OSG's Rob Quick and Kyle Gross Share Expertise in Rwanda and Italy](#) (12/6/2016)
- [Cancer Computer and OSG Partner for the Cure](#) (1/18/2017)
- [Free Supercomputing for Research: Scott Cole Introduces You to OSG](#) (2/10/2017)
- [For Neuroscientist Chris Cox, the OSG Helps Process Mountains of Data](#) (2/20/2017)

The Communication Team continues to maintain the web pages at [www.opensciencegrid.org](http://www.opensciencegrid.org) and to post updates and share collaborator activity on Twitter. This year, Twitter activity was greatly increased during the OSG All Hands Meeting and received positive feedback from both inside and outside OSG. Plans are underway to expand on this strategy. Effort levels do not allow for other forms of social media such as Facebook and Google groups to continue outside of voluntary activity.

### 5.3 Outreach

OSG staff participated in a number of national cyberinfrastructure development workshops and symposia, which are another form of outreach to the national scientific computing community.

- OSG contributed to the Southern Partnership for Advanced Networking (SPAN) conference held at University of Central Florida, March 9–10, 2016. The aim was to provide high-level guidance to computing directors and IT professionals for connecting both researchers and campus research computing resources to the national cyberinfrastructure systems provided by the OSG.
- In August 9–8, 2016, OSG hosted a session at the Rocky Mountain Advanced Computing Consortium's HPC Symposium held at Colorado State University in Fort Collins, Colorado. The session provided options for campus HPC integration using OSG managed services.
- In a broader context, OSG organized a session at the Advancing Research Computing on Campuses: Best Practices Workshop, held in Urbana, Illinois, March 22–24, 2016. The session focused on sustainability models for sharing resources across institutions to accelerate science.

Also during this reporting period, OSG prepared a curriculum and infrastructure for a three-day workshop that was tailored to researchers at Jefferson National Accelerator Laboratory and was held on May 17–19, 2017. The first two days focused on fundamentals of software development in scientific computing environments following the popular Software Carpentry format. The third day was focused on high throughput computing and job submission tutorials for the OSG. OSG also prepared for participation in

the Southern Partnership for Advanced Networking (SPAN), which was held at South Carolina State University, May 18–19, 2017. This workshop introduced universities in the region to strategies for integrating campus HPC resources with the national infrastructure using OSG hosted services, and options for researcher engagement using OSG Connect user infrastructure.

In addition, OSG leadership routinely engages with the community by giving seminars and 1–2 day visits focused on engagement with new communities at various institutions and conferences. Within the last year, a dozen such visits were undertaken including visits to LIGO centers in Germany and India.

Finally, the 2017 All Hands Meeting of the OSG was hosted by the San Diego Supercomputer Center at University of California San Diego. It attracted 140 researchers from across the country and the world, giving more than 50 invited talks in addition to the co-located US ATLAS and US CMS annual Tier-2 meetings. OSG organized three training events at that meeting; one for researchers that want to use OSG for their research, and two for system administrators focusing on software and security respectively.

## Appendix: Science Publications Enabled by OSG

### ATLAS

1. Measurement of the cross-section for producing a  $W$  boson in association with a single top quark in  $pp$  collisions at  $\sqrt{s} = 13$  TeV with ATLAS. By ATLAS Collaboration (Morad Aaboud et al.). arXiv:1612.07231 [hep-ex].
2. Measurements of top quark spin observables in  $t\bar{t}$  events using dilepton final states in  $\sqrt{s}=8$  TeV  $pp$  collisions with the ATLAS detector. By ATLAS Collaboration (Morad Aaboud et al.). arXiv:1612.07004 [hep-ex]. [10.1007/JHEP03\(2017\)113](https://doi.org/10.1007/JHEP03(2017)113). JHEP 1703 (2017) 113.
3. Measurements of top-quark pair differential cross-sections in the  $e\mu$  channel in  $pp$  collisions at  $\sqrt{s} = 13$  TeV using the ATLAS detector. By ATLAS Collaboration (Morad Aaboud et al.). arXiv:1612.05220 [hep-ex]. [10.1140/epjc/s10052-017-4821-x](https://doi.org/10.1140/epjc/s10052-017-4821-x). Eur.Phys.J. C77 (2017) no.5, 292.
4. Measurements of top-quark pair to  $Z$ -boson cross-section ratios at  $\sqrt{s} = 13, 8, 7$  TeV with the ATLAS detector. By ATLAS Collaboration (Morad Aaboud et al.). arXiv:1612.03636 [hep-ex]. [10.1007/JHEP02\(2017\)117](https://doi.org/10.1007/JHEP02(2017)117). JHEP 1702 (2017) 117.
5. Precision measurement and interpretation of inclusive  $W^+ + W^-$ ,  $Z\gamma$  production cross sections with the ATLAS detector. By ATLAS Collaboration (Morad Aaboud et al.). arXiv:1612.03016 [hep-ex].
6. Measurement of the prompt  $J/\psi$  pair production cross-section in  $pp$  collisions at  $\sqrt{s} = 8$  TeV with the ATLAS detector. By ATLAS Collaboration (Morad Aaboud et al.). arXiv:1612.02950 [hep-ex]. [10.1140/epjc/s10052-017-4644-9](https://doi.org/10.1140/epjc/s10052-017-4644-9). Eur.Phys.J. C77 (2017) no.2, 76.
7. Measurement of the  $W$  boson polarisation in  $t\bar{t}$  events from  $pp$  collisions at  $\sqrt{s} = 8$  TeV in the lepton+jets channel with ATLAS. By ATLAS Collaboration (Morad Aaboud et al.). arXiv:1612.02577 [hep-ex]. [10.1140/epjc/s10052-017-4819-4](https://doi.org/10.1140/epjc/s10052-017-4819-4). Eur.Phys.J. C77 (2017) no.4, 264.
8. Electron efficiency measurements with the ATLAS detector using 2012 LHC proton-proton collision data. By ATLAS Collaboration (Morad Aaboud et al.). arXiv:1612.01456 [hep-ex]. [10.1140/epjc/s10052-017-4756-2](https://doi.org/10.1140/epjc/s10052-017-4756-2). Eur.Phys.J. C77 (2017) no.3, 195.
9. Reconstruction of primary vertices at the ATLAS experiment in Run 1 proton–proton collisions at the LHC. By ATLAS Collaboration (Morad Aaboud et al.). arXiv:1611.10235 [physics.ins-det]. [10.1140/epjc/s10052-017-4887-5](https://doi.org/10.1140/epjc/s10052-017-4887-5). Eur.Phys.J. C77 (2017) no.5, 332.
10. Performance of the ATLAS Trigger System in 2015. By ATLAS Collaboration (Morad Aaboud et al.). arXiv:1611.09661 [hep-ex]. [10.1140/epjc/s10052-017-4852-3](https://doi.org/10.1140/epjc/s10052-017-4852-3). Eur.Phys.J. C77 (2017) no.5, 317.
11. High- $E_{\text{miss T}}$  isolated-photon plus jets production in  $pp$  collisions at  $\sqrt{s}=8$  TeV with the ATLAS detector. By ATLAS Collaboration (Morad Aaboud et al.). arXiv:1611.06586 [hep-ex]. [10.1016/j.nuclphysb.2017.03.006](https://doi.org/10.1016/j.nuclphysb.2017.03.006). Nucl.Phys. B918 (2017) 257-316.
12. Search for new phenomena in events containing a same-flavour opposite-sign dilepton pair, jets, and large missing transverse momentum in  $\sqrt{s}=13$   $pp$  collisions with the ATLAS detector. By ATLAS Collaboration (Morad Aaboud et al.). arXiv:1611.05791 [hep-ex]. [10.1140/epjc/s10052-017-4700-5](https://doi.org/10.1140/epjc/s10052-017-4700-5). Eur.Phys.J. C77 (2017) no.3, 144.

13. Measurement of  $W^{\pm}W^{\pm}$  vector-boson scattering and limits on anomalous quartic gauge couplings with the ATLAS detector. By ATLAS Collaboration (Morad Aaboud et al.). arXiv:1611.02428 [hep-ex].
14. Measurement of jet activity produced in top-quark events with an electron, a muon and two  $b$ -tagged jets in the final state in  $pp$  collisions at  $\sqrt{s}=13$  TeV with the ATLAS detector. By ATLAS Collaboration (Morad Aaboud et al.). arXiv:1610.09978 [hep-ex]. [10.1140/epjc/s10052-017-4766-0](https://doi.org/10.1140/epjc/s10052-017-4766-0). Eur.Phys.J. C77 (2017) no.4, 220.
15. Measurements of  $\psi(2S)$  and  $X(3872) \rightarrow J/\psi\pi^+\pi^-$  production in  $pp$  collisions at  $\sqrt{s} = 8$  TeV with the ATLAS detector. By ATLAS Collaboration (Morad Aaboud et al.). arXiv:1610.09303 [hep-ex]. [10.1007/JHEP01\(2017\)117](https://doi.org/10.1007/JHEP01(2017)117). JHEP 1701 (2017) 117.
16. Measurements of charge and CP asymmetries in  $b$ -hadron decays using top-quark events collected by the ATLAS detector in  $pp$  collisions at  $\sqrt{s}=8$  TeV. By ATLAS Collaboration (Morad Aaboud et al.). arXiv:1610.07869 [hep-ex]. [10.1007/JHEP02\(2017\)071](https://doi.org/10.1007/JHEP02(2017)071). JHEP 1702 (2017) 071.
17. Measurement of the  $ZZ$  production cross section in proton-proton collisions at  $\sqrt{s} = 8$  TeV using the  $ZZ \rightarrow ell^- ell^+ ell^+ ell^-$  and  $ZZ \rightarrow ell^- ell^+ nu bar{nu}$  channels with the ATLAS detector. By ATLAS Collaboration (Morad Aaboud et al.). arXiv:1610.07585 [hep-ex]. [10.1007/JHEP01\(2017\)099](https://doi.org/10.1007/JHEP01(2017)099). JHEP 1701 (2017) 099.
18. Search for triboson  $W^{\pm}W^{\pm}W^{\pm}$  production in  $pp$  collisions at  $\sqrt{s}=8$  TeV with the ATLAS detector. By ATLAS Collaboration (Morad Aaboud et al.). arXiv:1610.05088 [hep-ex]. [10.1140/epjc/s10052-017-4692-1](https://doi.org/10.1140/epjc/s10052-017-4692-1). Eur.Phys.J. C77 (2017) no.3, 141.
19. Performance of algorithms that reconstruct missing transverse momentum in  $\sqrt{s}=8$  TeV proton-proton collisions in the ATLAS detector. By ATLAS Collaboration (G. Aad et al.). arXiv:1609.09324 [hep-ex]. [10.1140/epjc/s10052-017-4780-2](https://doi.org/10.1140/epjc/s10052-017-4780-2). Eur.Phys.J. C77 (2017) no.4, 241.
20. Measurement of  $W$  boson angular distributions in events with high transverse momentum jets at  $\sqrt{s}=8$  TeV using the ATLAS detector. By ATLAS Collaboration (Morad Aaboud et al.). arXiv:1609.07045 [hep-ex]. [10.1016/j.physletb.2016.12.005](https://doi.org/10.1016/j.physletb.2016.12.005). Phys.Lett. B765 (2017) 132-153.
21. Measurements of long-range azimuthal anisotropies and associated Fourier coefficients for  $pp$  collisions at  $\sqrt{s}=5.02$  and  $13$  TeV and  $p+Pb$  collisions at  $\sqrt{s_{NN}}=5.02$  TeV with the ATLAS detector. By ATLAS Collaboration (Morad Aaboud et al.). arXiv:1609.06213 [nucl-ex].
22. Search for anomalous electroweak production of  $WW/WZ$  in association with a high-mass dijet system in  $pp$  collisions at  $\sqrt{s}=8$  TeV with the ATLAS detector. By ATLAS Collaboration (Morad Aaboud et al.). arXiv:1609.05122 [hep-ex]. [10.1103/PhysRevD.95.032001](https://doi.org/10.1103/PhysRevD.95.032001). Phys.Rev. D95 (2017) no.3, 032001.
23. Search for dark matter in association with a Higgs boson decaying to  $b$ -quarks in  $pp$  collisions at  $\sqrt{s}=13$  TeV with the ATLAS detector. By ATLAS Collaboration (Morad Aaboud et al.). arXiv:1609.04572 [hep-ex]. [10.1016/j.physletb.2016.11.035](https://doi.org/10.1016/j.physletb.2016.11.035). Phys.Lett. B765 (2017) 11-31.
24. A measurement of material in the ATLAS tracker using secondary hadronic interactions in 7 TeV pp collisions. By ATLAS Collaboration (Morad Aaboud et al.). arXiv:1609.04305 [hep-ex]. [10.1088/1748-0221/11/11/P11020](https://doi.org/10.1088/1748-0221/11/11/P11020). JINST 11 (2016) no.11, P11020.

25. Measurement of the inclusive cross-sections of single top-quark and top-antiquark \$t\\$-\$channel production in \$pp\$ collisions at \$\sqrt{s} = 13\$ TeV with the ATLAS detector. By ATLAS Collaboration (Morad Aaboud et al.). arXiv:1609.03920 [hep-ex]. [10.1007/JHEP04\(2017\)086](https://doi.org/10.1007/JHEP04(2017)086). JHEP 1704 (2017) 086.
26. Measurement of the \$t\bar{t}Z\$ and \$t\bar{t}W\$ production cross sections in multilepton final states using 3.2 fb\$^{-1}\$ of \$pp\$ collisions at \$\sqrt{s} = 13\$ TeV with the ATLAS detector. By ATLAS Collaboration (Morad Aaboud et al.). arXiv:1609.01599 [hep-ex]. [10.1140/epjc/s10052-016-4574-y](https://doi.org/10.1140/epjc/s10052-016-4574-y). Eur.Phys.J. C77 (2017) no.1, 40.
27. Luminosity determination in pp collisions at \$\sqrt{s} = 8\$ TeV using the ATLAS detector at the LHC. By ATLAS Collaboration (Morad Aaboud et al.). arXiv:1608.03953 [hep-ex]. [10.1140/epjc/s10052-016-4466-1](https://doi.org/10.1140/epjc/s10052-016-4466-1). Eur.Phys.J. C76 (2016) no.12, 653.
28. Measurement of \$W^+W^-\$ production in association with one jet in proton--proton collisions at \$\sqrt{s} = 8\$ TeV with the ATLAS detector. By ATLAS Collaboration (Morad Aaboud et al.). arXiv:1608.03086 [hep-ex]. [10.1016/j.physletb.2016.10.014](https://doi.org/10.1016/j.physletb.2016.10.014). Phys.Lett. B763 (2016) 114-133.
29. Search for dark matter produced in association with a hadronically decaying vector boson in \$pp\$ collisions at \$\sqrt{s} = 13\$ TeV with the ATLAS detector. By ATLAS Collaboration (Morad Aaboud et al.). arXiv:1608.02372 [hep-ex]. [10.1016/j.physletb.2016.10.042](https://doi.org/10.1016/j.physletb.2016.10.042). Phys.Lett. B763 (2016) 251-268.
30. Study of hard double-parton scattering in four-jet events in pp collisions at \$\sqrt{s}=7\$ TeV with the ATLAS experiment. By ATLAS Collaboration (Morad Aaboud et al.). arXiv:1608.01857 [hep-ex]. [10.1007/JHEP11\(2016\)110](https://doi.org/10.1007/JHEP11(2016)110). JHEP 1611 (2016) 110.
31. Search for Minimal Supersymmetric Standard Model Higgs bosons \$H/A\$ and for a \$Z^{\prime}\$ boson in the \$\tau\tau\$ final state produced in \$pp\$ collisions at \$\sqrt{s}=13\$ TeV with the ATLAS Detector. By ATLAS Collaboration (Morad Aaboud et al.). arXiv:1608.00890 [hep-ex]. [10.1140/epjc/s10052-016-4400-6](https://doi.org/10.1140/epjc/s10052-016-4400-6). Eur.Phys.J. C76 (2016) no.11, 585.
32. Dark matter interpretations of ATLAS searches for the electroweak production of supersymmetric particles in \$\sqrt{s}=8\$ TeV proton-proton collisions. By ATLAS Collaboration (Morad Aaboud et al.). arXiv:1608.00872 [hep-ex]. [10.1007/JHEP09\(2016\)175](https://doi.org/10.1007/JHEP09(2016)175). JHEP 1609 (2016) 175.
33. A measurement of the calorimeter response to single hadrons and determination of the jet energy scale uncertainty using LHC Run-1 \$pp\$-collision data with the ATLAS detector. By ATLAS Collaboration (Morad Aaboud et al.). arXiv:1607.08842 [hep-ex]. [10.1140/epjc/s10052-016-4580-0](https://doi.org/10.1140/epjc/s10052-016-4580-0). Eur.Phys.J. C77 (2017) no.1, 26.
34. Measurement of the \$b\bar{b}\$ dijet cross section in pp collisions at \$\sqrt{s} = 7\$ TeV with the ATLAS detector. By ATLAS Collaboration (Morad Aaboud et al.). arXiv:1607.08430 [hep-ex]. [10.1140/epjc/s10052-016-4521-y](https://doi.org/10.1140/epjc/s10052-016-4521-y). Eur.Phys.J. C76 (2016) no.12, 670.
35. Search for new phenomena in different-flavour high-mass dilepton final states in pp collisions at \$\sqrt{s}=13\$ TeV with the ATLAS detector. By ATLAS Collaboration (Morad Aaboud et al.). arXiv:1607.08079 [hep-ex]. [10.1140/epjc/s10052-016-4385-1](https://doi.org/10.1140/epjc/s10052-016-4385-1). Eur.Phys.J. C76 (2016) no.10, 541.
36. Measurement of top quark pair differential cross-sections in the dilepton channel in \$pp\$ collisions at \$\sqrt{s} = 7\$ and 8 TeV with ATLAS. By ATLAS Collaboration (Morad Aaboud et al.). arXiv:1607.07281 [hep-ex]. [10.1103/PhysRevD.94.092003](https://doi.org/10.1103/PhysRevD.94.092003). Phys.Rev. D94 (2016) no.9, 092003.

37. Measurement of the total cross section from elastic scattering in \$pp\$ collisions at  $\sqrt{s}=8$  TeV with the ATLAS detector. By ATLAS Collaboration (Morad Aaboud et al.). arXiv:1607.06605 [hep-ex]. [10.1016/j.physletb.2016.08.020](https://doi.org/10.1016/j.physletb.2016.08.020). Phys.Lett. B761 (2016) 158-178.
38. Search for heavy resonances decaying to a  $Z$  boson and a photon in \$pp\$ collisions at  $\sqrt{s}=13$  TeV with the ATLAS detector. By ATLAS Collaboration (Morad Aaboud et al.). arXiv:1607.06363 [hep-ex]. [10.1016/j.physletb.2016.11.005](https://doi.org/10.1016/j.physletb.2016.11.005). Phys.Lett. B764 (2017) 11-30.
39. Search for squarks and gluinos in events with hadronically decaying tau leptons, jets and missing transverse momentum in proton–proton collisions at  $\sqrt{s}=13$  TeV recorded with the ATLAS detector. By ATLAS Collaboration (Morad Aaboud et al.). arXiv:1607.05979 [hep-ex]. [10.1140/epjc/s10052-016-4481-2](https://doi.org/10.1140/epjc/s10052-016-4481-2). Eur.Phys.J. C76 (2016) no.12, 683.
40. Search for new resonances decaying to a  $W$  or  $Z$  boson and a Higgs boson in the  $e^+e^- b\bar{b}$ ,  $e^+\nu b\bar{b}$ , and  $\nu\bar{\nu} b\bar{b}$  channels with \$pp\$ collisions at  $\sqrt{s}=13$  TeV with the ATLAS detector. By ATLAS Collaboration (Morad Aaboud et al.). arXiv:1607.05621 [hep-ex]. [10.1016/j.physletb.2016.11.045](https://doi.org/10.1016/j.physletb.2016.11.045). Phys.Lett. B765 (2017) 32-52.
41. Measurement of exclusive  $\gamma\gamma \rightarrow W^+W^-$  production and search for exclusive Higgs boson production in \$pp\$ collisions at  $\sqrt{s}=8$  TeV using the ATLAS detector. By ATLAS Collaboration (Morad Aaboud et al.). arXiv:1607.03745 [hep-ex]. [10.1103/PhysRevD.94.032011](https://doi.org/10.1103/PhysRevD.94.032011). Phys.Rev. D94 (2016) no.3, 032011.
42. Search for high-mass new phenomena in the dilepton final state using proton-proton collisions at  $\sqrt{s}=13$  TeV with the ATLAS detector. By ATLAS Collaboration (Morad Aaboud et al.). arXiv:1607.03669 [hep-ex]. [10.1016/j.physletb.2016.08.055](https://doi.org/10.1016/j.physletb.2016.08.055). Phys.Lett. B761 (2016) 372-392.
43. Search for Higgs and  $Z$  Boson Decays to  $\phi\gamma$  with the ATLAS Detector. By ATLAS Collaboration (Morad Aaboud et al.). arXiv:1607.03400 [hep-ex]. [10.1103/PhysRevLett.117.111802](https://doi.org/10.1103/PhysRevLett.117.111802). Phys.Rev.Lett. 117 (2016) no.11, 111802.
44. Search for supersymmetry in a final state containing two photons and missing transverse momentum in  $\sqrt{s}=13$  TeV \$pp\$ collisions at the LHC using the ATLAS detector. By ATLAS Collaboration (Morad Aaboud et al.). arXiv:1606.09150 [hep-ex]. [10.1140/epjc/s10052-016-4344-x](https://doi.org/10.1140/epjc/s10052-016-4344-x). Eur.Phys.J. C76 (2016) no.9, 517.
45. Measurement of jet activity in top quark events using the  $e\mu$  final state with two  $b$ -tagged jets in \$pp\$ collisions at  $\sqrt{s}=8$  TeV with the ATLAS detector. By ATLAS Collaboration (Morad Aaboud et al.). arXiv:1606.09490 [hep-ex]. [10.1007/JHEP09\(2016\)074](https://doi.org/10.1007/JHEP09(2016)074). JHEP 1609 (2016) 074.
46. Search for bottom squark pair production in proton–proton collisions at  $\sqrt{s}=13$  TeV with the ATLAS detector. By ATLAS Collaboration (Morad Aaboud et al.). arXiv:1606.08772 [hep-ex]. [10.1140/epjc/s10052-016-4382-4](https://doi.org/10.1140/epjc/s10052-016-4382-4). Eur.Phys.J. C76 (2016) no.10, 547.
47. Search for the Higgs boson produced in association with a  $W$  boson and decaying to four  $b$ -quarks via two spin-zero particles in \$pp\$ collisions at 13 TeV with the ATLAS detector. By ATLAS Collaboration (Morad Aaboud et al.). arXiv:1606.08391 [hep-ex]. [10.1140/epjc/s10052-016-4418-9](https://doi.org/10.1140/epjc/s10052-016-4418-9). Eur.Phys.J. C76 (2016) no.11, 605.
48. Measurement of forward-backward multiplicity correlations in lead-lead, proton-lead and proton-proton collisions with the ATLAS detector. By ATLAS Collaboration (Morad Aaboud et al.). arXiv:1606.08170 [hep-ex].

49. The performance of the jet trigger for the ATLAS detector during 2011 data taking. By ATLAS Collaboration (Georges Aad et al.). arXiv:1606.07759 [hep-ex]. [10.1140/epjc/s10052-016-4325-0](https://doi.org/10.1140/epjc/s10052-016-4325-0). Eur.Phys.J. C76 (2016) no.10, 526.
50. Search for heavy long-lived charged \$R\$-hadrons with the ATLAS detector in  $3.2 \text{ fb}^{-1}$  of proton--proton collision data at  $\sqrt{s} = 13 \text{ TeV}$ . By ATLAS Collaboration (Morad Aaboud et al.). arXiv:1606.05129 [hep-ex]. [10.1016/j.physletb.2016.07.042](https://doi.org/10.1016/j.physletb.2016.07.042). Phys.Lett. B760 (2016) 647-665.
51. Searches for heavy diboson resonances in  $\text{pp}$  collisions at  $\sqrt{s}=13 \text{ TeV}$  with the ATLAS detector. By ATLAS Collaboration (Morad Aaboud et al.). arXiv:1606.04833 [hep-ex]. [10.1007/JHEP09\(2016\)173](https://doi.org/10.1007/JHEP09(2016)173). JHEP 1609 (2016) 173.
52. Search for pair production of Higgs bosons in the  $b\bar{b}b\bar{b}$  final state using proton--proton collisions at  $\sqrt{s} = 13 \text{ TeV}$  with the ATLAS detector. By ATLAS Collaboration (Morad Aaboud et al.). arXiv:1606.04782 [hep-ex]. [10.1103/PhysRevD.94.052002](https://doi.org/10.1103/PhysRevD.94.052002). Phys.Rev. D94 (2016) no.5, 052002.
53. Measurement of the  $W^{\pm}Z$  boson pair-production cross section in  $\text{pp}$  collisions at  $\sqrt{s}=13 \text{ TeV}$  with the ATLAS Detector. By ATLAS Collaboration (Morad Aaboud et al.). arXiv:1606.04017 [hep-ex]. [10.1016/j.physletb.2016.08.052](https://doi.org/10.1016/j.physletb.2016.08.052). Phys.Lett. B762 (2016) 1-22.
54. Search for new resonances in events with one lepton and missing transverse momentum in  $\text{pp}$  collisions at  $\sqrt{s} = 13 \text{ TeV}$  with the ATLAS detector. By ATLAS Collaboration (Morad Aaboud et al.). arXiv:1606.03977 [hep-ex]. [10.1016/j.physletb.2016.09.040](https://doi.org/10.1016/j.physletb.2016.09.040). Phys.Lett. B762 (2016) 334-352.
55. Search for top squarks in final states with one isolated lepton, jets, and missing transverse momentum in  $\sqrt{s}=13 \text{ TeV}$   $\text{pp}$  collisions with the ATLAS detector. By ATLAS Collaboration (Morad Aaboud et al.). arXiv:1606.03903 [hep-ex]. [10.1103/PhysRevD.94.052009](https://doi.org/10.1103/PhysRevD.94.052009). Phys.Rev. D94 (2016) no.5, 052009.
56. Search for resonances in diphoton events at  $\sqrt{s}=13 \text{ TeV}$  with the ATLAS detector. By ATLAS Collaboration (Morad Aaboud et al.). arXiv:1606.03833 [hep-ex]. [10.1007/JHEP09\(2016\)001](https://doi.org/10.1007/JHEP09(2016)001). JHEP 1609 (2016) 001.
57. Measurement of the  $t\bar{t}$  production cross-section using  $e\mu$  events with b-tagged jets in  $\text{pp}$  collisions at  $\sqrt{s}=13 \text{ TeV}$  with the ATLAS detector. By ATLAS Collaboration (Morad Aaboud et al.). arXiv:1606.02699 [hep-ex]. [10.1016/j.physletb.2016.08.019](https://doi.org/10.1016/j.physletb.2016.08.019). Phys.Lett. B761 (2016) 136-157.
58. Measurement of the Inelastic Proton-Proton Cross Section at  $\sqrt{s} = 13 \text{ TeV}$  with the ATLAS Detector at the LHC. By ATLAS Collaboration (M. Aaboud et al.). arXiv:1606.02625 [hep-ex]. [10.1103/PhysRevLett.117.182002](https://doi.org/10.1103/PhysRevLett.117.182002). Phys.Rev.Lett. 117 (2016) no.18, 182002.
59. Measurements of the Higgs boson production and decay rates and constraints on its couplings from a combined ATLAS and CMS analysis of the LHC pp collision data at  $\sqrt{s}=7 \text{ and } 8 \text{ TeV}$ . By ATLAS and CMS Collaborations (Georges Aad et al.). arXiv:1606.02266 [hep-ex]. [10.1007/JHEP08\(2016\)045](https://doi.org/10.1007/JHEP08(2016)045). JHEP 1608 (2016) 045.
60. Search for TeV-scale gravity signatures in high-mass final states with leptons and jets with the ATLAS detector at  $\sqrt{s}=13 \text{ TeV}$ . By ATLAS Collaboration (Morad Aaboud et al.). arXiv:1606.02265 [hep-ex]. [10.1016/j.physletb.2016.07.030](https://doi.org/10.1016/j.physletb.2016.07.030). Phys.Lett. B760 (2016) 520-537.

61. Search for the Standard Model Higgs boson produced by vector-boson fusion and decaying to bottom quarks in  $\sqrt{s}=8$  TeV pp collisions with the ATLAS detector. By ATLAS Collaboration (Morad Aaboud et al.). arXiv:1606.02181 [hep-ex]. [10.1007/JHEP11\(2016\)112](https://doi.org/10.1007/JHEP11(2016)112). JHEP 1611 (2016) 112.
62. Measurement of the top quark mass in the  $t\bar{t}$  dilepton channel from  $\sqrt{s}=8$  TeV ATLAS data. By ATLAS Collaboration (Morad Aaboud et al.). arXiv:1606.02179 [hep-ex]. [10.1016/j.physletb.2016.08.042](https://doi.org/10.1016/j.physletb.2016.08.042). Phys.Lett. B761 (2016) 350-371.
63. Measurement of the photon identification efficiencies with the ATLAS detector using LHC Run-1 data. By ATLAS Collaboration (Morad Aaboud et al.). arXiv:1606.01813 [hep-ex]. [10.1140/epjc/s10052-016-4507-9](https://doi.org/10.1140/epjc/s10052-016-4507-9). Eur.Phys.J. C76 (2016) no.12, 666.
64. Measurement of the double-differential high-mass Drell-Yan cross section in pp collisions at  $\sqrt{s}=8$  TeV with the ATLAS detector. By ATLAS Collaboration (Georges Aad et al.). arXiv:1606.01736 [hep-ex]. [10.1007/JHEP08\(2016\)009](https://doi.org/10.1007/JHEP08(2016)009). JHEP 1608 (2016) 009.
65. Charged-particle distributions at low transverse momentum in  $\sqrt{s} = 13$  TeV pp interactions measured with the ATLAS detector at the LHC. By ATLAS Collaboration (Morad Aaboud et al.). arXiv:1606.01133 [hep-ex]. [10.1140/epjc/s10052-016-4335-y](https://doi.org/10.1140/epjc/s10052-016-4335-y). Eur.Phys.J. C76 (2016) no.9, 502.
66. Measurement of the angular coefficients in Z-boson events using electron and muon pairs from data taken at  $\sqrt{s}=8$  TeV with the ATLAS detector. By ATLAS Collaboration (Georges Aad et al.). arXiv:1606.00689 [hep-ex]. [10.1007/JHEP08\(2016\)159](https://doi.org/10.1007/JHEP08(2016)159). JHEP 1608 (2016) 159.
67. Search for pair production of gluinos decaying via stop and sbottom in events with b-jets and large missing transverse momentum in pp collisions at  $\sqrt{s} = 13$  TeV with the ATLAS detector. By ATLAS Collaboration (Georges Aad et al.). arXiv:1605.09318 [hep-ex]. [10.1103/PhysRevD.94.032003](https://doi.org/10.1103/PhysRevD.94.032003). Phys.Rev. D94 (2016) no.3, 032003.
68. Measurement of the relative width difference of the  $B^0 - \bar{B}^0$  system with the ATLAS detector. By ATLAS Collaboration (Morad Aaboud et al.). arXiv:1605.07485 [hep-ex]. [10.1007/JHEP06\(2016\)081](https://doi.org/10.1007/JHEP06(2016)081). JHEP 1606 (2016) 081.
69. Transverse momentum, rapidity, and centrality dependence of inclusive charged-particle production in  $\sqrt{s_{NN}}=5.02$  TeV p + Pb collisions measured by the ATLAS experiment. By ATLAS Collaboration (Georges Aad et al.). arXiv:1605.06436 [hep-ex]. [10.1016/j.physletb.2016.10.053](https://doi.org/10.1016/j.physletb.2016.10.053). Phys.Lett. B763 (2016) 313-336.
70. Search for scalar leptoquarks in pp collisions at  $\sqrt{s} = 13$  TeV with the ATLAS experiment. By ATLAS Collaboration (Morad Aaboud et al.). arXiv:1605.06035 [hep-ex]. [10.1088/1367-2630/18/9/093016](https://doi.org/10.1088/1367-2630/18/9/093016). New J.Phys. 18 (2016) no.9, 093016.
71. Search for gluinos in events with an isolated lepton, jets and missing transverse momentum at  $\sqrt{s} = 13$  TeV with the ATLAS detector. By ATLAS Collaboration (Georges Aad et al.). arXiv:1605.04285 [hep-ex]. [10.1140/epjc/s10052-016-4397-x](https://doi.org/10.1140/epjc/s10052-016-4397-x). Eur.Phys.J. C76 (2016) no.10, 565.
72. Search for squarks and gluinos in final states with jets and missing transverse momentum at  $\sqrt{s} = 13$  TeV with the ATLAS detector. By ATLAS Collaboration (Morad Aaboud et al.). arXiv:1605.03814 [hep-ex]. [10.1140/epjc/s10052-016-4184-8](https://doi.org/10.1140/epjc/s10052-016-4184-8). Eur.Phys.J. C76 (2016) no.7, 392.

73. Measurement of the inclusive isolated prompt photon cross section in pp collisions at  $\sqrt{s}=8$  TeV with the ATLAS detector. By ATLAS Collaboration (Georges Aad et al.). arXiv:1605.03495 [hep-ex]. [10.1007/JHEP08\(2016\)005](https://doi.org/10.1007/JHEP08(2016)005). JHEP 1608 (2016) 005.
74. Search for new phenomena in final states with an energetic jet and large missing transverse momentum in  $\text{pp}$  collisions at  $\sqrt{s}=13$  TeV using the ATLAS detector. By ATLAS Collaboration (Morad Aaboud et al.). arXiv:1604.07773 [hep-ex]. [10.1103/PhysRevD.94.032005](https://doi.org/10.1103/PhysRevD.94.032005). Phys. Rev. D94 (2016) no.3, 032005.
75. Search for lepton-flavour-violating decays of the Higgs and  $Z$  bosons with the ATLAS detector. By ATLAS Collaboration (Georges Aad et al.). arXiv:1604.07730 [hep-ex]. [10.1140/epjc/s10052-017-4624-0](https://doi.org/10.1140/epjc/s10052-017-4624-0). Eur.Phys.J. C77 (2017) no.2, 70.
76. Measurements of the charge asymmetry in top-quark pair production in the dilepton final state at  $\sqrt{s}=8$  TeV with the ATLAS detector. By ATLAS Collaboration (Georges Aad et al.). arXiv:1604.05538 [hep-ex]. [10.1103/PhysRevD.94.032006](https://doi.org/10.1103/PhysRevD.94.032006). Phys. Rev. D94 (2016) no.3, 032006.
77. Measurements of  $Z\gamma\gamma$  and  $Z\gamma\gamma\gamma$  production in  $\text{pp}$  collisions at  $\sqrt{s}=8$  TeV with the ATLAS detector. By ATLAS Collaboration (Georges Aad et al.). arXiv:1604.05232 [hep-ex]. [10.1103/PhysRevD.93.112002](https://doi.org/10.1103/PhysRevD.93.112002). Phys. Rev. D93 (2016) no.11, 112002.
78. Search for metastable heavy charged particles with large ionization energy loss in pp collisions at  $\sqrt{s} = 13$  TeV using the ATLAS experiment. By ATLAS Collaboration (Morad Aaboud et al.). arXiv:1604.04520 [hep-ex]. [10.1103/PhysRevD.93.112015](https://doi.org/10.1103/PhysRevD.93.112015). Phys. Rev. D93 (2016) no.11, 112015.
79. Study of the rare decays of  $B^0_s$  and  $B^0$  into muon pairs from data collected during the LHC Run 1 with the ATLAS detector. By ATLAS Collaboration (Morad Aaboud et al.). arXiv:1604.04263 [hep-ex]. [10.1140/epjc/s10052-016-4338-8](https://doi.org/10.1140/epjc/s10052-016-4338-8). Eur.Phys.J. C76 (2016) no.9, 513.
80. Search for the Standard Model Higgs boson decaying into  $b\bar{b}$  produced in association with top quarks decaying hadronically in pp collisions at  $\sqrt{s}=8$  TeV with the ATLAS detector. By ATLAS Collaboration (Georges Aad et al.). arXiv:1604.03812 [hep-ex]. [10.1007/JHEP05\(2016\)160](https://doi.org/10.1007/JHEP05(2016)160). JHEP 1605 (2016) 160.
81. Measurement of fiducial differential cross sections of gluon-fusion production of Higgs bosons decaying to  $WW^{*}\rightarrow e\nu\mu\nu$  with the ATLAS detector at  $\sqrt{s}=8$  TeV. By ATLAS Collaboration (Georges Aad et al.). arXiv:1604.02997 [hep-ex]. [10.1007/JHEP08\(2016\)104](https://doi.org/10.1007/JHEP08(2016)104). JHEP 1608 (2016) 104.
82. Search for new phenomena in events with a photon and missing transverse momentum in  $\text{pp}$  collisions at  $\sqrt{s}=13$  TeV with the ATLAS detector. By ATLAS Collaboration (Morad Aaboud et al.). arXiv:1604.01306 [hep-ex]. [10.1007/JHEP06\(2016\)059](https://doi.org/10.1007/JHEP06(2016)059). JHEP 1606 (2016) 059.
83. Measurement of  $W^{*\pm}$  and  $Z$ -boson production cross sections in  $\text{pp}$  collisions at  $\sqrt{s}=13$  TeV with the ATLAS detector. By ATLAS Collaboration (Georges Aad et al.). arXiv:1603.09222 [hep-ex]. [10.1016/j.physletb.2016.06.023](https://doi.org/10.1016/j.physletb.2016.06.023). Phys.Lett. B759 (2016) 601-621.
84. Search for charged Higgs bosons produced in association with a top quark and decaying via  $H^{*\pm}\rightarrow\tau\nu$  using  $\text{pp}$  collision data recorded at  $\sqrt{s} = 13$  TeV by the ATLAS detector. By ATLAS Collaboration (Morad Aaboud et al.). arXiv:1603.09203 [hep-ex]. [10.1016/j.physletb.2016.06.017](https://doi.org/10.1016/j.physletb.2016.06.017). Phys.Lett. B759 (2016) 555-574.

85. Beam-induced and cosmic-ray backgrounds observed in the ATLAS detector during the LHC 2012 proton-proton running period. By ATLAS Collaboration (Georges Aad et al.). arXiv:1603.09202 [hep-ex]. [10.1088/1748-0221/11/05/P05013](https://doi.org/10.1088/1748-0221/11/05/P05013). JINST 11 (2016) no.05, P05013.
86. Search for resonances in the mass distribution of jet pairs with one or two jets identified as \$b\$-jets in proton--proton collisions at  $\sqrt{s}=13$  TeV with the ATLAS detector. By ATLAS Collaboration (Morad Aaboud et al.). arXiv:1603.08791 [hep-ex]. [10.1016/j.physletb.2016.05.064](https://doi.org/10.1016/j.physletb.2016.05.064). Phys.Lett. B759 (2016) 229-246.
87. Muon reconstruction performance of the ATLAS detector in proton–proton collision data at  $\sqrt{s}=13$  TeV. By ATLAS Collaboration (Georges Aad et al.). arXiv:1603.05598 [hep-ex]. [10.1140/epjc/s10052-016-4120-y](https://doi.org/10.1140/epjc/s10052-016-4120-y). Eur.Phys.J. C76 (2016) no.5, 292.
88. Identification of high transverse momentum top quarks in  $p\bar{p}$  collisions at  $\sqrt{s}=8$  TeV with the ATLAS detector. By ATLAS Collaboration (Georges Aad et al.). arXiv:1603.03127 [hep-ex]. [10.1007/JHEP06\(2016\)093](https://doi.org/10.1007/JHEP06(2016)093). JHEP 1606 (2016) 093.
89. Topological cell clustering in the ATLAS calorimeters and its performance in LHC Run 1. By ATLAS Collaboration (Georges Aad et al.). arXiv:1603.02934 [hep-ex].
90. Charged-particle distributions in  $p\bar{p}$  interactions at  $\sqrt{s}=8$  TeV measured with the ATLAS detector. By ATLAS Collaboration (Georges Aad et al.). arXiv:1603.02439 [hep-ex]. [10.1140/epjc/s10052-016-4203-9](https://doi.org/10.1140/epjc/s10052-016-4203-9). Eur.Phys.J. C76 (2016) no.7, 403.
91. Measurements of  $W^{\pm} Z$  production cross sections in  $p\bar{p}$  collisions at  $\sqrt{s}=8$  TeV with the ATLAS detector and limits on anomalous gauge boson self-couplings. By ATLAS Collaboration (Georges Aad et al.). arXiv:1603.02151 [hep-ex]. [10.1103/PhysRevD.93.092004](https://doi.org/10.1103/PhysRevD.93.092004). Phys.Rev. D93 (2016) no.9, 092004.
92. Measurement of total and differential  $W^+ W^-$  production cross sections in proton-proton collisions at  $\sqrt{s}=8$  TeV with the ATLAS detector and limits on anomalous triple-gauge-boson couplings. By ATLAS Collaboration (Georges Aad et al.). arXiv:1603.01702 [hep-ex]. [10.1007/JHEP09\(2016\)029](https://doi.org/10.1007/JHEP09(2016)029). JHEP 1609 (2016) 029.
93. Search for supersymmetry at  $\sqrt{s}=13$  TeV in final states with jets and two same-sign leptons or three leptons with the ATLAS detector. By ATLAS Collaboration (Georges Aad et al.). arXiv:1602.09058 [hep-ex]. [10.1140/epjc/s10052-016-4095-8](https://doi.org/10.1140/epjc/s10052-016-4095-8). Eur.Phys.J. C76 (2016) no.5, 259.
94. Measurement of event-shape observables in  $Z \rightarrow e^+ e^-$  events in  $p\bar{p}$  collisions at  $\sqrt{s}=7$  TeV with the ATLAS detector at the LHC. By ATLAS Collaboration (Georges Aad et al.). arXiv:1602.08980 [hep-ex]. [10.1140/epjc/s10052-016-4176-8](https://doi.org/10.1140/epjc/s10052-016-4176-8). Eur.Phys.J. C76 (2016) no.7, 375.
95. Search for new phenomena in final states with large jet multiplicities and missing transverse momentum with ATLAS using  $\sqrt{s}=13$  TeV proton-proton collisions. By ATLAS Collaboration (Georges Aad et al.). arXiv:1602.06194 [hep-ex]. [10.1016/j.physletb.2016.04.005](https://doi.org/10.1016/j.physletb.2016.04.005). Phys.Lett. B757 (2016) 334-355.
96. Search for single production of a vector-like quark via a heavy gluon in the  $4b$  final state with the ATLAS detector in  $p\bar{p}$  collisions at  $\sqrt{s}=8$  TeV. By ATLAS Collaboration (Georges Aad et al.). arXiv:1602.06034 [hep-ex]. [10.1016/j.physletb.2016.04.061](https://doi.org/10.1016/j.physletb.2016.04.061). Phys.Lett. B758 (2016) 249-268.

97. Search for single production of vector-like quarks decaying into Wb in pp collisions at  $\sqrt{s} = 8$  TeV with the ATLAS detector. By ATLAS Collaboration (Georges Aad et al.). arXiv:1602.05606 [hep-ex]. [10.1140/epjc/s10052-016-4281-8](https://doi.org/10.1140/epjc/s10052-016-4281-8). Eur.Phys.J. C76 (2016) no.8, 442.
98. Test of CP Invariance in vector-boson fusion production of the Higgs boson using the Optimal Observable method in the ditau decay channel with the ATLAS detector. By ATLAS Collaboration (Georges Aad et al.). arXiv:1602.04516 [hep-ex]. [10.1140/epjc/s10052-016-4499-5](https://doi.org/10.1140/epjc/s10052-016-4499-5). Eur.Phys.J. C76 (2016) no.12, 658.
99. Charged-particle distributions in  $\sqrt{s} = 13$  TeV pp interactions measured with the ATLAS detector at the LHC. By ATLAS Collaboration (Georges Aad et al.). arXiv:1602.01633 [hep-ex]. [10.1016/j.physletb.2016.04.050](https://doi.org/10.1016/j.physletb.2016.04.050). Phys.Lett. B758 (2016) 67-88.
100. Measurement of the charged-particle multiplicity inside jets from  $\sqrt{s}=8$  TeV \$pp\$ collisions with the ATLAS detector. By ATLAS Collaboration (Georges Aad et al.). arXiv:1602.00988 [hep-ex]. [10.1140/epjc/s10052-016-4126-5](https://doi.org/10.1140/epjc/s10052-016-4126-5). Eur.Phys.J. C76 (2016) no.6, 322.
101. A search for top squarks with R-parity-violating decays to all-hadronic final states with the ATLAS detector in  $\sqrt{s} = 8$  TeV proton-proton collisions. By ATLAS Collaboration (Georges Aad et al.). arXiv:1601.07453 [hep-ex]. [10.1007/JHEP06\(2016\)067](https://doi.org/10.1007/JHEP06(2016)067). JHEP 1606 (2016) 067.
102. A search for an excited muon decaying to a muon and two jets in \$pp\$ collisions at  $\sqrt{s} = 8$  TeV with the ATLAS detector. By ATLAS Collaboration (Georges Aad et al.). arXiv:1601.05627 [hep-ex]. [10.1088/1367-2630/18/7/073021](https://doi.org/10.1088/1367-2630/18/7/073021). New J.Phys. 18 (2016) no.7, 073021.
103. Probing lepton flavour violation via neutrinoless  $\tau \rightarrow \mu$  decays with the ATLAS detector. By ATLAS Collaboration (Georges Aad et al.). arXiv:1601.03567 [hep-ex]. [10.1140/epjc/s10052-016-4041-9](https://doi.org/10.1140/epjc/s10052-016-4041-9). Eur.Phys.J. C76 (2016) no.5, 232.
104. Measurement of the CP-violating phase  $\phi_s$  and the  $B^0_s \rightarrow J/\psi \phi$  meson decay width difference with  $B^0_s \rightarrow J/\psi \phi$  decays in ATLAS. By ATLAS Collaboration (Georges Aad et al.). arXiv:1601.03297 [hep-ex]. [10.1007/JHEP08\(2016\)147](https://doi.org/10.1007/JHEP08(2016)147). JHEP 1608 (2016) 147.
105. Measurement of the charge asymmetry in highly boosted top-quark pair production in  $\sqrt{s} = 8$  TeV \$pp\$ collision data collected by the ATLAS experiment. By ATLAS Collaboration (Georges Aad et al.). arXiv:1512.06092 [hep-ex]. [10.1016/j.physletb.2016.02.055](https://doi.org/10.1016/j.physletb.2016.02.055). Phys.Lett. B756 (2016) 52-71.
106. Reconstruction of hadronic decay products of tau leptons with the ATLAS experiment. By ATLAS Collaboration (Georges Aad et al.). arXiv:1512.05955 [hep-ex]. [10.1140/epjc/s10052-016-4110-0](https://doi.org/10.1140/epjc/s10052-016-4110-0). Eur.Phys.J. C76 (2016) no.5, 295.
107. Search for new phenomena with photon+jet events in proton-proton collisions at  $\sqrt{s}=13$  TeV with the ATLAS detector. By ATLAS Collaboration (Georges Aad et al.). arXiv:1512.05910 [hep-ex]. [10.1007/JHEP03\(2016\)041](https://doi.org/10.1007/JHEP03(2016)041). JHEP 1603 (2016) 041.
108. Measurement of the ZZ Production Cross Section in \$pp\$ Collisions at  $\sqrt{s} = 13$  TeV with the ATLAS Detector. By ATLAS Collaboration (Georges Aad et al.). arXiv:1512.05314 [hep-ex]. [10.1103/PhysRevLett.116.101801](https://doi.org/10.1103/PhysRevLett.116.101801). Phys.Rev.Lett. 116 (2016) no.10, 101801.
109. Combination of searches for WW\$, WZ\$, and ZZ\$ resonances in \$pp\$ collisions at  $\sqrt{s} = 8$  TeV with the ATLAS detector. By ATLAS Collaboration (Georges Aad et al.). arXiv:1512.05099 [hep-ex]. [10.1016/j.physletb.2016.02.015](https://doi.org/10.1016/j.physletb.2016.02.015). Phys.Lett. B755 (2016) 285-305.

110. Search for charged Higgs bosons in the  $H^{\pm} \rightarrow tb$  decay channel in  $\text{pp}$  collisions at  $\sqrt{s}=8$  TeV using the ATLAS detector. By ATLAS Collaboration (Georges Aad et al.). arXiv:1512.03704 [hep-ex]. [10.1007/JHEP03\(2016\)127](https://doi.org/10.1007/JHEP03(2016)127). JHEP 1603 (2016) 127.
111. Measurement of the differential cross-sections of prompt and non-prompt production of  $J/\psi$  and  $\psi(2\text{m}\chi)$  in  $\text{pp}$  collisions at  $\sqrt{s} = 7$  and 8 TeV with the ATLAS detector. By ATLAS Collaboration (Georges Aad et al.). arXiv:1512.03657 [hep-ex]. [10.1140/epjc/s10052-016-4050-8](https://doi.org/10.1140/epjc/s10052-016-4050-8). Eur.Phys.J. C76 (2016) no.5, 283.
112. Measurement of  $D^{*\pm}$ ,  $D^{\pm}$  and  $D_s^{\pm}$  meson production cross sections in  $\text{pp}$  collisions at  $\sqrt{s}=7$  TeV with the ATLAS detector. By ATLAS Collaboration (Georges Aad et al.). arXiv:1512.02913 [hep-ex]. [10.1016/j.nuclphysb.2016.04.032](https://doi.org/10.1016/j.nuclphysb.2016.04.032). Nucl.Phys. B907 (2016) 717-763.
113. Search for strong gravity in multijet final states produced in  $\text{pp}$  collisions at  $\sqrt{s} = 13$  TeV using the ATLAS detector at the LHC. By ATLAS Collaboration (Georges Aad et al.). arXiv:1512.02586 [hep-ex]. [10.1007/JHEP03\(2016\)026](https://doi.org/10.1007/JHEP03(2016)026). JHEP 1603 (2016) 026.
114. Measurement of the transverse momentum and  $\phi_{\eta}$  distributions of Drell–Yan lepton pairs in proton–proton collisions at  $\sqrt{s}=8$  TeV with the ATLAS detector. By ATLAS Collaboration (Georges Aad et al.). arXiv:1512.02192 [hep-ex]. [10.1140/epjc/s10052-016-4070-4](https://doi.org/10.1140/epjc/s10052-016-4070-4). Eur.Phys.J. C76 (2016) no.5, 291.
115. Search for new phenomena in dijet mass and angular distributions from  $\text{pp}$  collisions at  $\sqrt{s}=13$  TeV with the ATLAS detector. By ATLAS Collaboration (Georges Aad et al.). arXiv:1512.01530 [hep-ex]. [10.1016/j.physletb.2016.01.032](https://doi.org/10.1016/j.physletb.2016.01.032). Phys.Lett. B754 (2016) 302-322.
116. Performance of  $b$ -Jet Identification in the ATLAS Experiment. By ATLAS Collaboration (Georges Aad et al.). arXiv:1512.01094 [hep-ex]. [10.1088/1748-0221/11/04/P04008](https://doi.org/10.1088/1748-0221/11/04/P04008). JINST 11 (2016) no.04, P04008.
117. Measurement of the dependence of transverse energy production at large pseudorapidity on the hard-scattering kinematics of proton-proton collisions at  $\sqrt{s} = 2.76$  TeV with ATLAS. By ATLAS Collaboration (Georges Aad et al.). arXiv:1512.00197 [hep-ex]. [10.1016/j.physletb.2016.02.056](https://doi.org/10.1016/j.physletb.2016.02.056). Phys.Lett. B756 (2016) 10-28.
118. Search for the Standard Model Higgs boson produced in association with a vector boson and decaying into a tau pair in  $\text{pp}$  collisions at  $\sqrt{s} = 8$  TeV with the ATLAS detector. By ATLAS Collaboration (Georges Aad et al.). arXiv:1511.08352 [hep-ex]. [10.1103/PhysRevD.93.092005](https://doi.org/10.1103/PhysRevD.93.092005). Phys.Rev. D93 (2016) no.9, 092005.
119. Evidence for single top-quark production in the  $s\bar{s}$ -channel in proton-proton collisions at  $\sqrt{s}=8$  TeV with the ATLAS detector using the Matrix Element Method. By ATLAS Collaboration (Georges Aad et al.). arXiv:1511.05980 [hep-ex]. [10.1016/j.physletb.2016.03.017](https://doi.org/10.1016/j.physletb.2016.03.017). Phys.Lett. B756 (2016) 228-246.
120. A search for prompt lepton-jets in  $\text{pp}$  collisions at  $\sqrt{s}=8$  TeV with the ATLAS detector. By ATLAS Collaboration (Georges Aad et al.). arXiv:1511.05542 [hep-ex]. [10.1007/JHEP02\(2016\)062](https://doi.org/10.1007/JHEP02(2016)062). JHEP 1602 (2016) 062.
121. Measurements of top-quark pair differential cross-sections in the lepton+jets channel in  $\text{pp}$  collisions at  $\sqrt{s}=8$  TeV using the ATLAS detector. By ATLAS Collaboration (Georges Aad et al.). arXiv:1511.04716 [hep-ex]. [10.1140/epjc/s10052-016-4366-4](https://doi.org/10.1140/epjc/s10052-016-4366-4). Eur.Phys.J. C76 (2016) no.10, 538.

122. Dijet production in  $\sqrt{s} = 7$  TeV  $pp$  collisions with large rapidity gaps at the ATLAS experiment. By ATLAS Collaboration (Georges Aad et al.). arXiv:1511.00502 [hep-ex]. [10.1016/j.physletb.2016.01.028](https://doi.org/10.1016/j.physletb.2016.01.028). Phys.Lett. B754 (2016) 214-234.
123. Measurement of the correlations between the polar angles of leptons from top quark decays in the helicity basis at  $\sqrt{s} = 7$  TeV using the ATLAS detector. By ATLAS Collaboration (Georges Aad et al.). arXiv:1510.07478 [hep-ex]. [10.1103/PhysRevD.93.012002](https://doi.org/10.1103/PhysRevD.93.012002). Phys.Rev. D93 (2016) no.1, 012002.
124. Search for dark matter produced in association with a Higgs boson decaying to two bottom quarks in  $pp$  collisions at  $\sqrt{s} = 8$  TeV with the ATLAS detector. By ATLAS Collaboration (Georges Aad et al.). arXiv:1510.06218 [hep-ex]. [10.1103/PhysRevD.93.072007](https://doi.org/10.1103/PhysRevD.93.072007). Phys.Rev. D93 (2016) no.7, 072007.
125. Identification of boosted, hadronically decaying W bosons and comparisons with ATLAS data taken at  $\sqrt{s} = 8$  TeV. By ATLAS Collaboration (Georges Aad et al.). arXiv:1510.05821 [hep-ex]. [10.1140/epjc/s10052-016-3978-z](https://doi.org/10.1140/epjc/s10052-016-3978-z). Eur.Phys.J. C76 (2016) no.3, 154.
126. Performance of pile-up mitigation techniques for jets in  $pp$  collisions at  $\sqrt{s} = 8$  TeV using the ATLAS detector. By ATLAS Collaboration (Georges Aad et al.). arXiv:1510.03823 [hep-ex]. [10.1140/epjc/s10052-016-4395-z](https://doi.org/10.1140/epjc/s10052-016-4395-z). Eur.Phys.J. C76 (2016) no.11, 581.
127. Measurement of the differential cross-section of highly boosted top quarks as a function of their transverse momentum in  $\sqrt{s} = 8$  TeV proton-proton collisions using the ATLAS detector. By ATLAS Collaboration (Georges Aad et al.). arXiv:1510.03818 [hep-ex]. [10.1103/PhysRevD.93.032009](https://doi.org/10.1103/PhysRevD.93.032009). Phys.Rev. D93 (2016) no.3, 032009.
128. Search for anomalous couplings in the  $Wtb$  vertex from the measurement of double differential angular decay rates of single top quarks produced in the  $t$ -channel with the ATLAS detector. By ATLAS Collaboration (Georges Aad et al.). arXiv:1510.03764 [hep-ex]. [10.1007/JHEP04\(2016\)023](https://doi.org/10.1007/JHEP04(2016)023). JHEP 1604 (2016) 023.
129. Measurement of the production cross-section of a single top quark in association with a  $W$  boson at 8 TeV with the ATLAS experiment. By ATLAS Collaboration (Georges Aad et al.). arXiv:1510.03752 [hep-ex]. [10.1007/JHEP01\(2016\)064](https://doi.org/10.1007/JHEP01(2016)064). JHEP 1601 (2016) 064.
130. Search for the production of single vector-like and excited quarks in the  $Wt$  final state in  $pp$  collisions at  $\sqrt{s} = 8$  TeV with the ATLAS detector. By ATLAS Collaboration (Georges Aad et al.). arXiv:1510.02664 [hep-ex]. [10.1007/JHEP02\(2016\)110](https://doi.org/10.1007/JHEP02(2016)110). JHEP 1602 (2016) 110.
131. Search for magnetic monopoles and stable particles with high electric charges in 8 TeV  $pp$  collisions with the ATLAS detector. By ATLAS Collaboration (Georges Aad et al.). arXiv:1509.08059 [hep-ex]. [10.1103/PhysRevD.93.052009](https://doi.org/10.1103/PhysRevD.93.052009). Phys.Rev. D93 (2016) no.5, 052009.
132. Measurements of four-lepton production in  $pp$  collisions at  $\sqrt{s} = 8$  TeV with the ATLAS detector. By ATLAS Collaboration (Georges Aad et al.). arXiv:1509.07844 [hep-ex]. [10.1016/j.physletb.2015.12.048](https://doi.org/10.1016/j.physletb.2015.12.048). Phys.Lett. B753 (2016) 552-572.
133. Search for the electroweak production of supersymmetric particles in  $\sqrt{s} = 8$  TeV  $pp$  collisions with the ATLAS detector. By ATLAS Collaboration (Georges Aad et al.). arXiv:1509.07152 [hep-ex]. [10.1103/PhysRevD.93.052002](https://doi.org/10.1103/PhysRevD.93.052002). Phys.Rev. D93 (2016) no.5, 052002.

134. Measurement of jet charge in dijet events from  $\sqrt{s}=8$  TeV pp collisions with the ATLAS detector. By ATLAS Collaboration (Georges Aad et al.). arXiv:1509.05190 [hep-ex]. [10.1103/PhysRevD.93.052003](https://doi.org/10.1103/PhysRevD.93.052003). Phys.Rev. D93 (2016) no.5, 052003.
135. Search for new phenomena in events with at least three photons collected in \$pp\$ collisions at  $\sqrt{s} = 8$  TeV with the ATLAS detector. By ATLAS Collaboration (Georges Aad et al.). arXiv:1509.05051 [hep-ex]. [10.1140/epjc/s10052-016-4034-8](https://doi.org/10.1140/epjc/s10052-016-4034-8). Eur.Phys.J. C76 (2016) no.4, 210.
136. Search for direct top squark pair production in final states with two tau leptons in pp collisions at  $\sqrt{s}=8$  TeV with the ATLAS detector. By ATLAS Collaboration (Georges Aad et al.). arXiv:1509.04976 [hep-ex]. [10.1140/epjc/s10052-016-3897-z](https://doi.org/10.1140/epjc/s10052-016-3897-z). Eur.Phys.J. C76 (2016) no.2, 81.
137. A new method to distinguish hadronically decaying boosted  $Z$  bosons from  $W$  bosons using the ATLAS detector. By ATLAS Collaboration (Georges Aad et al.). arXiv:1509.04939 [hep-ex]. [10.1140/epjc/s10052-016-4065-1](https://doi.org/10.1140/epjc/s10052-016-4065-1). Eur.Phys.J. C76 (2016) no.5, 238.
138. Observation of Long-Range Elliptic Azimuthal Anisotropies in  $\sqrt{s}=13$  and 2.76 TeV \$pp\$ Collisions with the ATLAS Detector. By ATLAS Collaboration (Georges Aad et al.). arXiv:1509.04776 [hep-ex]. [10.1103/PhysRevLett.116.172301](https://doi.org/10.1103/PhysRevLett.116.172301). Phys.Rev.Lett. 116 (2016) no.17, 172301.
139. Measurement of the charge asymmetry in top-quark pair production in the lepton-plus-jets final state in pp collision data at  $\sqrt{s}=8\text{ TeV}$  with the ATLAS detector. By ATLAS Collaboration (Georges Aad et al.). arXiv:1509.02358 [hep-ex]. [10.1140/epjc/s10052-016-3910-6](https://doi.org/10.1140/epjc/s10052-016-3910-6). Eur.Phys.J. C76 (2016) no.2, 87.
140. Search for a high-mass Higgs boson decaying to a  $WW$  boson pair in \$pp\$ collisions at  $\sqrt{s} = 8$  TeV with the ATLAS detector. By ATLAS Collaboration (Georges Aad et al.). arXiv:1509.00389 [hep-ex]. [10.1007/JHEP01\(2016\)032](https://doi.org/10.1007/JHEP01(2016)032). JHEP 1601 (2016) 032.
141. Search for single top-quark production via flavour-changing neutral currents at 8 TeV with the ATLAS detector. By ATLAS Collaboration (Georges Aad et al.). arXiv:1509.00294 [hep-ex]. [10.1140/epjc/s10052-016-3876-4](https://doi.org/10.1140/epjc/s10052-016-3876-4). Eur.Phys.J. C76 (2016) no.2, 55.
142. Search for invisible decays of a Higgs boson using vector-boson fusion in \$pp\$ collisions at  $\sqrt{s}=8$  TeV with the ATLAS detector. By ATLAS Collaboration (Georges Aad et al.). arXiv:1508.07869 [hep-ex]. [10.1007/JHEP01\(2016\)172](https://doi.org/10.1007/JHEP01(2016)172). JHEP 1601 (2016) 172.
143. Measurements of fiducial cross-sections for  $t\bar{t}$  production with one or two additional b-jets in pp collisions at  $\sqrt{s}=8$  TeV using the ATLAS detector. By ATLAS Collaboration (Georges Aad et al.). arXiv:1508.06868 [hep-ex]. [10.1140/epjc/s10052-015-3852-4](https://doi.org/10.1140/epjc/s10052-015-3852-4). Eur.Phys.J. C76 (2016) no.1, 11.
144. Search for flavour-changing neutral current top-quark decays to  $qZ$  in \$pp\$ collision data collected with the ATLAS detector at  $\sqrt{s} = 8$  TeV. By ATLAS Collaboration (Georges Aad et al.). arXiv:1508.05796 [hep-ex]. [10.1140/epjc/s10052-015-3851-5](https://doi.org/10.1140/epjc/s10052-015-3851-5). Eur.Phys.J. C76 (2016) no.1, 12.
145. Searches for scalar leptoquarks in pp collisions at  $\sqrt{s} = 8$  TeV with the ATLAS detector. By ATLAS Collaboration (Georges Aad et al.). arXiv:1508.04735 [hep-ex]. [10.1140/epjc/s10052-015-3823-9](https://doi.org/10.1140/epjc/s10052-015-3823-9). Eur.Phys.J. C76 (2016) no.1, 5.
146. Constraints on non-Standard Model Higgs boson interactions in an effective Lagrangian using differential cross sections measured in the  $H \rightarrow \gamma\gamma$  decay channel at

- $\sqrt{s} = 8\text{TeV}$  with the ATLAS detector. By ATLAS Collaboration (Georges Aad et al.). arXiv:1508.02507 [hep-ex]. [10.1016/j.physletb.2015.11.071](https://doi.org/10.1016/j.physletb.2015.11.071). Phys.Lett. B753 (2016) 69-85.
147. Measurement of the centrality dependence of the charged-particle pseudorapidity distribution in proton-lead collisions at  $\sqrt{s_{\text{NN}}} = 5.02\text{TeV}$  with the ATLAS detector. By ATLAS Collaboration (Georges Aad et al.). arXiv:1508.00848 [hep-ex]. [10.1140/epjc/s10052-016-4002-3](https://doi.org/10.1140/epjc/s10052-016-4002-3). Eur.Phys.J. C76 (2016) no.4, 199.
  148. Study of the  $B_c^+ \rightarrow J/\psi D_s^+$  and  $B_c^+ \rightarrow J/\psi D_s^{*+}$  decays with the ATLAS detector. By ATLAS Collaboration (Georges Aad et al.). arXiv:1507.07099 [hep-ex]. [10.1140/epjc/s10052-015-3743-8](https://doi.org/10.1140/epjc/s10052-015-3743-8). Eur.Phys.J. C76 (2016) no.1, 4.
  149. Search for an additional, heavy Higgs boson in the  $H \rightarrow ZZ$  decay channel at  $\sqrt{s} = 8\text{TeV}$  in  $p\bar{p}$  collision data with the ATLAS detector. By ATLAS Collaboration (Georges Aad et al.). arXiv:1507.05930 [hep-ex]. [10.1140/epjc/s10052-015-3820-z](https://doi.org/10.1140/epjc/s10052-015-3820-z). Eur.Phys.J. C76 (2016) no.1, 45.
  150. Measurements of the Higgs boson production and decay rates and coupling strengths using  $p\bar{p}$  collision data at  $\sqrt{s}=7\text{TeV}$  and 8 TeV in the ATLAS experiment. By ATLAS Collaboration (Georges Aad et al.). arXiv:1507.04548 [hep-ex]. [10.1140/epjc/s10052-015-3769-y](https://doi.org/10.1140/epjc/s10052-015-3769-y). Eur.Phys.J. C76 (2016) no.1, 6.
  151. Centrality, rapidity and transverse momentum dependence of isolated prompt photon production in lead-lead collisions at  $\sqrt{s_{\text{NN}}} = 2.76\text{TeV}$  measured with the ATLAS detector. By ATLAS Collaboration (Georges Aad et al.). arXiv:1506.08552 [hep-ex]. [10.1103/PhysRevC.93.034914](https://doi.org/10.1103/PhysRevC.93.034914). Phys.Rev. C93 (2016) no.3, 034914.

### CHTC (University of Wisconsin-Madison)

152. Bastide, H., Lange, J. D., Lack, J. B., Yassin, A., & Pool, J. E. (2016). A variable genetic architecture of melanic evolution in *Drosophila melanogaster*. *Genetics*, 204:1307-1319.
153. Burnett, B. A., & Williams, B. S. (2016). Design strategy for terahertz quantum dot cascade lasers. *Optics Express*, 24, 25471–25481. <https://doi.org/10.1364/OE.24.025471>
154. Burritt, N. L., Foss, N. J., Neeno-Eckwall, E. C., Church, J. O., Hilger, A. M., Hildebrand, J. A., et al. (2016). Sepsis and hemocyte loss in honey bees (*Apis mellifera*) infected with *Serratia marcescens* strain sicaria. *PLoS One*. 2016 Dec 21;11(12):e0167752. <https://doi.org/10.1371/journal.pone.0167752>
155. Chasman, D., Walters, K. B., Lopes, T. J. S., Eisfeld, A. J., Kawaoka, Y., & Roy, S. (2016). Integrating transcriptomic and proteomic data using predictive regulatory network models of host response to pathogens. *PLOS Computational Biology*. <https://doi.org/10.1371/journal.pcbi.1005013>
156. Dolan, N. S., Scamp, R. J., Yang, T., Berry, J. F., & Schomaker, J. M. (2016). Catalyst-controlled and tunable, chemoselective silver-catalyzed intermolecular nitrene transfer: Experimental and computational studies. *Journal of the American Chemical Society*, 138, 14658–14667. <https://doi.org/10.1021/jacs.6b07981>
157. Ganta, S., Van Veen, B. D., & Hagness, S. C. (2016, January). A classification framework for methods of uncertainty quantification in computational electromagnetics. National Radio Science Meeting, Boulder, CO.

158. Gofman, M. (2017). Efficiency and stability of a financial architecture with too-interconnected- to-fail institutions. *Journal of Financial Economics*, 124, 113-146.
159. Kim, D. (2016). Statistical inference for unified GARCH-Ito models with high-frequency financial data. *Journal of Time Series Analysis*, 37, 513-532.
160. Kim, H., Smith, B. M., Adluru, N., Dyer, C. R., Johnson, S. C., & Singh, V. (2016). Abundant inverse regression using sufficient reduction and its applications. *Proceedings of European Conference on Computer Vision*.
161. Kim, W. H., Kim, H. J., Adluru, N., & Singh, V. (2016). Latent variable graphical model selection using harmonic analysis: Applications to the Human Connectome Project. *Proceedings of IEEE Conference on Computer Vision and Pattern Recognition*.
162. Kim, W., Hwang, S., Adluru, N., Johnson, S. C., & Singh, V. (2016). Adaptive signal recovery on graphs via harmonic analysis for experimental design in neuroimaging. *Proceedings of European Conference on Computer Vision*.
163. Lack, J. B., Lange, J. D., Tang, A. D., Corbett-Detig, R. B., & Pool, J. E. (2016). A thousand genomes: An expanded *Drosophila* Genome Nexus. *Mol Biol Evol*, 33:3308-3313.
164. Lange, J. D., & Pool, J. E. (2016). A haplotype method detects diverse signatures of local adaptation from genomic sequence variation. *Mol Ecol* 25:3081-3100.
165. Liu, J., Ye, Z., Mayer, J. G., Hoch, B. A., Green, C., Rolak, L., et al. (2016). Phenome-wide association study maps new diseases to the human major histocompatibility complex region. *J Med Genet*. 2016 Oct;53(10):681-9. doi: 10.1136/jmedgenet-2016-103867
166. Marx H., Minogue, C. E., Jayaraman, D., Richards, A. L., Kwiecien, N. W., Siahpirani, A. F., et al. (2016). A proteomic atlas of the legume *Medicago truncatula* and its nitrogen-fixing endosymbiont *Sinorhizobium meliloti*. *Nature Biotechnology*, 34, 1198–1205. <https://doi.org/10.1038/nbt.3681>
167. Niu, Z., Chasman, D., Eisfeld, A. J., Kawaoka, Y., & Roy, S. (2016). Multi-task consensus clustering of genome-wide transcriptomes from related biological conditions. *Bioinformatics*, 32, 1509-1517. <https://doi.org/10.1093/bioinformatics/btw007>
168. Oswal, U., Cox, C., Rogers, T., & Nowak, R. (2016). Representational similarity learning with application to brain networks. *International Conference on Machine Learning*.
169. Pool, J. E. (2016). Genetic mapping by bulk segregant analysis in *Drosophila*: Experimental design and simulation-based inference. *Genetics*, 204:1295-1306.
170. Ravi, S. N., Ithapu, V. K., Johnson, S. C., & Singh, V. Experimental design on a budget for sparse linear models and applications. *Proceedings of International Conference on Machine Learning*.
171. Roth, J. D., Smith, C. R., & Thelen, D. G. (2017). Do simulated ligament releases to reduce imbalance after total knee arthroplasty compromise knee stability? Annual Meeting of the Orthopedic Research Society San Diego, CA.
172. Siahpirani, A. F., & Roy, S. (2016). A prior-based integrative framework for functional transcriptional regulatory network inference. *Nucleic Acids Research*, 45(4). <https://doi.org/10.1093/nar/gkw963>
173. Siahpirani, A. F., Ay, F., & Roy, S. (2016). A multi-task graph-clustering approach for chromosome conformation capture data sets identifies conserved modules of chromosomal interactions. *Genome Biology*, 17, 114. <https://doi.org/10.1186/s13059-016-0962-8>

174. Sievers, C. K., Zou, L. S., Pickhardt, P. J., Matkowskyj, K. A., Albrecht, D. M., Clipson, L., et al. (2016). Subclonal diversity arises early even in small colorectal tumours and contributes to differential growth fates. *Gut* 0, 1-9. doi:10.1136/gutjnl-2016-312232
175. Smith, C. R., & Thelen, D. (2016, August). Effects of muscle strength variations on simulated muscle loads and knee mechanics during walking. 40th Annual Meeting American Society of Biomechanics, Raleigh, NC.
176. Smith, C. R., & Thelen, D. (2016, June). The interaction of muscle coordination and knee mechanics. Biomechanics and Neural Motor Control of Movement, Mt. Sterling, OH.
177. Smith, C. R., & Thelen, D. (2017, March). Stochastic simulation of functional knee mechanics enabled via statistical shape modeling and high throughput computing. NIH IMAG Multiscale Modeling Consortium Meeting, Bethesda, MD.
178. Smith, C. R., Clouthier, A., Vignos, M., Brandon, S., & Thelen, D. (2016, August). A high throughput computing approach to stochastic simulation of cartilage loading during walking. 4th International Workshop on Biomechanical and Parametric Modeling of Human Anatomy, Vancouver, Canada.
179. Smith, C. R., Vignos, M., & Thelen, D. (2016, March). The influence of the ACL femoral attachment on knee mechanics during gait: A simulation study. Orthopedic Research Society Annual Meeting, Orlando, FL.
180. Smith, C. R., & Thelen, D. (2016, September). Simulation of coupled neuromuscular coordination and knee joint mechanics during movement. Podium Presentation. 14th International Symposium Computer Methods in Biomechanics and Biomedical Engineering, Tel Aviv, Israel.
181. Smith, C. R., & Thelen, D. (2017, July). Stochastic simulation of knee mechanics enabled via novel solution techniques and high throughput computing. XXVI Congress of the International Society of Biomechanics, Brisbane, Australia.
182. Smith, C. R., Koch, C., & Thelen, D. G. (2016). Enabling stochastic simulation of human movement with high throughput computing. OpenSim Webinar Series. <https://youtu.be/u8Cjvn9xMd0>
183. Wright, E. S., & Vetsigian, K. (2016). DesignSignatures: A tool for designing primers that yield amplicons with distinct signatures. *Bioinformatics*.
184. Wright, E. S., & Vetsigian, K. (2016). Inhibitory interactions promote frequent bistability among competing bacteria. *Nature Communications*, 7, 11274.
185. Wright, E. S., & Vetsigian, K. (2016). Quality filtering of Illumina index reads mitigates sample cross-talk. *BMC Genomics*, Nov., 1-7.

## CMS

186. Khachatryan, V., et al. (2017). Search for heavy gauge W' boson in events with an energetic lepton and large missing transverse momentum at  $\sqrt{s} = 13$  TeV. *Phys. Lett.*, B770, 278-301. doi:10.1016/j.physletb.2017.04.043. arXiv:1612.09274 [hep-ex].
187. Sirunyan, A., et al. (2017). Search for massive resonances decaying into WW, WZ or ZZ bosons in proton-proton collisions at  $\sqrt{s} = 13$  TeV. *JHEP*, 03, 162. doi:10.1007/JHEP03(2017)162. arXiv:1612.09159 [hep-ex].

188. Sirunyan, A., et al. (2017). Search for electroweak production of a vector-like quark decaying to a top quark and a Higgs boson using boosted topologies in fully hadronic final states. JHEP, 04, 136. doi:10.1007/JHEP04(2017)136. arXiv:1612.05336 [hep-ex].
189. Sirunyan, A., et al. (2017). Searches for pair production of third-generation squarks in  $\sqrt{s}=13 \text{ TeV}$  pp collisions. Eur. Phys. J., C77, 327. doi:10.1140/epjc/s10052-017-4853-2. arXiv:1612.03877 [hep-ex].
190. Khachatryan, V., et al. (2017). Search for heavy neutrinos or third-generation leptoquarks in final states with two hadronically decaying  $\tau$  leptons and two jets in proton-proton collisions at  $\sqrt{s}=13 \text{ TeV}$ . JHEP, 03, 077. doi:10.1007/JHEP03(2017)077. arXiv:1612.01190 [hep-ex].
191. Khachatryan, V., et al. (2017). Search for single production of a heavy vector-like T quark decaying to a Higgs boson and a top quark with a lepton and jets in the final state. Phys. Lett., B771, 80-105. doi:10.1016/j.physletb.2017.05.019. arXiv:1612.00999 [hep-ex].
192. Khachatryan, V., et al. (2017). Search for CP violation in  $t\bar{t}$  production and decay in proton-proton collisions at  $\sqrt{s}=8 \text{ TeV}$ . JHEP, 03, 101. doi:10.1007/JHEP03(2017)101. arXiv:1611.08931 [hep-ex].
193. Khachatryan, V., et al. (2017). Search for supersymmetry in events with photons and missing transverse energy in pp collisions at 13 TeV. Phys. Lett., B769, 391-412. doi:10.1016/j.physletb.2017.04.005. arXiv:1611.06604 [hep-ex].
194. Khachatryan, V., et al. (2017). Search for heavy resonances decaying to tau lepton pairs in proton-proton collisions at  $\sqrt{s}=13 \text{ TeV}$ . JHEP, 02, 048. doi:10.1007/JHEP02(2017)048. arXiv:1611.06594 [hep-ex].
195. Khachatryan, V., et al. (2017). Measurement of the  $t\bar{t}$  production cross section using events in the  $e\mu$  final state in pp collisions at  $\sqrt{s} = 13 \text{ TeV}$ . Eur. Phys. J., C77, 172. doi:10.1140/epjc/s10052-017-4718-8. arXiv:1611.04040 [hep-ex].
196. Khachatryan, V., et al. (2017). Measurements of differential production cross sections for a Z boson in association with jets in pp collisions at  $\sqrt{s}=8 \text{ TeV}$ . JHEP, 04, 022. doi:10.1007/JHEP04(2017)022. arXiv:1611.03844 [hep-ex].
197. Sirunyan, A., et al. (2017). Search for dijet resonances in proton–proton collisions at  $\sqrt{s} = 13 \text{ TeV}$  and constraints on dark matter and other models. Phys. Lett., B769, 520-542. doi:10.1016/j.physletb.2017.02.012. arXiv:1611.03568 [hep-ex].
198. Khachatryan, V., et al. (2017). Charged-particle nuclear modification factors in PbPb and pPb collisions at  $\sqrt{s_{\text{NN}}} = 5.02 \text{ TeV}$ . JHEP, 04, 039. doi:10.1007/JHEP04(2017)039. arXiv:1611.01664 [nucl-ex].
199. Khachatryan, V., et al. (2017). Suppression of  $\Upsilon(1S)$ ,  $\Upsilon(2S)$  and  $\Upsilon(3S)$  production in PbPb collisions at  $\sqrt{s_{\text{NN}}} = 2.76 \text{ TeV}$ . Phys. Lett., B770, 357-379. doi:10.1016/j.physletb.2017.04.031. arXiv:1611.01510 [nucl-ex].
200. Sirunyan, A., et al. (2017). Relative Modification of Prompt  $\psi(2S)$  and  $J/\psi$  Yields from pp to PbPb Collisions at  $\sqrt{s_{\text{NN}}} = 5.02 \text{ TeV}$ . Phys. Rev. Lett., 118, 162301. doi:10.1103/PhysRevLett.118.162301. arXiv:1611.01438 [nucl-ex].
201. Khachatryan, V., et al. (2017). A search for new phenomena in pp collisions at  $\sqrt{s} = 13 \text{ TeV}$  in final states with missing transverse momentum and at least one jet using the  $\alpha$

- $\_ \{\mathrm{T}\}$  variable. Eur. Phys. J., C77, 294. doi:10.1140/epjc/s10052-017-4787-8.  
arXiv:1611.00338 [hep-ex].
202. Chatrchyan, S., et al. (2017). Measurement of the mass difference between top quark and antiquark in pp collisions at  $\sqrt{s} = 8$  TeV. Phys. Lett., B770, 50-71. doi:10.1016/j.physletb.2017.04.028.  
arXiv:1610.09551 [hep-ex].
  203. Khachatryan, V., et al. (2017). Searches for invisible decays of the Higgs boson in pp collisions at  $\sqrt{s} = 7, 8$ , and 13 TeV. JHEP, 02, 135. doi:10.1007/JHEP02(2017)135. arXiv:1610.09218 [hep-ex].
  204. Khachatryan, V., et al. (2017). Search for heavy resonances decaying into a vector boson and a Higgs boson in final states with charged leptons, neutrinos, and b quarks. Phys. Lett., B768, 137-162. doi:10.1016/j.physletb.2017.02.040. arXiv:1610.08066 [hep-ex].
  205. Khachatryan, V., et al. (2017). Observation of  $\Upsilon(1S)$  pair production in proton-proton collisions at  $\sqrt{s}=8$  TeV. JHEP, 05, 013. doi:10.1007/JHEP05(2017)013. arXiv:1610.07095 [hep-ex].
  206. Khachatryan, V., et al. (2016). Search for R-parity violating supersymmetry with displaced vertices in proton-proton collisions at  $\sqrt{s} = 8$  TeV. Phys. Rev. D. doi:10.1103/PhysRevD.95.012009.  
arXiv:1610.05133 [hep-ex].
  207. Khachatryan, V., et al. (2017). Search for electroweak production of charginos in final states with two  $\tau$  leptons in pp collisions at  $\sqrt{s}=8$  TeV. JHEP, 04, 018. doi:10.1007/JHEP04(2017)018.  
arXiv:1610.04870 [hep-ex].
  208. Khachatryan, V., et al. (2017). Search for top quark decays via Higgs-boson-mediated flavor-changing neutral currents in pp collisions at  $\sqrt{s}=8$  TeV. JHEP, 02, 079.  
doi:10.1007/JHEP02(2017)079. arXiv:1610.04857 [hep-ex].
  209. Khachatryan, V., et al. (2016). Measurements of differential cross sections for associated production of a W boson and jets in proton-proton collisions at  $\sqrt{s} = 8$  TeV. Phys. Rev. D.  
doi:10.1103/PhysRevD.95.052002. arXiv:1610.04222 [hep-ex].
  210. Khachatryan, V., et al. (2017). Measurement of differential cross sections for top quark pair production using the lepton+jets final state in proton-proton collisions at 13 TeV. Phys. Rev., D95, 092001. doi:10.1103/PhysRevD.95.092001. arXiv:1610.04191 [hep-ex].
  211. Khachatryan, V., et al. (2017). Search for anomalous Wtb couplings and flavour-changing neutral currents in t-channel single top quark production in pp collisions at  $\sqrt{s} = 7$  and 8 TeV. JHEP, 02, 028. doi:10.1007/JHEP02(2017)028. arXiv:1610.03545 [hep-ex].
  212. Khachatryan, V., et al. (2017). Search for high-mass Z $\gamma$  resonances in  $e^+ e^- \gamma \gamma$  and  $\mu^+ \mu^- \gamma \gamma$  final states in proton-proton collisions at  $\sqrt{s} = 8$  and 13 TeV. JHEP, 01, 076. doi:10.1007/JHEP01(2017)076.  
arXiv:1610.02960 [hep-ex].
  213. Khachatryan, V., et al. (2017). Suppression and azimuthal anisotropy of prompt and nonprompt  $J/\psi$  production in PbPb collisions at  $\sqrt{s_{\text{NN}}} = 2.76$  TeV. Eur. Phys. J., C77, 252. doi:10.1140/epjc/s10052-017-4781-1.  
arXiv:1610.00613 [nucl-ex].

214. Khachatryan, V., et al. (2017). Observation of charge-dependent azimuthal correlations in  $\text{Pb}+\text{Pb}$  collisions and its implication for the search for the chiral magnetic effect. *Phys. Rev. Lett.*, 118, 122301. doi:10.1103/PhysRevLett.118.122301. arXiv:1610.00263 [nucl-ex].
215. Khachatryan, V., et al. (2017). Search for supersymmetry in events with one lepton and multiple jets in proton-proton collisions at  $\sqrt{s} = 13 \text{ TeV}$ . *Phys. Rev.*, D95, 012011. doi:10.1103/PhysRevD.95.012011. arXiv:1609.09386 [hep-ex].
216. Khachatryan, V., et al. (2016). Search for long-lived charged particles in proton-proton collisions at  $\sqrt{s} = 13 \text{ TeV}$ . *Phys. Rev.*, D94, 112004. doi:10.1103/PhysRevD.94.112004. arXiv:1609.08382 [hep-ex].
217. Khachatryan, V., et al. (2017). Inclusive search for supersymmetry using razor variables in pp collisions at  $\sqrt{s} = 13 \text{ TeV}$ . *Phys. Rev.*, D95, 012003. doi:10.1103/PhysRevD.95.012003. arXiv:1609.07658 [hep-ex].
218. Khachatryan, V., et al. (2017). Measurement of the  $WZ$  production cross section in pp collisions at  $\sqrt{s} = 7 \text{ and } 8 \text{ TeV}$  and search for anomalous triple gauge couplings at  $\sqrt{s} = 8 \text{ TeV}$ . *Eur. Phys. J.*, C77, 236. doi:10.1140/epjc/s10052-017-4730-z. arXiv:1609.05721 [hep-ex].
219. Khachatryan, V., et al. (2017). Search for narrow resonances in dilepton mass spectra in proton-proton collisions at  $\sqrt{s} = 13 \text{ TeV}$  and combination with 8 TeV data. *Phys. Lett.*, B768, 57-80. doi:10.1016/j.physletb.2017.02.010. arXiv:1609.05391 [hep-ex].
220. Khachatryan, V., et al. (2017). Measurement and QCD analysis of double-differential inclusive jet cross sections in pp collisions at  $\sqrt{s} = 8 \text{ TeV}$  and cross section ratios to 2.76 and 7 TeV. *JHEP*, 03, 156. doi:10.1007/JHEP03(2017)156. arXiv:1609.05331 [hep-ex].
221. Khachatryan, V., et al. (2016). Studies of inclusive four-jet production with two  $b$ -tagged jets in proton-proton collisions at 7 TeV. *Phys. Rev.*, D94, 112005. doi:10.1103/PhysRevD.94.112005. arXiv:1609.03489 [hep-ex].
222. Khachatryan, V., et al. (2017). Search for high-mass diphoton resonances in proton–proton collisions at 13 TeV and combination with 8 TeV search. *Phys. Lett.*, B767, 147-170. doi:10.1016/j.physletb.2017.01.027. arXiv:1609.02507 [hep-ex].
223. Khachatryan, V., et al. (2016). Decomposing transverse momentum balance contributions for quenched jets in PbPb collisions at  $\sqrt{s} = 2.76 \text{ TeV}$ . *JHEP*, 11, 055. doi:10.1007/JHEP11(2016)055. arXiv:1609.02466 [nucl-ex].
224. Khachatryan, V., et al. (2017). The CMS trigger system. *JINST*, 12, P01020. doi:10.1088/1748-0221/12/01/P01020. arXiv:1609.02366 [physics.ins-det].
225. Khachatryan, V., et al. (2016). Measurement of the total and differential inclusive  $B(+)$  hadron cross sections in pp collisions at  $\sqrt{s} = 13 \text{ TeV}$ . *Phys. Lett. B*. doi:10.1016/j.physletb.2017.05.074. arXiv:1609.00873 [hep-ex].
226. Khachatryan, V., et al. (2017). Measurement of the production cross section of a  $W$  boson in association with two  $b$  jets in pp collisions at  $\sqrt{s} = 8 \text{ TeV}$ . *Eur. Phys. J.*, C77, 92. doi:10.1140/epjc/s10052-016-4573-z. arXiv:1608.07561 [hep-ex].
227. Khachatryan, V., et al. (2016). Measurement of the mass of the top quark in decays with a  $J/\psi$  meson in pp collisions at 8 TeV. *JHEP*, 12, 123. doi:10.1007/JHEP12(2016)123. arXiv:1608.03560 [hep-ex].

228. Khachatryan, V., et al. (2017). Search for new phenomena in events with high jet multiplicity and low missing transverse momentum in proton–proton collisions at  $\sqrt{s}=8$  TeV. Phys. Lett., B770, 257-267. doi:10.1016/j.physletb.2017.01.073. arXiv:1608.01224 [hep-ex].
229. Khachatryan, V., et al. (2016). Measurement of the ZZ production cross section and Z  $\rightarrow \ell^+\ell^-\ell^+\ell^-$  branching fraction in pp collisions at  $\sqrt{s}=13$  TeV. Phys. Lett., B763, 280-303. doi:10.1016/j.physletb.2016.10.054. arXiv:1607.08834 [hep-ex].
230. Khachatryan, V., et al. (2016). Measurement of electroweak production of a W boson and two forward jets in proton-proton collisions at  $\sqrt{s}=8$  TeV. JHEP, 11, 147. doi:10.1007/JHEP11(2016)147. arXiv:1607.06975 [hep-ex].
231. Khachatryan, V., et al. (2017). Measurement of the WZ production cross section in pp collisions at  $\sqrt{s}=13$  TeV. Phys. Lett., B766, 268-290. doi:10.1016/j.physletb.2017.01.011. arXiv:1607.06943 [hep-ex].
232. Khachatryan, V., et al. (2016). Search for dark matter in proton-proton collisions at 8 TeV with missing transverse momentum and vector boson tagged jets. JHEP, 12, 083. doi:10.1007/JHEP12(2016)083. arXiv:1607.05764 [hep-ex].
233. Khachatryan, V., et al. (2017). Jet energy scale and resolution in the CMS experiment in pp collisions at 8 TeV. JINST, 12, P02014. doi:10.1088/1748-0221/12/02/P02014. arXiv:1607.03663 [hep-ex].
234. Khachatryan, V., et al. (2016). Search for lepton flavour violating decays of the Higgs boson to  $e\tau$  and  $e\mu$  in proton–proton collisions at  $\sqrt{s}=8$  TeV. Phys. Lett., B763, 472-500. doi:10.1016/j.physletb.2016.09.062. arXiv:1607.03561 [hep-ex].
235. Khachatryan, V., et al. (2017). Observation of the decay  $B^+ \rightarrow \psi(2S) \phi(1020) K^+$  in pp collisions at  $\sqrt{s}=8$  TeV. Phys. Lett., B764, 66-86. doi:10.1016/j.physletb.2016.11.001. arXiv:1607.02638 [hep-ex].
236. Khachatryan, V., et al. (2016). Search for new physics in final states with two opposite-sign, same-flavor leptons, jets, and missing transverse momentum in pp collisions at  $\sqrt{s}=13$  TeV. JHEP, 12, 013. doi:10.1007/JHEP12(2016)013. arXiv:1607.00915 [hep-ex].
237. Khachatryan, V., et al. (2016). Measurement of the differential cross sections for top quark pair production as a function of kinematic event variables in pp collisions at  $\sqrt{s}=7$  and 8 TeV. Phys. Rev., D94, 052006. doi:10.1103/PhysRevD.94.052006. arXiv:1607.00837 [hep-ex].
238. Khachatryan, V., et al. (2016). Searches for R-parity-violating supersymmetry in pp collisions at  $\sqrt{s}=8$  TeV in final states with 0-4 leptons. Phys. Rev., D94, 112009. doi:10.1103/PhysRevD.94.112009. arXiv:1606.08076 [hep-ex].
239. Khachatryan, V., et al. (2017). Evidence for collectivity in pp collisions at the LHC. Phys. Lett., B765, 193-220. doi:10.1016/j.physletb.2016.12.009. arXiv:1606.06198 [nucl-ex].
240. Khachatryan, V., et al. (2017). Measurement of the transverse momentum spectra of weak vector bosons produced in proton-proton collisions at  $\sqrt{s}=8$  TeV. JHEP, 02, 096. doi:10.1007/JHEP02(2017)096. arXiv:1606.05864 [hep-ex].
241. Khachatryan, V., et al. (2016). Search for Resonant Production of High-Mass Photon Pairs in Proton-Proton Collisions at  $\sqrt{s}=8$  and 13 TeV. Phys. Rev. Lett., 117, 051802. doi:10.1103/PhysRevLett.117.051802. arXiv:1606.04093 [hep-ex].

242. Khachatryan, V., et al. (2016). Phenomenological MSSM interpretation of CMS searches in pp collisions at  $\sqrt{s} = 7$  and 8 TeV. JHEP, 10, 129. doi:10.1007/JHEP10(2016)129. arXiv:1606.03577 [hep-ex].
243. Aad, G., et al. (2016). Measurements of the Higgs boson production and decay rates and constraints on its couplings from a combined ATLAS and CMS analysis of the LHC pp collision data at  $\sqrt{s}=7$  and 8 TeV. JHEP, 08, 045. doi:10.1007/JHEP08(2016)045. arXiv:1606.02266 [hep-ex].
244. Khachatryan, V., et al. (2017). Measurement of the transverse momentum spectrum of the Higgs boson produced in pp collisions at  $\sqrt{s}=8$  TeV using  $H \rightarrow WW$  decays. JHEP, 03, 032. doi:10.1007/JHEP03(2017)032. arXiv:1606.01522 [hep-ex].
245. Khachatryan, V., et al. (2017). Search for Dark Matter and Supersymmetry with a Compressed Mass Spectrum in the Vector Boson Fusion Topology in Proton-Proton Collisions at  $\sqrt{s} = 8$  TeV. Phys. Rev. Lett., 118, 021802. doi:10.1103/PhysRevLett.118.021802. arXiv:1605.09305 [hep-ex].
246. Khachatryan, V., et al. (2016). Measurement of the W boson helicity fractions in the decays of top quark pairs to lepton + jets final states produced in pp collisions at  $\sqrt{s}=8$  TeV. Phys. Lett., B762, 512-534. doi:10.1016/j.physletb.2016.10.007. arXiv:1605.09047 [hep-ex].
247. Khachatryan, V., et al. (2017). Search for top squark pair production in compressed-mass-spectrum scenarios in proton-proton collisions at  $\sqrt{s} = 8$  TeV using the  $\alpha_T$  variable. Phys. Lett., B767, 403-430. doi:10.1016/j.physletb.2017.02.007. arXiv:1605.08993 [hep-ex].
248. Khachatryan, V., et al. (2017). Multiplicity and rapidity dependence of strange hadron production in pp, pPb, and PbPb collisions at the LHC. Phys. Lett., B768, 103-129. doi:10.1016/j.physletb.2017.01.075. arXiv:1605.06699 [nucl-ex].
249. Khachatryan, V., et al. (2016). Search for supersymmetry in pp collisions at  $\sqrt{s}=13$  TeV in the single-lepton final state using the sum of masses of large-radius jets. JHEP, 08, 122. doi:10.1007/JHEP08(2016)122. arXiv:1605.04608 [hep-ex].
250. Khachatryan, V., et al. (2016). Measurement of the double-differential inclusive jet cross section in proton–proton collisions at  $\sqrt{s} = 13\text{TeV}$ . Eur. Phys. J., C76, 451. doi:10.1140/epjc/s10052-016-4286-3. arXiv:1605.04436 [hep-ex].
251. Khachatryan, V., et al. (2016). Search for new physics in same-sign dilepton events in proton–proton collisions at  $\sqrt{s} = 13\text{TeV}$ . Eur. Phys. J., C76, 439. doi:10.1140/epjc/s10052-016-4261-z. arXiv:1605.03171 [hep-ex].
252. Khachatryan, V., et al. (2016). Search for Higgs boson off-shell production in proton-proton collisions at 7 and 8 TeV and derivation of constraints on its total decay width. JHEP, 09, 051. doi:10.1007/JHEP09(2016)051. arXiv:1605.02329 [hep-ex].
253. Khachatryan, V., et al. (2016). Measurement of the integrated and differential  $t\bar{t}$  production cross sections for high- $p_t$  top quarks in  $p\bar{p}$  collisions at  $\sqrt{s}=8$  TeV. Phys. Rev., D94, 072002. doi:10.1103/PhysRevD.94.072002. arXiv:1605.00116 [hep-ex].
254. Khachatryan, V., et al. (2016). Search for narrow resonances in dijet final states at  $\sqrt{s}=8$  TeV with the novel CMS technique of data scouting. Phys. Rev. Lett., 117, 031802. doi:10.1103/PhysRevLett.117.031802. arXiv:1604.08907 [hep-ex].
255. Khachatryan, V., et al. (2016). Search for lepton flavour violating decays of heavy resonances and quantum black holes to an  $e^-\mu^+$  pair in proton-proton collisions at  $\sqrt{s}=8$  TeV. Eur. Phys. J., C76, 317. doi:10.1140/epjc/s10052-016-4149-y. arXiv:1604.05239 [hep-ex].

256. Khachatryan, V., et al. (2016). Evidence for exclusive  $\gamma\gamma \rightarrow W^+ W^-$  production and constraints on anomalous quartic gauge couplings in  $p\bar{p}$  collisions at  $\sqrt{s}=7$  and 8 TeV. *JHEP*, 08, 119. doi:10.1007/JHEP08(2016)119. arXiv:1604.04464 [hep-ex].
257. Khachatryan, V., et al. (2016). Search for dark matter particles in proton-proton collisions at  $\sqrt{s}=8$  TeV using the razor variables. *JHEP*, 12, 088. doi:10.1007/JHEP12(2016)088. arXiv:1603.08914 [hep-ex].
258. Khachatryan, V., et al. (2016). Search for two Higgs bosons in final states containing two photons and two bottom quarks in proton-proton collisions at 8 TeV. *Phys. Rev.*, D94, 052012. doi:10.1103/PhysRevD.94.052012. arXiv:1603.06896 [hep-ex].
259. Khachatryan, V., et al. (2016). Measurement of the top quark mass using charged particles in pp collisions at  $\sqrt{s} = 8$  TeV. *Phys. Rev.*, D93, 092006. doi:10.1103/PhysRevD.93.092006. arXiv:1603.06536 [hep-ex].
260. Khachatryan, V., et al. (2016). Measurements of  $t\bar{t}$  charge asymmetry using dilepton final states in pp collisions at  $\sqrt{s}=8$  TeV. *Phys. Lett.*, B760, 365-386. doi:10.1016/j.physletb.2016.07.006. arXiv:1603.06221 [hep-ex].
261. Khachatryan, V., et al. (2016). Search for new physics with the  $M_{T2}$  variable in all-jets final states produced in pp collisions at  $\sqrt{s}=13$  TeV. *JHEP*, 10, 006. doi:10.1007/JHEP10(2016)006. arXiv:1603.04053 [hep-ex].
262. Khachatryan, V., et al. (2016). Search for neutral resonances decaying into a Z boson and a pair of b jets or  $\tau$  leptons. *Phys. Lett.*, B759, 369-394. doi:10.1016/j.physletb.2016.05.087. arXiv:1603.02991 [hep-ex].
263. Khachatryan, V., et al. (2016).  $\Upsilon(nS)$  polarizations versus particle multiplicity in pp collisions at  $\sqrt{s} = 7$  TeV. *Phys. Lett.*, B761, 31-52. doi:10.1016/j.physletb.2016.07.065. arXiv:1603.02913 [hep-ex].
264. Khachatryan, V., et al. (2016). Search for s channel single top quark production in pp collisions at  $\sqrt{s}=7$  and 8 TeV. *JHEP*, 09, 027. doi:10.1007/JHEP09(2016)027. arXiv:1603.02555 [hep-ex].
265. Khachatryan, V., et al. (2016). Measurement of the t-bar production cross section in the e-mu channel in proton-proton collisions at  $\sqrt{s} = 7$  and 8 TeV. *JHEP*, 08, 029. doi:10.1007/JHEP08(2016)029. arXiv:1603.02303 [hep-ex].
266. Khachatryan, V., et al. (2016). Search for heavy Majorana neutrinos in  $e^\pm e^\pm$  jets and  $e^\pm \mu^\pm$  jets events in proton-proton collisions at  $\sqrt{s}=8$  TeV. *JHEP*, 04, 169. doi:10.1007/JHEP04(2016)169. arXiv:1603.02248 [hep-ex].
267. Khachatryan, V., et al. (2016). Measurement of the differential cross section and charge asymmetry for inclusive  $p\bar{p} \rightarrow W^{\pm} + X$  production at  $\sqrt{s} = 8$  TeV. *Eur. Phys. J.*, C76, 469. doi:10.1140/epjc/s10052-016-4293-4. arXiv:1603.01803 [hep-ex].
268. Khachatryan, V., et al. (2016). Search for direct pair production of supersymmetric top quarks decaying to all-hadronic final states in pp collisions at  $\sqrt{s} = 8$  TeV. *Eur. Phys. J.*, C76, 460. doi:10.1140/epjc/s10052-016-4292-5. arXiv:1603.00765 [hep-ex].
269. Khachatryan, V., et al. (2017). Measurements of the  $t\bar{t}$  production cross section in lepton+jets final states in pp collisions at 8 TeV and ratio of 8

- to 7 TeV cross sections. Eur. Phys. J., C77, 15. doi:10.1140/epjc/s10052-016-4504-z. arXiv:1602.09024 [hep-ex].
270. Khachatryan, V., et al. (2016). Search for supersymmetry in electroweak production with photons and large missing transverse energy in pp collisions at  $\sqrt{s} = 8$  TeV. Phys. Lett., B759, 479-500. doi:10.1016/j.physletb.2016.05.088. arXiv:1602.08772 [hep-ex].
271. Khachatryan, V., et al. (2016). Search for heavy resonances decaying to two Higgs bosons in final states containing four b quarks. Eur. Phys. J., C76, 371. doi:10.1140/epjc/s10052-016-4206-6. arXiv:1602.08762 [hep-ex].
272. Khachatryan, V., et al. (2016). Measurement of the  $Z \rightarrow \gamma\gamma$  production cross section in pp collisions at  $\sqrt{s}=8$  TeV and limits on anomalous  $ZZ \rightarrow \gamma\gamma$  and  $Z\gamma\gamma$  trilinear gauge boson couplings. Phys. Lett., B760, 448-468. doi:10.1016/j.physletb.2016.06.080. arXiv:1602.07152 [hep-ex].
273. Khachatryan, V., et al. (2016). Search for supersymmetry in the multijet and missing transverse momentum final state in pp collisions at 13 TeV. Phys. Lett., B758, 152-180. doi:10.1016/j.physletb.2016.05.002. arXiv:1602.06581 [hep-ex].
274. Khachatryan, V., et al. (2016). Measurement of dijet azimuthal decorrelation in pp collisions at  $\sqrt{s}=8$  TeV. Eur. Phys. J., C76, 536. doi:10.1140/epjc/s10052-016-4346-8. arXiv:1602.04384 [hep-ex].
275. Khachatryan, V., et al. (2016). Search for R-parity violating decays of a top squark in proton-proton collisions at  $\sqrt{s}=8$  TeV. Phys. Lett., B760, 178-201. doi:10.1016/j.physletb.2016.06.039. arXiv:1602.04334 [hep-ex].
276. Khachatryan, V., et al. (2016). Combined search for anomalous pseudoscalar HVV couplings in  $VH(H \rightarrow b\bar{b})$  production and  $H \rightarrow VV$  decay. Phys. Lett., B759, 672-696. doi:10.1016/j.physletb.2016.06.004. arXiv:1602.04305 [hep-ex].
277. Khachatryan, V., et al. (2016). Search for direct pair production of scalar top quarks in the single- and dilepton channels in proton-proton collisions at  $\sqrt{s}=8$  TeV. JHEP, 07, 027. doi:10.1007/JHEP07(2016)027, 10.1007/JHEP09(2016)056. arXiv:1602.03169 [hep-ex].
278. Khachatryan, V., et al. (2016). Search for supersymmetry in pp collisions at  $\sqrt{s}=8$  TeV in final states with boosted W bosons and b jets using razor variables. Phys. Rev., D93, 092009. doi:10.1103/PhysRevD.93.092009. arXiv:1602.02917 [hep-ex].
279. Khachatryan, V., et al. (2016). Azimuthal decorrelation of jets widely separated in rapidity in pp collisions at  $\sqrt{s}=7$  TeV. JHEP, 08, 139. doi:10.1007/JHEP08(2016)139. arXiv:1601.06713 [hep-ex].
280. Khachatryan, V., et al. (2016). Search for massive WH resonances decaying into the  $\ell\nu$  final state at  $\sqrt{s}=8$  TeV. Eur. Phys. J., C76, 237. doi:10.1140/epjc/s10052-016-4067-z. arXiv:1601.06431 [hep-ex].
281. Khachatryan, V., et al. (2016). Forward-backward asymmetry of Drell-Yan lepton pairs in pp collisions at  $\sqrt{s}=8$  TeV. Eur. Phys. J., C76, 325. doi:10.1140/epjc/s10052-016-4156-z. arXiv:1601.04768 [hep-ex].

282. Khachatryan, V., et al. (2016). Measurement of inclusive jet production and nuclear modifications in pPb collisions at  $\sqrt{s_{\text{NN}}} = 5.02$  TeV. *Eur. Phys. J.*, C76, 372. doi:10.1140/epjc/s10052-016-4205-7. arXiv:1601.02001 [nucl-ex].
283. Khachatryan, V., et al. (2016). Measurements of t t-bar spin correlations and top quark polarization using dilepton final states in pp collisions at  $\sqrt{s} = 8$  TeV. *Phys. Rev.*, D93, 052007. doi:10.1103/PhysRevD.93.052007. arXiv:1601.01107 [hep-ex].
284. Khachatryan, V., et al. (2016). Correlations between jets and charged particles in PbPb and pp collisions at  $\sqrt{s_{\text{NN}}} = 2.76$  TeV. *JHEP*, 02, 156. doi:10.1007/JHEP02(2016)156. arXiv:1601.00079 [nucl-ex].
285. Khachatryan, V., et al. (2016). Measurement of differential and integrated fiducial cross sections for Higgs boson production in the four-lepton decay channel in pp collisions at  $\sqrt{s}=7$  and 8 TeV. *JHEP*, 04, 005. doi:10.1007/JHEP04(2016)005. arXiv:1512.08377 [hep-ex].
286. Khachatryan, V., et al. (2016). Search for supersymmetry in events with soft leptons, low jet multiplicity, and missing transverse energy in proton–proton collisions at  $\sqrt{s}=8$  TeV. *Phys. Lett.*, B759, 9-35. doi:10.1016/j.physletb.2016.05.033. arXiv:1512.08002 [hep-ex].
287. Khachatryan, V., et al. (2016). Study of Z boson production in pPb collisions at  $\sqrt{s_{\text{NN}}} = 5.02$  TeV. *Phys. Lett.*, B759, 36-57. doi:10.1016/j.physletb.2016.05.044. arXiv:1512.06461 [hep-ex].
288. Khachatryan, V., et al. (2016). Measurement of the inclusive jet cross section in pp collisions at  $\sqrt{s} = 2.76$  TeV. *Eur. Phys. J.*, C76, 265. doi:10.1140/epjc/s10052-016-4083-z. arXiv:1512.06212 [hep-ex].
289. Khachatryan, V., et al. (2016). Search for narrow resonances decaying to dijets in proton-proton collisions at  $\sqrt{s} = 13$  TeV. *Phys. Rev. Lett.*, 116, 071801. doi:10.1103/PhysRevLett.116.071801. arXiv:1512.01224 [hep-ex].
290. Khachatryan, V., et al. (2016). Event generator tunes obtained from underlying event and multiparton scattering measurements. *Eur. Phys. J.*, C76, 155. doi:10.1140/epjc/s10052-016-3988-x. arXiv:1512.00815 [hep-ex].
291. Khachatryan, V., et al. (2016). Search for dark matter and unparticles produced in association with a Z boson in proton-proton collisions at  $\sqrt{s}=8$  TeV. *Phys. Rev.*, D93, 052011. doi:10.1103/PhysRevD.93.052011. arXiv:1511.09375 [hep-ex].
292. Khachatryan, V., et al. (2016). Measurement of spin correlations in  $t\bar{t}$  production using the matrix element method in the muon+jets final state in pp collisions at  $\sqrt{s} = 8$  TeV. *Phys. Lett.*, B758, 321-346. doi:10.1016/j.physletb.2016.05.005. arXiv:1511.06170 [hep-ex].
293. Khachatryan, V., et al. (2016). Search for anomalous single top quark production in association with a photon in pp collisions at  $\sqrt{s}=8$  TeV. *JHEP*, 04, 035. doi:10.1007/JHEP04(2016)035. arXiv:1511.03951 [hep-ex].
294. Khachatryan, V., et al. (2016). Search for a low-mass pseudoscalar Higgs boson produced in association with a  $b\bar{b}$  pair in pp collisions at  $\sqrt{s} = 8$  TeV. *Phys. Lett.*, B758, 296-320. doi:10.1016/j.physletb.2016.05.003. arXiv:1511.03610 [hep-ex].
295. Khachatryan, V., et al. (2016). Measurement of top quark polarisation in t-channel single top quark production. *JHEP*, 04, 073. doi:10.1007/JHEP04(2016)073. arXiv:1511.02138 [hep-ex].

296. Khachatryan, V., et al. (2016). Search for excited leptons in proton-proton collisions at  $\sqrt{s} = 8$  TeV. *JHEP*, 03, 125. doi:10.1007/JHEP03(2016)125. arXiv:1511.01407 [hep-ex].
297. Khachatryan, V., et al. (2016). Reconstruction and identification of  $\tau$  lepton decays to hadrons and  $\nu\tau$  at CMS. *JINST*, 11, P01019. doi:10.1088/1748-0221/11/01/P01019. arXiv:1510.07488 [physics.ins-det].
298. Khachatryan, V., et al. (2016). Search for a very light NMSSM Higgs boson produced in decays of the 125 GeV scalar boson and decaying into  $\tau$  leptons in pp collisions at  $\sqrt{s}=8$  TeV. *JHEP*, 01, 079. doi:10.1007/JHEP01(2016)079. arXiv:1510.06534 [hep-ex].
299. Khachatryan, V., et al. (2016). Measurement of the top quark pair production cross section in proton-proton collisions at  $\sqrt{s} = 13$  TeV. *Phys. Rev. Lett.*, 116, 052002. doi:10.1103/PhysRevLett.116.052002. arXiv:1510.05302 [hep-ex].
300. Khachatryan, V., et al. (2016). Transverse momentum spectra of inclusive b jets in pPb collisions at  $\sqrt{s_{NN}} = 5.02$  TeV. *Phys. Lett.*, B754, 59. doi:10.1016/j.physletb.2016.01.010. arXiv:1510.03373 [nucl-ex].
301. Khachatryan, V., et al. (2016). Measurement of  $t\bar{t}$  production with additional jet activity, including b quark jets, in the dilepton decay channel using pp collisions at  $\sqrt{s} = 8$  TeV. *Eur. Phys. J.*, C76, 379. doi:10.1140/epjc/s10052-016-4105-x. arXiv:1510.03072 [hep-ex].
302. Khachatryan, V., et al. (2016). Measurement of long-range near-side two-particle angular correlations in pp collisions at  $\sqrt{s} = 13$  TeV. *Phys. Rev. Lett.*, 116, 172302. doi:10.1103/PhysRevLett.116.172302. arXiv:1510.03068 [nucl-ex].
303. Khachatryan, V., et al. (2016). Searches for a heavy scalar boson H decaying to a pair of 125 GeV Higgs bosons hh or for a heavy pseudoscalar boson A decaying to Zh, in the final states with  $h \rightarrow \tau\tau$ . *Phys. Lett.*, B755, 217-244. doi:10.1016/j.physletb.2016.01.056. arXiv:1510.01181 [hep-ex].
304. Khachatryan, V., et al. (2016). Observation of top quark pairs produced in association with a vector boson in pp collisions at  $\sqrt{s}=8$  TeV. *JHEP*, 01, 096. doi:10.1007/JHEP01(2016)096. arXiv:1510.01131 [hep-ex].
305. Khachatryan, V., et al. (2016). Measurement of transverse momentum relative to dijet systems in PbPb and pp collisions at  $\sqrt{s_{NN}}=2.76$  TeV. *JHEP*, 01, 006. doi:10.1007/JHEP01(2016)006. arXiv:1509.09029 [nucl-ex].
306. Khachatryan, V., et al. (2016). Search for the associated production of a Higgs boson with a single top quark in proton-proton collisions at  $\sqrt{s}=8$  TeV. *JHEP*, 06, 177. doi:10.1007/JHEP06(2016)177. arXiv:1509.08159 [hep-ex].
307. Khachatryan, V., et al. (2016). Search for the production of an excited bottom quark decaying to  $tW$  in proton-proton collisions at  $\sqrt{s}=8$  TeV. *JHEP*, 01, 166. doi:10.1007/JHEP01(2016)166. arXiv:1509.08141 [hep-ex].
308. Khachatryan, V., et al. (2016). Measurement of the  $t\bar{t}$  production cross section in the all-jets final state in pp collisions at  $\sqrt{s}=8$  TeV. *Eur. Phys. J.*, C76, 128. doi:10.1140/epjc/s10052-016-3956-5. arXiv:1509.06076 [hep-ex].
309. Khachatryan, V., et al. (2016). Search for  $W' \rightarrow tb$  in proton-proton collisions at  $\sqrt{s} = 8$  TeV. *JHEP*, 02, 122. doi:10.1007/JHEP02(2016)122. arXiv:1509.06051 [hep-ex].

310. Khachatryan, V., et al. (2016). Search for vector-like charge 2/3 T quarks in proton-proton collisions at  $\sqrt{s} = 8$  TeV. Phys. Rev., D93, 012003. doi:10.1103/PhysRevD.93.012003. arXiv:1509.04177 [hep-ex].
311. Khachatryan, V., et al. (2016). Measurement of the top quark mass using proton-proton data at  $\sqrt{s} = 7$  and 8 TeV. Phys. Rev., D93, 072004. doi:10.1103/PhysRevD.93.072004. arXiv:1509.04044 [hep-ex].
312. Khachatryan, V., et al. (2016). Measurement of the inelastic cross section in proton–lead collisions at  $\sqrt{s_{NN}} = 5.02$  TeV. Phys. Lett., B759, 641-662. doi:10.1016/j.physletb.2016.06.027. arXiv:1509.03893 [hep-ex].
313. Khachatryan, V., et al. (2016). Search for single production of scalar leptoquarks in proton-proton collisions at  $\sqrt{s} = 8$  TeV. Phys. Rev., D93, 032005. doi:10.1103/PhysRevD.95.039906, 10.1103/PhysRevD.93.032005. arXiv:1509.03750 [hep-ex].
314. Khachatryan, V., et al. (2016). Search for pair production of first and second generation leptoquarks in proton-proton collisions at  $\sqrt{s} = 8$  TeV. Phys. Rev., D93, 032004. doi:10.1103/PhysRevD.93.032004. arXiv:1509.03744 [hep-ex].
315. Khachatryan, V., et al. (2016). Measurement of differential cross sections for Higgs boson production in the diphoton decay channel in pp collisions at  $\sqrt{s}=8$  TeV. Eur. Phys. J., C76, 13. doi:10.1140/epjc/s10052-015-3853-3. arXiv:1508.07819 [hep-ex].
316. Khachatryan, V., et al. (2016). Study of B Meson Production in p+\$Pb Collisions at  $\sqrt{s_{NN}}=5.02$  TeV Using Exclusive Hadronic Decays. Phys. Rev. Lett., 116, 032301. doi:10.1103/PhysRevLett.116.032301. arXiv:1508.06678 [nucl-ex].
317. Khachatryan, V., et al. (2016). Search for W' decaying to tau lepton and neutrino in proton-proton collisions at  $\sqrt{s} = 8$  TeV. Phys. Lett., B755, 196-216. doi:10.1016/j.physletb.2016.02.002. arXiv:1508.04308 [hep-ex].
318. Khachatryan, V., et al. (2016). Measurement of the charge asymmetry in top quark pair production in pp collisions at  $\sqrt{s} = 8$  TeV using a template method. Phys. Rev., D93, 034014. doi:10.1103/PhysRevD.93.034014. arXiv:1508.03862 [hep-ex].
319. Khachatryan, V., et al. (2016). Search for neutral MSSM Higgs bosons decaying to  $\mu^+ \mu^-$  in pp collisions at  $\sqrt{s} = 7$  and 8 TeV. Phys. Lett., B752, 221-246. doi:10.1016/j.physletb.2015.11.042. arXiv:1508.01437 [hep-ex].
320. Khachatryan, V., et al. (2016). Search for supersymmetry in events with a photon, a lepton, and missing transverse momentum in pp collisions at  $\sqrt{s} = 8$  TeV. Phys. Lett., B757, 6-31. doi:10.1016/j.physletb.2016.03.039. arXiv:1508.01218 [hep-ex].
321. Khachatryan, V., et al. (2016). Angular analysis of the decay  $B^0 \rightarrow K^{*0} \mu^+ \mu^-$  from pp collisions at  $\sqrt{s} = 8$  TeV. Phys. Lett., B753, 424-448. doi:10.1016/j.physletb.2015.12.020. arXiv:1507.08126 [hep-ex].
322. Khachatryan, V., et al. (2016). Measurement of the CP-violating weak phase  $\phi_s$  and the decay width difference  $\Delta \Gamma_s$  using the  $B^- \rightarrow J/\psi \phi(1020)$  decay channel in pp collisions at  $\sqrt{s} = 8$  TeV. Phys. Lett., B757, 97-120. doi:10.1016/j.physletb.2016.03.046. arXiv:1507.07527 [hep-ex].

323. Khachatryan, V., et al. (2016). Search for pair-produced vectorlike B quarks in proton-proton collisions at  $\sqrt{s}=8$  TeV. Phys. Rev., D93, 112009. doi:10.1103/PhysRevD.93.112009. arXiv:1507.07129 [hep-ex].
324. Khachatryan, V., et al. (2016). Measurement of the  $\langle W^+ W^- \rangle$  cross section in pp collisions at  $\sqrt{s} = 8$  TeV and limits on anomalous gauge couplings. Eur. Phys. J., C76, 401. doi:10.1140/epjc/s10052-016-4219-1. arXiv:1507.03268 [hep-ex].
325. Khachatryan, V., et al. (2016). Inclusive and differential measurements of the  $\overline{t}$  charge asymmetry in pp collisions at  $\sqrt{s} = 8$  TeV. Phys. Lett., B757, 154-179. doi:10.1016/j.physletb.2016.03.060. arXiv:1507.03119 [hep-ex].
326. Khachatryan, V., et al. (2016). Search for a Higgs boson decaying into  $\gamma^* \gamma \rightarrow \ell\bar{\ell}$  with low dilepton mass in pp collisions at  $\sqrt{s} = 8$  TeV. Phys. Lett., B753, 341-362. doi:10.1016/j.physletb.2015.12.039. arXiv:1507.03031 [hep-ex].
327. Khachatryan, V., et al. (2016). Search for exotic decays of a Higgs boson into undetectable particles and one or more photons. Phys. Lett., B753, 363-388. doi:10.1016/j.physletb.2015.12.017. arXiv:1507.00359 [hep-ex].
328. Khachatryan, V., et al. (2016). Search for resonant  $t\bar{t}$  production in proton-proton collisions at  $\sqrt{s}=8$  TeV. Phys. Rev., D93, 012001. doi:10.1103/PhysRevD.93.012001. arXiv:1506.03062 [hep-ex].
329. Khachatryan, V., et al. (2016). Search for a massive resonance decaying into a Higgs boson and a W or Z boson in hadronic final states in proton-proton collisions at  $\sqrt{s}=8$  TeV. JHEP, 02, 145. doi:10.1007/JHEP02(2016)145. arXiv:1506.01443 [hep-ex].
330. Khachatryan, V., et al. (2016). A search for pair production of new light bosons decaying into muons. Phys. Lett., B752, 146-168. doi:10.1016/j.physletb.2015.10.067. arXiv:1506.00424 [hep-ex].
331. Khachatryan, V., et al. (2015). Comparison of the  $Z/\gamma\gamma + \text{jets}$  to  $\gamma\gamma + \text{jets}$  cross sections in pp collisions at  $\sqrt{s}=8$  TeV. JHEP, 10, 128. doi:10.1007/JHEP04(2016)010, 10.1007/JHEP10(2015)128. arXiv:1505.06520 [hep-ex].
332. Khachatryan, V., et al. (2015). Search for Third-Generation Scalar Leptoquarks in the  $t\tau$  Channel in Proton-Proton Collisions at  $\sqrt{s}=8$  TeV. JHEP, 07, 042. doi:10.1007/JHEP11(2016)056, 10.1007/JHEP07(2015)042. arXiv:1503.09049 [hep-ex].
333. Khachatryan, V., et al. (2016). Measurement of the ratio  $B(B^0_s \rightarrow J/\psi f_0(980)) / B(B^0_s \rightarrow J/\psi \phi(1020))$  in pp collisions at  $\sqrt{s}=7$  TeV. Phys. Lett., B756, 84-102. doi:10.1016/j.physletb.2016.02.047. arXiv:1501.06089 [hep-ex].
334. Khachatryan, V., et al. (2016). Search for new phenomena in monophoton final states in proton-proton collisions at  $\sqrt{s}=8$  TeV. Phys. Lett., B755, 102-124. doi:10.1016/j.physletb.2016.01.057. arXiv:1410.8812 [hep-ex].
335. Khachatryan, V., et al. (2015). Measurement of the  $pp \rightarrow ZZ$  production cross section and constraints on anomalous triple gauge couplings in four-lepton final states at  $\sqrt{s}=8$  TeV. Phys. Lett., B740, 250-272. doi:10.1016/j.physletb.2016.04.010, 10.1016/j.physletb.2014.11.059. arXiv:1406.0113 [hep-ex].

## FIFE

336. Abbott, B. P., Abbott, R., Abbott, T. D., Abernathy, M. R., Acernese, F., Ackley, K., et al. (2016). Localization and broadband follow-up of the gravitational-wave transient GW150914. *Astrophysical Journal Letters*, 826(1). <http://iopscience.iop.org/article/10.3847/2041-8205/826/1/L13>
337. Adamson, P., et al. (Daya Bay Collaboration, MINOS Collaboration). (2016). Limits on active to sterile neutrino oscillations from disappearance searches in the MINOS, Daya Bay, and Bugey-3 experiments. *Phys. Rev. Lett.* 117, 151801. <https://doi.org/10.1103/PhysRevLett.117.151801>
338. Adamson, P., et al. (MINOS Collaboration). (2016). Constraints on large extra dimensions from the MINOS experiment. *Phys. Rev. D* 94, 111101(R). <https://doi.org/10.1103/PhysRevD.94.111101>
339. Adamson, P., et al. (MINOS Collaboration). (2016). Search for sterile neutrinos mixing with muon neutrinos in MINOS. *Phys. Rev. Lett.* 117, 151803. <https://doi.org/10.1103/PhysRevLett.117.151803>
340. Adamson, P., et al. (MINOS Collaboration). (2017). A search for flavor-changing non-standard neutrino interactions using ve appearance in MINOS. *Phys. Rev. D* 95, 012005. <https://doi.org/10.1103/PhysRevD.95.012005>
341. Adamson, P., et al. (NOvA Collaboration). (2016). First measurement of electron neutrino appearance in NOvA. *Phys. Rev. Lett.* 116, 151806. <https://doi.org/10.1103/PhysRevLett.116.151806>
342. Adamson, P., et al. (NOvA Collaboration). (2016). First measurement of muon-neutrino disappearance in NOvA. *Phys. Rev. D* 93, 051104(R). <https://doi.org/10.1103/PhysRevD.93.051104>
343. Adamson, P., et al. (NOvA Collaboration). (2017). Measurement of the neutrino mixing angle  $\theta_{23}$  in NOvA. *Phys. Rev. Lett.* 118, 151802. <https://doi.org/10.1103/PhysRevLett.118.151802>
344. Aliaga, L., et al. (MINERvA Collaboration). (2016). Neutrino flux predictions for the NuMI beam. *Phys. Rev. D* 94, 092005. <https://doi.org/10.1103/PhysRevD.94.092005>
345. Annis, J., Soares-Santos, M., Berger, E., Brout, D., Chen, H., Chornock, R. (2016). A Dark Energy Camera search for missing supergiants in the LMC after the Advanced LIGO gravitational wave event GW150914. *Astrophysical Journal Letters*, 823(2). <http://iopscience.iop.org/article/10.3847/2041-8205/823/2/L34>
346. Cowperthwaite, P. S., Berger, E., Soares-Santos, M., Annis, J., Brout, D., Brown, D. A., et al. (2016). A DECam search for an optical counterpart to the LIGO gravitational wave event GW151226. *Astrophysical Journal Letters*, 826(2). <http://iopscience.iop.org/article/10.3847/2041-8205/826/2/L29>
347. Devan, J., et al. (The MINERvA Collaboration). (2016). Measurements of the inclusive neutrino and antineutrino charged current cross sections in MINERvA using the low-v flux method. *Phys. Rev. D* 94, 112007. <https://doi.org/10.1103/PhysRevD.94.112007>
348. Gerdes, D. W., Sako, M., Hamilton, S., Zhang, K., Khain, T., Becker, J. C., et al. (2017). Discovery and physical characterization of a large scattered disk object at 92 AU. *Astrophysical Journal Letters*, 839(1). <http://iopscience.iop.org/article/10.3847/2041-8213/aa64d8>

349. Marshall, C. M., et al. (MINERvA Collaboration). (2016). Measurement of K<sup>+</sup> production in charged-current νμ interactions. *Phys. Rev. D* 94, 012002. <https://doi.org/10.1103/PhysRevD.94.012002>
350. McGivern, C. L., et al. (MINERvA Collaboration). (2016). Cross sections for neutrino and antineutrino induced pion production on hydrocarbon in the few-GeV region using MINERvA. *Phys. Rev. D* 94, 052005. <https://doi.org/10.1103/PhysRevD.94.052005>
351. Mousseau, J., et al. (The MINERvA Collaboration). (2016). Measurement of partonic nuclear effects in deep-inelastic neutrino scattering using MINERvA. *Phys. Rev. D* 93, 071101. <https://doi.org/10.1103/PhysRevD.93.071101>
352. Park, J., et al. (MINERvA Collaboration). (2016). Measurement of neutrino flux using neutrino-electron elastic scattering. *Phys. Rev. D* 93, 112007. <https://doi.org/10.1103/PhysRevD.93.112007>
353. Rodrigues, P. A., et al. (MINERvA Collaboration). (2016). Identification of nuclear effects in neutrino-carbon interactions at low three-momentum transfer. *Phys. Rev. Lett.* 116, 071802. <https://doi.org/10.1103/PhysRevLett.116.071802>
354. Soares-Santos, M., Kessler, R., Berger, E., Annis, J., Brout, D., Buckley-Geer, E., et al. (2016). A Dark Energy Camera search for an optical counterpart to the first advanced LIGO gravitational wave event GW150914. *Astrophysical Journal Letters*, 823(2). <http://iopscience.iop.org/article/10.3847/2041-8205/823/2/L33>
355. Wang, Z., et al. (MINERvA Collaboration). (2016). First evidence of coherent K<sup>+</sup> meson production in neutrino-nucleus scattering. *Phys. Rev. Lett.* 117, 061802. <https://doi.org/10.1103/PhysRevLett.117.061802>
356. Wolcott, J., et al. (MINERvA Collaboration). (2016). Evidence for neutral-current diffractive neutral pion production from hydrogen in neutrino interactions on hydrocarbon. *Phys. Rev. Lett.* 117, 111801. <https://doi.org/10.1103/PhysRevLett.117.111801>
357. Wolcott, J., et al. (MINERvA Collaboration). (2016). Measurement of electron neutrino quasielastic and quasielastic-like scattering on hydrocarbon at average E<sub>V</sub> of 3.6 GeV. *Phys. Rev. Lett.* 116, 081802. <https://doi.org/10.1103/PhysRevLett.116.081802>

## **IceCube**

358. Neutrinos and Cosmic Rays Observed by IceCube. By IceCube Collaboration (M.G. Aartsen et al.). [arXiv:1701.03731 [astro-ph.HE]].
359. The IceCube Realtime Alert System. By IceCube Collaboration (M.G. Aartsen et al.). [arXiv:1612.06028 [astro-ph.HE]]. 10.1016/j.astropartphys.2017.05.002. *Astropart.Phys.* 92 (2017) 30-41.
360. Search for annihilating dark matter in the Sun with 3 years of IceCube data. By IceCube Collaboration (M.G. Aartsen et al.). [arXiv:1612.05949 [astro-ph.HE]]. 10.1140/epjc/s10052-017-4689-9. *Eur.Phys.J. C*77 (2017) no.3, 146.
361. The IceCube Neutrino Observatory: Instrumentation and Online Systems. By IceCube Collaboration (M.G. Aartsen et al.). [arXiv:1612.05093 [astro-ph.IM]]. 10.1088/1748-0221/12/03/P03012. *JINST* 12 (2017) no.03, P03012.

362. The contribution of Fermi-2LAC blazars to the diffuse TeV-PeV neutrino flux. By IceCube Collaboration (M.G. Aartsen et al.). [arXiv:1611.03874 [astro-ph.HE]]. 10.3847/1538-4357/835/1/45. *Astrophys.J.* 835 (2017) no.1, 45.
363. Measurement of the mass difference between top quark and antiquark in pp collisions at  $\sqrt{s} = 8$  TeV. By CMS Collaboration (Serguei Chatrchyan et al.). [arXiv:1610.09551 [hep-ex]]. 10.1016/j.physletb.2017.04.028. *Phys.Lett.B* 770 (2017) 50-71.
364. Very High-Energy Gamma-Ray Follow-Up Program Using Neutrino Triggers from IceCube. By IceCube and MAGIC and VERITAS Collaborations (M.G. Aartsen et al.). [arXiv:1610.01814 [hep-ex]]. 10.1088/1748-0221/11/11/P11009. *JINST* 11 (2016) no.11, P11009.
365. All-sky Search for Time-integrated Neutrino Emission from Astrophysical Sources with 7 yr of IceCube Data. By IceCube Collaboration (M.G. Aartsen et al.). [arXiv:1609.04981 [astro-ph.HE]]. 10.3847/1538-4357/835/2/151. *Astrophys.J.* 835 (2017) no.2, 151.
366. First search for dark matter annihilations in the Earth with the IceCube Detector. By IceCube Collaboration (M.G. Aartsen et al.). [arXiv:1609.01492 [astro-ph.HE]]. 10.1140/epjc/s10052-016-4582-y. *Eur.Phys.J.C* 77 (2017) no.2, 82.
367. Observation and Characterization of a Cosmic Muon Neutrino Flux from the Northern Hemisphere using six years of IceCube data. By IceCube Collaboration (M.G. Aartsen et al.). [arXiv:1607.08006 [astro-ph.HE]]. 10.3847/0004-637X/833/1/3. *Astrophys.J.* 833 (2016) no.1, 3.
368. Constraints on Ultrahigh-Energy Cosmic-Ray Sources from a Search for Neutrinos above 10 PeV with IceCube. By IceCube Collaboration (M.G. Aartsen et al.). [arXiv:1607.05886 [astro-ph.HE]]. 10.1103/PhysRevLett.117.241101. *Phys.Rev.Lett.* 117 (2016) no.24, 241101.
369. Search for Sources of High-Energy Neutrons with four Years of Data from the IceTop Detector. By IceCube Collaboration (M.G. Aartsen et al.). [arXiv:1607.05614 [astro-ph.HE]]. 10.3847/0004-637X/830/2/129. *Astrophys.J.* 830 (2016) no.2, 129.
370. PINGU: A Vision for Neutrino and Particle Physics at the South Pole. By IceCube Collaboration (M.G. Aartsen et al.). [arXiv:1607.02671 [hep-ex]]. 10.1088/1361-6471/44/5/054006. *J.Phys.G* 44 (2017) no.5, 054006.
371. All-flavour Search for Neutrinos from Dark Matter Annihilations in the Milky Way with IceCube/DeepCore. By IceCube Collaboration (M.G. Aartsen et al.). [arXiv:1606.00209 [astro-ph.HE]]. 10.1140/epjc/s10052-016-4375-3. *Eur.Phys.J.C* 76 (2016) no.10, 531.
372. Neutrino oscillation studies with IceCube-DeepCore. By M.G. Aartsen et al.. 10.1016/j.nuclphysb.2016.03.028. *Nucl.Phys.B* 908 (2016) 161-177.
373. Searches for Sterile Neutrinos with the IceCube Detector. By IceCube Collaboration (M.G. Aartsen et al.). [arXiv:1605.01990 [hep-ex]]. 10.1103/PhysRevLett.117.071801. *Phys.Rev.Lett.* 117 (2016) no.7, 071801.
374. Lowering IceCube's Energy Threshold for Point Source Searches in the Southern Sky. By IceCube Collaboration (M.G. Aartsen et al.). [arXiv:1605.00163 [astro-ph.HE]]. 10.3847/2041-8205/824/2/L28. *Astrophys.J.* 824 (2016) no.2, L28.
375. Anisotropy in Cosmic-ray Arrival Directions in the Southern Hemisphere Based on six Years of Data From the Icecube Detector. By IceCube Collaboration (M.G. Aartsen et al.). [arXiv:1603.01227 [astro-ph.HE]]. 10.3847/0004-637X/826/2/220. *Astrophys.J.* 826 (2016) no.2, 220.

376. High-energy Neutrino follow-up search of Gravitational Wave Event GW150914 with ANTARES and IceCube. By ANTARES and IceCube and LIGO Scientific and Virgo Collaborations (S. Adrian-Martinez et al.). [arXiv:1602.05411 [astro-ph.HE]]. 10.1103/PhysRevD.93.122010. Phys. Rev. D93 (2016) no.12, 122010.
377. An All-Sky Search for Three Flavors of Neutrinos from Gamma-Ray Bursts with the IceCube Neutrino Observatory. By IceCube Collaboration (M.G. Aartsen et al.). [arXiv:1601.06484 [astro-ph.HE]]. 10.3847/0004-637X/824/2/115. *Astrophys.J.* 824 (2016) no.2, 115.
378. Improved limits on dark matter annihilation in the Sun with the 79-string IceCube detector and implications for supersymmetry. By IceCube Collaboration (M.G. Aartsen et al.). [arXiv:1601.00653 [hep-ph]]. 10.1088/1475-7516/2016/04/022. *JCAP* 1604 (2016) no.04, 022.
379. Characterization of the atmospheric muon flux in IceCube. IceCube Collaboration (M. G. Aartsen, et al.). *Astroparticle Physics*, 78, 1–17. <https://doi.org/10.1016/j.astropartphys.2016.01.006>
380. First combined search for neutrino point-sources in the Southern Hemisphere with the ANTARES and IceCube neutrino telescopes. ANTARES and IceCube Collaborations (S. Adrián-Martínez, et al.). *Astrophysical Journal*, 823(1). <https://doi.org/10.3847/0004-637X/823/1/65>
381. Search for astrophysical tau neutrinos in three years of IceCube data. Icecube Collaboration (M. G. Aartsen, et al.). *Physical Review D*, 93, 022001. <https://doi.org/10.1103/PhysRevD.93.022001>
382. Search for correlations between the arrival directions of IceCube neutrino events and ultrahigh-energy cosmic rays detected by the Pierre Auger Observatory and the Telescope Array. The IceCube, Pierre Auger, and Telescope Array Collaborations (M. G. Aartsen, et al.). *Journal of Cosmology and Astroparticle Physics*, 2016. <https://doi.org/10.1088/1475-7516/2016/01/037>
383. Search for transient astrophysical neutrino emission with IceCube-DeepCore. IceCube Collaboration (M. G. Aartsen, et al.). *Astrophysical Journal*, 816(2). <https://doi.org/10.3847/0004-637X/816/2/75>
384. Searches for relativistic magnetic monopoles in IceCube. IceCube Collaboration (M. G. Aartsen, et al.). *European Physical Journal C*, 76, 133. <https://doi.org/10.1140/epjc/s10052-016-3953-8>
385. Halzen, F. (2016). High-energy neutrino astrophysics. *Nature Phys.* 13, 232–238. <https://doi.org/10.1038/nphys3816>
386. Halzen, F., & Klein, S. (2016). IceCube seeks to expand. *CERN Courier*, 56, 40–41. <http://cerncourier.com/cws/article/cern/65508>

## Other

387. Burrill, D., & Del Maestro, A. (2016). Ab initio electronic properties of organometallic solid solutions of  $\beta-(CuPc)_{1-x}(H_2Pc)_x$ . Manuscript in preparation.
388. Chekanov, S. & Kotwal, A. (2016, May). Complex detector simulations of proton collisions for FCC. *FCC News*. Retrieved from <https://fcc.web.cern.ch/Pages/news/Complex-detector-simulations-of-proton-collisions-for-FCC-.aspx>
389. Chekanov, S. V. (2016). Public repository with Monte Carlo simulations for high-energy particle collision experiments. *ICHEP2016 Proceedings* (Chicago, 2016). Retrieved from <https://arxiv.org/abs/1609.04455>
390. Chekanov, S. V., & Demarteau, M. (2016). Conceptual design studies for a CEPC Detector. arXiv:1604.01994 (April 7, 2016). A white paper contributed to the IAS Program on High Energy

Physics (4-29 Jan, 2016), International Journal of Modern Physics A (IJMPA) Volume No.31, Issue No. 33, 1644021-1.

391. Chekanov, S. V., Beydler, M., Kotwal, A. V., Gray, L., Sen, S., Tran, N. V., et al. (2016). Initial performance studies of a general-purpose detector for multi-TeV physics at a 100 TeV pp collider. Submitted to NIM. Retrieved from <https://arxiv.org/abs/1612.07291>
392. Gladstein, A. L., Pistorius, J. L., Quinto-Cortés, C. D., Skodiak, M. A., Watkins, J. C., Woerner, A. E., & Hammer, M.F. (in preparation) Efficient pipeline for whole genome simulation and summary statistic calculation with flexible demographic models.
393. Gladstein, A. L., Pistorius, J. L., Quinto-Cortés, C. D., Watkins, J. C., & Hammer, M. F. (2016). Population substructure within Ashkenazi Jews inferred with Approximate Bayesian Computation. Manuscript in preparation.
394. Golling, T., Hance, M., Harris, P., Mangano, M. L., McCullough, M., Moortgat, F., et al. Physics at a 100 TeV pp collider: Beyond the Standard Model phenomena (CERN-TH-2016-111). Retrieved from <https://arxiv.org/abs/1606.00947>
395. Huizinga, J., Mouret, J. B., Clune, J. (2016). Does aligning phenotypic and genotypic modularity improve the evolution of neural networks? Proceedings of the Genetic and Evolutionary Computation Conference (pp. 125-132).
396. Robertson, K., & Del Maestro, A. (2016). Superfluid helium-4 confined inside hexagonal nanopores. Manuscript in preparation.
397. Saadatzi, M., & Celik, O. (2016). A passive hip exoskeleton for reducing metabolic cost of walking: A simulation study. Manuscript in preparation.
398. Saadatzi, M., & Celik, O. (2016). Predictive simulation framework for combined device and human mechanics. Manuscript in preparation.
399. Santos, R., Nguyen, M., Webster, J., Ryu, S., Adelman, J., Chekanov, S., et al. (2016). Machine learning techniques in searches for  $t\bar{t}h$  in the  $h \rightarrow bb^-$  decay channel. Submitted to Physical Review D. Retrieved from <https://arxiv.org/abs/1610.03088>
400. Sen, S., Kotwal, A., Chekanov, S., Gray, L., Tran, N. V., & Yu, S.-S. (2016). Detectors for superboosted  $\tau$ -leptons at future circular colliders. Proceedings of Science (ICHEP2016) 788. Retrieved from [https://pos.sissa.it/archive/conferences/282/788/ICHEP2016\\_788.pdf](https://pos.sissa.it/archive/conferences/282/788/ICHEP2016_788.pdf)
401. Xie, B., Nguyen, T. H., & Minh, D. D. L. (in press). Absolute binding free energies between T4 lysozyme and 141 small molecules: Calculations based on multiple rigid receptor structures. Journal of Chemical Theory and Computation.
402. Xu, Y., Cao, S., Nahrgang, M., Bernhard, J. E., Bass, S. A. (2016). Data-driven analysis of the temperature dependence of the heavy-quark transport coefficient. Hard Probe 2016 proceeding (published in Nuclear and Particle Physics proceedings by Elsevier).
403. Yu, S.-S., Chekanov, S., Gray, L., Kotwal, A., Sen, S., Tran, N. V. (2016). Study of boosted W-jets and Higgs-jets with the SiFCC detector. Proceedings for the 38th International Conference on High Energy Physics, 3-10 August 2016, Chicago, USA. Retrieved from <https://arxiv.org/abs/1611.01136>
404. Zhang C., Freddolino, P. L., & Zhang, Y. (in press). COFACTOR: Improved protein function prediction by combining structure, sequence, and protein-protein interaction information. Nucleic Acids Research.